universität wien

MASTERARBEIT / MASTER'S THESIS

Titel der Masterarbeit / Title of the Master's Thesis

„Glycolipid profiling of colon cancer samples using liquid chromatography, high resolution mass spectrometry and multistage fragmentation“

verfasst von / submitted by

Richard Urban, BSc

angestrebter akademischer Grad / in partial fulfilment of the requirements for the degree of

Master of Science (MSc)

Wien, 2023 / Vienna 2023

Studienkennzahl lt. Studienblatt / degree programme code as it appears on the student record sheet:	A 066 862
Studienrichtung lt. Studienblatt / degree programme as it appears on the student record sheet:	Masterstudium Chemie
Betreut von / Supervisor:	Dipl.-Ing. Evelyn Rampler, Privatdoz. Bakk. PhD

Table of contents

1. Introduction 1
1.1 Lipidomics research 1
1.2 Sphingolipids 3
1.3 Glycosphingolipids (GSL) 7
1.3.1 Lactosylceramide 8
1.3.2 Globoside 9
1.3.3 Ganglioside 11
1.3.4 Impact of GSLs on cancer development 12
2. Material and methods 15
2.1 Requirements for sample and standard preparation 15
2.2 Lipid based Liquid chromatograhy 16
2.2.1 Reversed phase-chromatography with Lipids 17
2.2.2 Retention time 17
2.3 High resolution mass spectrometry 18
2.3.1 Targeted lipid analysis 18
2.3.2 Untargeted lipid analysis 18
2.3.3 Data acquisiton modes 19
2.3.4 Lipid identification 20
2.3.5 MS-based approaches for quantification 21
2.4 Chemical reagents 22
2.4.1 Eluents for the liquid chromatography 22
2.5 Reference Standards 22
2.5.1 Standard preparation method 24
2.6 HCT116 colon cancer sample 25
2.6.1 HCT116 sample preparation method 26
2.7 LC-MS/MS measurements 27

2.8 Methods 28
2.8.1 Lipid QC - 23 minutes method 28
2.8.2 Experiments - 30 minutes method 30
2.8.3 Data interpretation of the Lipids via Skyline 31
3. Results and discussion 33
3.1 GSL-specific method development 33
3.1.1 Targeted analysis of GSLs in the standard pool and cancer sample 33
3.1.2 Target- and inclusion list 34
3.1.3 Cancer studies on GSLs species 34
3.2 Method performance 37
3.2.1 Chromatographic seperation of the studied GSL classes and species 37
3.2.2 Retention time stability 40
3.2.3 Ionisation methods for glycosphingolipids 42
3.2.4 Setup for the HESI-source parameter validation 43
3.2.5 HESI-source parameter 44
3.2.6 Comparison of HESI modes 46
3.3 Analysis of colon cancer samples using the developed glycosphingolipid assay 52
3.3.1 GSLs in standard pool and HCT116 samples 55
3.4 GSL annotation based on fragmentation patterns in MS2 57
3.4.1 Nomenclature of GSL fragments 57
3.4.2 Glycosidic fragments 59
3.4.3 Ceramide fragments 61
3.5 Conclusion and outlook 68
4. References 70

List of figures

Figure 1. Structures of the respective lipid categories [2] 2
Figure 2. Structural details and IUPAC-IUBMB nomenclature of a phosphatidylcholine (PC) species [3] 3
Figure 3. Overview of central sphingolipid metabolism [12] 5
Figure 4. Ceramide - Involvement in tumorigenesis processes and site of action of individual ceramide-associated drugs [18] 7
Figure 5. biosynthetic pathway of the glycosphingolipid series [30] 8
Figure 6. structure of Lactosylceramide (LacCer) and galactosylceramide (GalCer) [28] 8
Figure 7. GSL sugar structures of the blood group antigens [28] 9
Figure 8. structure of Gb3Cer and Gb4Cer [28] 10
Figure 9. structure of Globo-H (created with ChemDraw 21.0.0) 10
Figure 10 A. structure of GD3 34:1, B. ganglioside biosynthesis (adapted from Sibille et al. [33]) 11
Figure 11. overview of puplished papers for different GSL in the up- and downregulation of cancer [39] 13
Figure 12. overview of different analytical approaches in screening by Schymanski et al.[82] .. 19
Figure 13. differences in the data acquisition mode when measuring with a CID-MS/MS [88] . 20
Figure 14. TLC on ingredients of item number 29358 - Cayman Chemical Company[156] 23
Figure 15. TLC on ingredients of item number 29360 - Cayman Chemical Company[156] 23
Figure 16. TLC on ingredients of item number 29361 - Cayman Chemical Company[156] 24
Figure 17. progression of the gradient for the 23 minutes method 28
Figure 18. course of the running average gradient for the 23 minutes method 29
Figure 19. progression of the gradient for the 30 minutes method 30
Figure 20. course of the running average gradient for the 30 minutes method 31
Figure 21. table of transition list of the lipid-QC and the visualization by skyline 31
Figure 22. reproducibility comparison of the peakarea of the last 8 lipid QC measurements, created by Skyline 32
Figure 23. reproducibility comparison of the retention time of the last 8 lipid QC measurements 32
Figure 24. lipid class content of the LILY-Lipid-QC [83] 32

Figure 25. elution order of all studied GSL classes for d18:1_16:0 (d34:1 species) - positive mode, typical total ion current (TIC) chromatogram created using Freestyle 1.8 38
Figure 26. comparison and effects on retention time of different carbon chain lengths and double bonds in lactosylceramide species – positiv mode – created using FreeStyle 1.8 39
Figure 27. comparison of peakarea in the standard pool/HCT116 sample replicates for LacCer d34:1 41
Figure 28. comparison of retention time in the standard pool/HCT116 sample replicates for LacCer d34:1 41
Figure 29. new HESI-source positive method for LacCer analysis (created with Skyline) 47
Figure 30. new HESI-source negative method for LacCer analysis (created with Skyline) 47
Figure 31. origin HESI-source positive method for LacCer analysis (created with Skyline) 48
Figure 32. origin HESI-source negative method for LacCer analysis (created with Skyline) 48
Figure 33. origin HESI-source positive method for Gb4 analysis (created with Skyline) 49
Figure 34. new HESI-source positive method for Gb4 analysis (created with Skyline) 49
Figure 35. origin HESI-source negative method for Gb4 analysis (created with Skyline) 50
Figure 36. new HESI-source negative method for Gb4 analysis (created with Skyline) 50
Figure 37. comparison highest Peakarea origin/new method for LacCer analysis in standard pool 51
Figure 38. comparison highest Peakarea origin/new method for Gb4 analysis in standard pool 51
Figure 39. new method positive mode for LacCer analysis in HCT116 sample (created with Skyline) 52
Figure 40. comparison highest Peakarea origin/new positive mode method for LacCer analysis in HCT116 sample 52
Figure 41. new method positive mode for Gb4 analysis in HCT116 sample (created with Skyline) 53
Figure 42. comparison highest Peakarea origin/new positive mode method for Gb4 analysis in HCT116 sample 53
Figure 43. comparison Peakarea new method for d34:1/d42:1 species in HCT116 sample 54
Figure 44. distribution of GSL classes in standard pool and HCT116 sample 54
Figure 45. sections and nomeclature of the individual fragments of GSL with MS/MS 58
Figure 46. Structure and fragmentation behavior of LacCer d34:1 (d18:1/16:0) 62

Figure 47. MS2 spectrum of LacCer d34:1 (d18:1/16:0) in positive mode (spectrum created using Freestyle 1.8) 62
Figure 48. Structure and fragmentation behavior of Gb4 d42:1 (d18:1/24:0) 64
Figure 49. MS2 spectrum of Gb4 d42:1 (d18:1/24:0) in positive mode (spectrum created using Freestyle 1.8) 65
Figure 50. MS2 spectrum of Gb4 d42:1 (d18:1/24:0) in negative mode (spectrum created using Freestyle 1.8) 66

List of tables

Table 1. Differences of structural resolution [3] 3
Table 2. Structures of the Globo series [28] 10
Table 3. composition of eluent A for LC 22
Table 4. Composition of eluent B for LC 22
Table 5. calculated molar concentration of each standard 24
Table 6. used standard concentration for the method validation 25
Table 7. HCT116 cell conditions 26
Table 8. ESI-source settings for the Lipid QC 29
Table 9. Major GSLs in breast cancer tissues and paired peritumoral tissues [121] 36
Table 10. composition of Gb3 species in different cell lines [103] 37
Table 11. overview of the used parameters of the RP-HRMS/MS methods in negative mode 45
Table 12. overview of the used parameters of the RP-HRMS/MS methods in positive mode 46
Table 13. most occurring species of the researched GSL classes identified in the standard pool sample and the HCT116 cancer cell line using negative and positive ion mode 56
Table 14. Overview of the fragment calculation of the respective lipid class 60
Table 15. observed fragmentation in MS2 of LacCer d34:1 in positive mode (d18:1/16:0) ... 63
Table 16. observed fragmentation in MS2 of Gb4 d42:1 in positive mode (d18:1/24:0)..... 65
Table 17. observed fragmentation in MS2 of Gb4 d42:1 in negative mode (d18:1/24:0) 66

Selbstständigkeitserklärung

Ich erkläre eidesstattlich, dass ich die eingereichte Masterarbeit selbstständig angefertigt und die mit ihr unmittelbar verbundenen Tätigkeiten selbst erbracht habe. Ich erkläre weiters, dass ich keine anderen als die angegebenen Hilfsmittel benutzt habe. Alle aus gedruckten und ungedruckten Werken oder dem Internet im Wortlaut oder im wesentlichen Inhalt übernommenen Formulierungen und Konzepte sind gemäß den Regeln für wissenschaftliche Arbeiten zitiert und durch genaue Quellenangaben gekennzeichnet. Die eingereichte Masterarbeit ist noch keiner anderen Prüfungsbehörde vorgelegt worden. Ich bin mir bewusst, dass eine falsche Erklärung rechtliche Folgen haben wird.

Wien, Mai 2023 

Ort, Datum | Unterschrift

Acknowledgement

I would like to express my gratitude to a couple of people who provided me the possibility to complete my master's thesis as it is presented here.

First of all, I want to thank my supervisor Dipl.-Ing. Evelyn Rampler, Bakk.techn. PhD, who gave me the great opportunity to work in her analysis group at the faculty of chemistry at University of Vienna. Her insightful comments, valuable feedback, and continuous encouragement were essential in shaping my research and completing this thesis. I would also like to thank my co-supervisor Katharina Hohenwallner MSc, who provided great support and advise during the whole project. She was there for all kinds of questions and always took time to explain the devices and software in detail. They never hesitated to help me during my experimental work and were always open to discuss new ideas. Through them I got to know and to appreciate the fascinating science field of lipidomics. My sincere thanks also go to the rest of the Rampler and Köllensperger working group, who made every working day pleasant due to friendly talks and the constructive working atmosphere.

Last but not least, many thanks go to my family and my friends for their support during my whole studies and beyond.

Abstract

Glycosphingolipids (GSLs) are an important bioactive lipid group involved in many cellular processes and considered biomarkers for certain diseases. Despite their importance in diagnostics and research, numerous functional questions remain unanswered. In order to answer these questions and facilitate meaningful analysis of organic samples, the research discipline lipidomics uses liquid chromatography coupled to mass spectrometry. Proper matching of the method to the respective lipid class ensures desired separation and characterization.

The aim of this work was to develop a reversed-phase liquid chromatography and mass spectrometry method for the detection and interpretation of certain glycosphingolipid (GSL) classes in a GSL standard pool and to examine the selected lipids for their occurrence in a colon cancer sample (HCT116). In particular, three GSL subclasses were discussed: lactosylceramides, globosides (Gb3, Gb4, Globo-H) and gangliosides (GM3). For method validation, liquid chromatography was coupled with high-resolution tandem mass spectrometry and the spectra were recorded at the MS1 and MS2 levels. Furthermore, several electrospray ionization (ESI) source parameters were varied and checked for changes at the MS1 level for each lipid class.

The identification of lipid fragments at the MS2 level with FreeStyle[154] enables the precise assignment of individual lipids. With the help of a target list and Skyline[78], an overview of the lipid species could be created. The functionality of the method and separation of the GSL classes were presented and discussed in detail about polarity, retention times and analytical limits. The new method proved to be fit for purpose for GSL analysis in complex samples revealing structural details up to the molecular lipid species level. All GSL classes could be separated by the reverse phase chromatography and hydroxylated saturated long-chain fatty acids with a chain length of 38 carbon atoms were detected alongside very short-chain fatty acids with 2 carbon atoms, including odd FA chains. The investigated colon cancer sample revealed over 50 species in different levels in each GSLs class. The developed workflow was the first step towards a comprehensive assay for GSL classes by RP-MS/MS and could pave the way to a better understanding of GSL structures and their occurrence in cancer.

Kurzfassung

Glykosphingolipide (GSL) sind eine wichtige bioaktive Lipidgruppe, die in vielen zellulären Prozessen mitwirken und als Biomarker für bestimmte Krankheiten gelten. Trotz ihrer Bedeutung in der Diagnostik und Forschung sind noch zahlreiche Funktionsfragen offen. Um bestimmte Fragestellungen zu beantworten und eine aussagekräftige Analyse von organischen Proben zu ermöglichen, bedient sich die Forschungsdisziplin Lipidomik der Flüssigchromatographie und der Massenspektrometrie. Durch die richtige Abstimmung der Methode auf die jeweilige Lipidklasse kann eine gewünschte Auftrennung und Charakterisierung gewährleistet werden. Das Ziel der Arbeit war es, eine Umkehrphasen-Flüssigchromatographie (RP-LC) und Massenspektrometrie Methode zum Nachweis und zur Deutung bestimmter Glykosphingolipid Klassen in einem GSL-Standardpool zu entwickeln, sowie die ausgewählten Lipide auf das Vorkommen in einer Darmkrebs Probe (HCT116) zu untersuchen. Insbesondere wurde auf drei GSL-Unterklassen: Lactosylceramide, Globoside (Gb3, Gb4, Globo-H) und Ganglioside (GM3) näher eingegangen. Zur Methodenvalidierung wurde Flüssigchromatographie mit hochauflösender Tandem-Massenspektrometrie gekoppelt und die Spektren auf MS1 und MS2 Level untersucht. Des Weiteren wurden mehrere HESI (erhitzte Elektrospray-Ionisierung) Parameter variiert und auf die Veränderungen auf MS1 Ebene überprüft. Die Identifizierung von Lipidfragmenten auf MS2 Level mit Freestyle[154] ermöglichte die genaue Zuordnung von einzelnen Lipiden. Mithilfe von Skyline[78] und einer „Target“-Liste konnte eine definierte Übersicht, der in den Proben enthaltenen GSL erstellt werden. Die Funktionsweise der Methode und die Trennung der GSL-Klassen wurden vorgestellt und ausführlich über Polarität, Retentionszeiten und analytische Grenzen diskutiert. Die neue Methode erwies sich als geeignet für die GSL-Analyse in komplexen Proben, die strukturelle Details bis hin zur Ebene der molekularen Lipidspezies offenlegt. Alle GSL-Klassen konnten durch RP-LC getrennt werden und es wurden hydroxylierte gesättigte langkettige Fettsäuren mit einer Kettenlänge von 38 Kohlenstoffatomen neben sehr kurzkettigen Fettsäuren mit 2 Kohlenstoffatomen, einschließlich ungerader FA-Ketten, nachgewiesen. Die Untersuchung der Darmkrebsprobe ergab über 50 Lipid-Spezies in unterschiedlichen Konzentrationen in jeder GSL-Klasse. Der entwickelte Arbeitsablauf war der erste Schritt hin zu einem umfassenden Assay für GSL-Klassen mittels RP-MS/MS und könnte zukünftig den Weg zu einem besseren Verständnis der GSL-Strukturen und ihres Auftretens bei Krebs ebnen.

List of Abbreviation

ACN	Acetonitrile
AF	Ammonium formate
Cer	Ceramide
CerP	Ceramide 1-phospahte
DB	Double bond
d	Dihydroxylated
dd	Data dependent
ddMS2	Data-dependent-tandem MS
ESI	Electrospray ionization
FA	Formic acid
FAs	Fatty acyls
GalCer	Galactosylceramide
Gb3	Globotriaosylceramide
Gb4	Globotetrahexosylceramide
GC	Gas chromatography
GL	Glycerolipid
GlcCer	Glucosylceramide
GSL	Glycosphingolipid
Hex	Hexose
HexCer	Hexosylceramide
HESI	Heated electrospray ionization
HDL	High-density lipoprotein
HILIC	Hydrophilic interaction liquid chromatography
HPLC	High-pressure liquid chromatography
HR	High resolution
HR-MS	High resolution-mass spectrometry
IC	Ion chromatography
IPA	2-propanol
ISO	International Organization for Standardization
ISTD	Internal standard
IUPAC-IUBMB	International Union of Pure and Applied Chemists and the International Union of Biochemistry and Molecular Biology
LacCer	Lactosylceramide
LC	Liquid chromatography
LC-MS	Liquid chromatography coupled to mass spectrometry
LCB	Long-chain base
LDA	Lipid Data Analyzer
LDL	Low-density lipoprotein
LILY	Lipidome isotope labeling of yeast

m/z	Mass-to-charge
MeOH	Methanol
MIT	Maximum (ion) injection time
MRM	Multiple reaction monitoring
MS	Mass spectrometry
MS1	Full MS
MS^n	Multi stage mass spectrometry
MTBE	Methyl-tert-butyl ether
NIST	National Institute of Standards & Technology
NP	Normal-phase
NMR	Nuclear magnetic resonance
PC	Phosphatidylcholine
PRM	Parallel reaction monitoring
Q	Quadrupole
QC	Quality Control
RI	Retention index
RP	Reversed phase
RT	Retention time
S1P	Sphingosine 1-phosphate
SM	Sphingomyelin
SP	Sphingolipid
SPE	Solid phase extraction
t	Trihydroxylated
TLC	Thin layer chromatography
(U)HPLC	(Ultra) high performance liquid chromatography

1. Introduction

1.1 Lipidomics research

Lipidomic research focuses on studying all lipids found in cells, tissues and organisms, using numerous instrumental analysis techniques to identify and interpret them. It is an integral part of systems biology, which focuses on the broad study of complex interactions of substances in biological systems. The ultimate goal is to develop a comprehensive omics science that includes genes, transcripts, metabolites and proteins for the identification of specific biomarkers for lipid-related diseases and for diagnostics.[1]

Lipids are nowadays classified into eight large lipid groups (glycerophospholipids, glycerolipids, saccharolipids, prenols, sterols, polyketides, fatty acycls and sphingolipids), which are visible in Figure 1. The further classification schemes of the individual subgroups are based on the different hydrophobic and hydrophilic elements of a lipid.[2]

Lipids have diverse and unique structures and encode for many different functions in an organism. They play an essential role in signaling, transport and inflammation of body processes. The combination of head groups, linkages and non-lipid units (e.g. proteins or carbohydrates) results in numerous structural possibilities, which possess specific chemical functions. An important aspect of the biological properties of lipids is also their isomers. The absence or presence of a double bond at a specific position can influence the lipid's functionality.[3]

Researchers have shown through conjugated linoleic acid isomers that the trans-11 isomer, in contrast to cis-9 isomers, inhibits tumor development in vitro. Moreover, the trans-10 and cis-12 isomers increased human blood lipid concentration and the ratio of HDL to LDL cholesterol, compared to cis-9 and trans-11 isomers.[4,5]

The matter of lipid nomenclature was taken up by the Commission on Biochemical Nomenclature of the International Union of Biochemistry and Molecular Biology (IUPAC-IUBMB) in 1976. The structural description of a phosphatidylcholine (PC) species is shown in Figure 2. To classify newly discovered lipid classes and support the growing field of lipidomics research, the International Lipid Classification and Nomenclature Committee (ILCNC) developed a "Comprehensive Classification System for Lipids," which was published in 2005

from Fahy et al.[2] In order to include eukaryotic and prokaryotic lipid structures, the classification system was updated in 2009 from Fahy et al.[6] In addition, a description for structures of complex MS-lipid data was introduced in 2013 from Liebisch et al.[7] Based on this classification, Koelmel et al. systematically characterized high-resolution MS data with exact mass and fragmentation patterns.[3] The details of the structural resolution and annotation is listed in Table 1.

The LIPID MAPS database (LMSD) serves as the most current and comprehensive catalog of lipid molecules, containing over 40,000 lipids, as well as systematic nomenclature, classification, structural representations and ontology of lipids along with mass spectrometric characterization.[8]

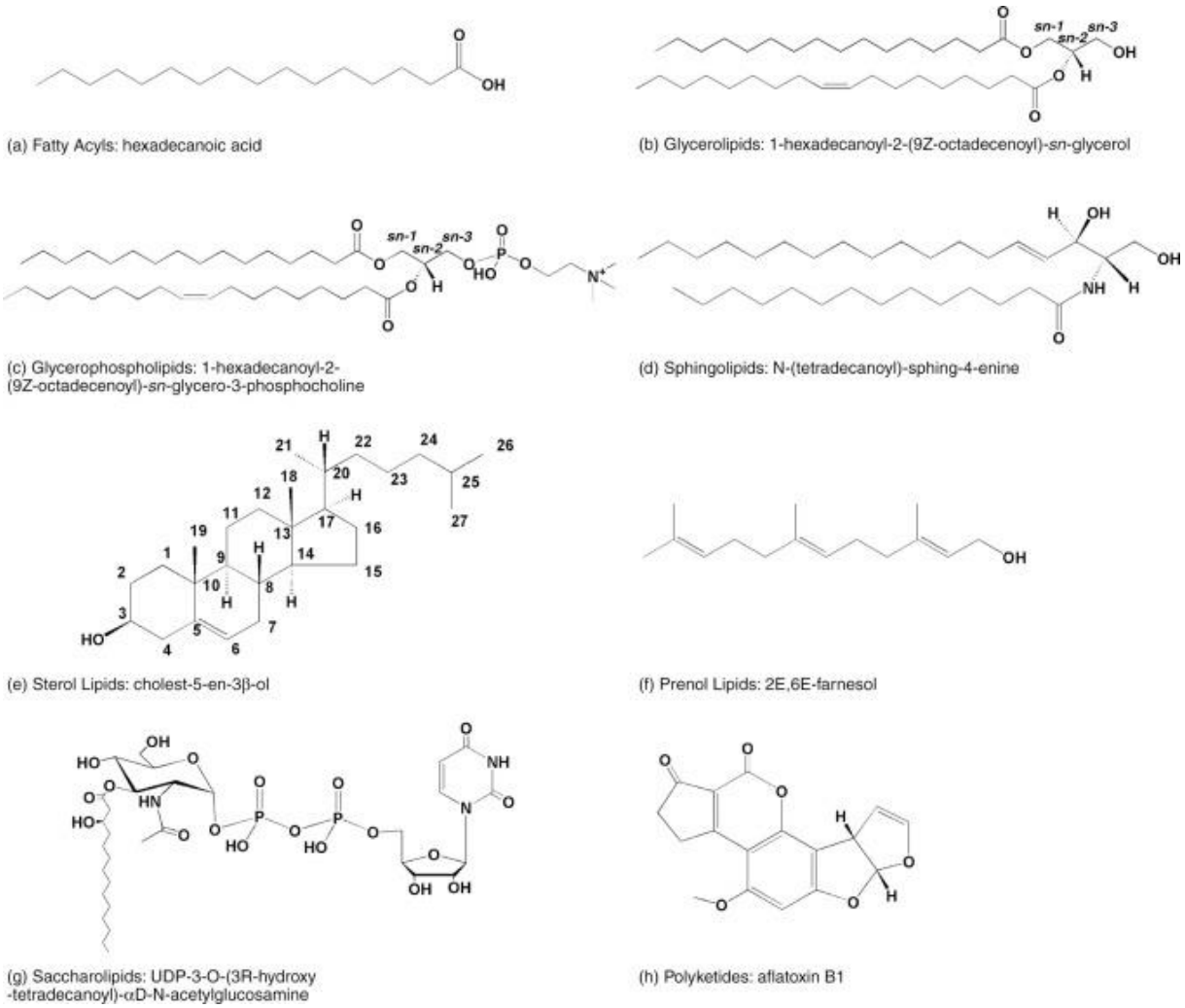

Figure 1. Structures of the respective lipid categories [2]

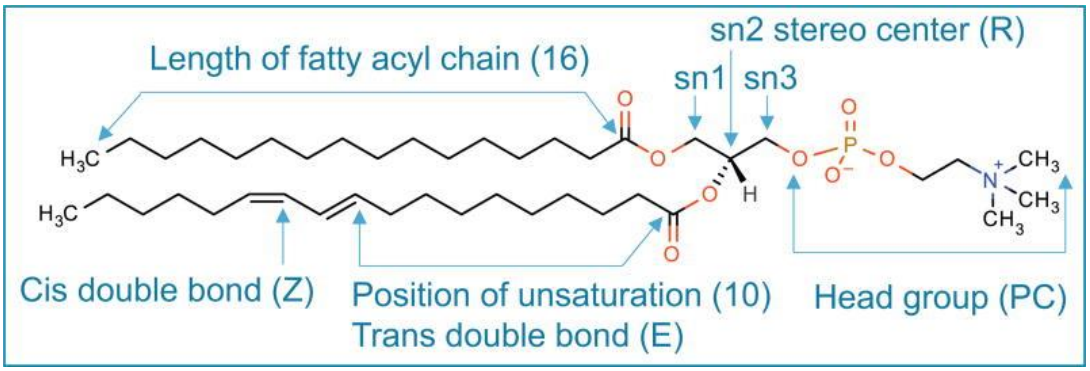

Figure 2. Structural details and IUPAC-IUBMB nomenclature of a phosphatidylcholine (PC) species [3]

Structural resolution	Annotation
Carbons and double bonds	PC(34:2)
Fatty acyl constituents	PC(16:0_18:2)
Positional isomers	PC(16:0/18:2)
Double bond position	PC(16:0/18:2(10,12))
Double bond Cis/Trans	PC(16:0/18:2(10E,12Z))
Stereochemistry	PC(16:0/18:2(10E,12Z)[R])

Table 1. Differences of structural resolution [3]

The MS lipid structure nomenclature is based on the classification of lipids according to their class and the molecular sum formula of carbons and double bonds in fatty acyl chains. From a technical perspective, only one fatty acyl chain is necessary to designate fatty acyl chains/fragments since the exact mass can be used to deduce the second. However, incorrect assignments could occur when annotating by lipid class, since certain fragments are not specific to only one lipid class. An underscore is used to describe unknown positional isomers, as many instrumental methods do not reveal precise double bond positions. The slash represents lipids where the isomeric level of the fatty acyl chains is known. Depending on the instrumental method, an exact assignment of double bond position isomers is also possible. A correct and generalized nomenclature of lipid structures is crucial to present new findings in the field of lipidomic accurately.[3]

1.2 Sphingolipids

The sphingolipids are one of the eight lipid classes and have different biological meanings. They can be found in different areas of the organism and play an important role in signal transmission, the regulation of numerous cell functions and as a structural component. Due to their unique structure, they were named after the "Sphinx" and have both hydrophobic and

hydrophilic properties. All sphingolipids consist of a sphingoid base (phytoceramide or sphinganine) attached to a fatty acid, also known as a long-chain base.[9]

Sghingosine-1-phosphate (S1P) and ceramide play the key roles. S1P is an antiapoptotic regulator, which is important for cell proliferation and motility.[10] On the other hand, ceramide promotes cell death by activating mitochondrial permeabilization. This releases caspases into the cell interior and initiates apoptosis.[11] In addition, numerous enzymes (sphingosine kinases, S1P phosphatases, ceramide synthases, ceramidases) are involved in the regulation of sphingolipid levels and serve as extra- and intracellular agonists.[12] Certain changes in sphingolipid balance can have adverse pathological implications. Chronic dysregulations can lead to neurodegeneration, cancer, Alzheimer's disease, Parkinson's disease and lysosomal storage diseases.[13]

Ceramide

Ceramide is an precursor molecule in the metabolism of sphingolipids, which has regulatory properties within the cell such as the initiation of apoptosis, differentiation and growth inhibition. Ceramide biosynthesis can be occurred from the de novo pathway or the sphingomyelinase pathway.[12] In the de novo pathway, serine and palmitate-CoA are used to synthesize ceramide through the actions of serine palmitoyl transferase and ceramide synthase.[14, 15] Sphingomyelin (SM) or glycosphingolipids (GSL) are generated from ceramides in the organism (sphingomyelinases and glycosylceramidases) and are partially used as a membrane compartment.[12] Moreover, ceramide can be converted into sphingosine, which can be phosphorylated to form S1P. Ceramides, sphingosine, and S1P can be interconverted by specific phosphatases, synthases, and kinases.[16] The central sphingolipid metabolism is shown in Figure 3 and gives a short overview of the most important reactions.

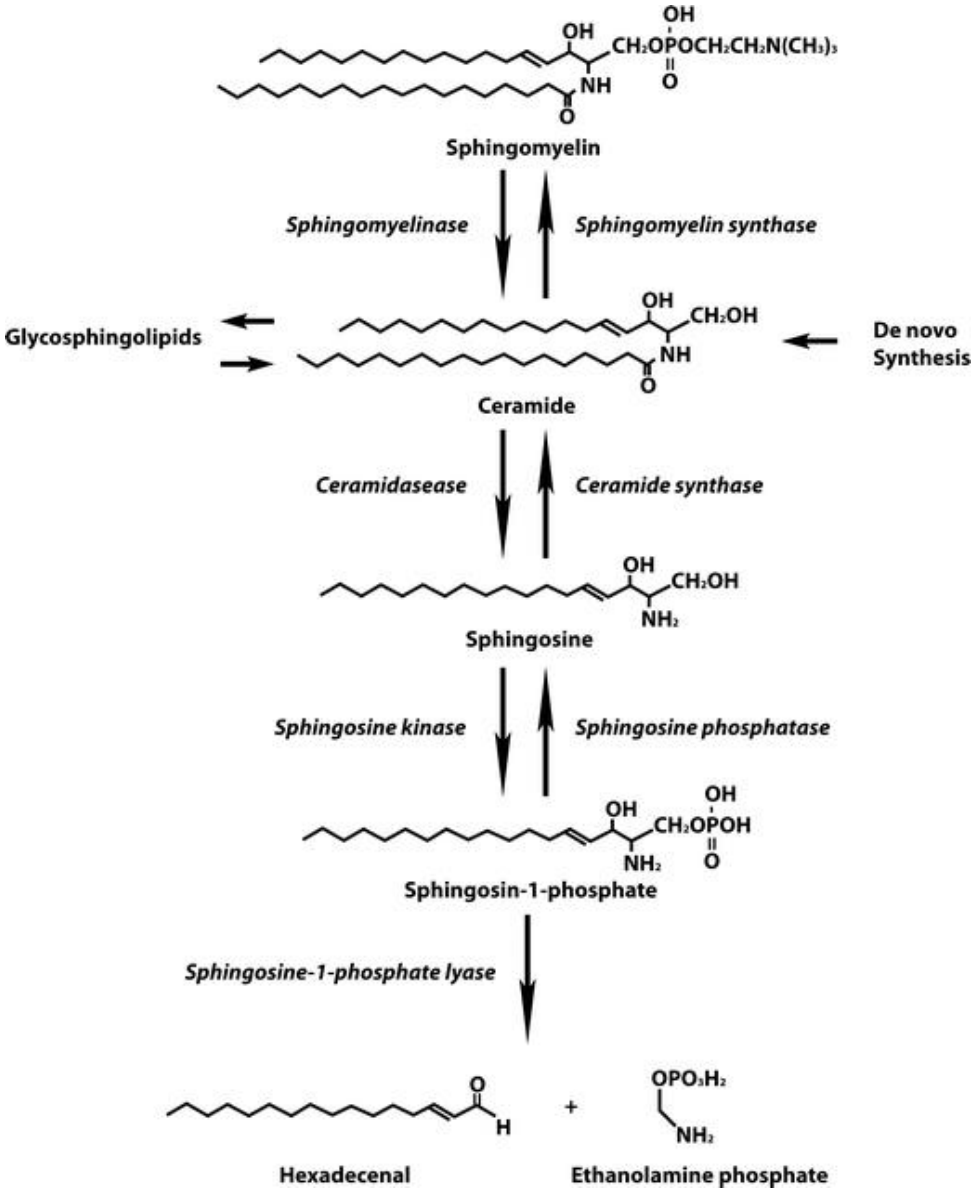

Figure 3. Overview of central sphingolipid metabolism [12]

Involvement of ceramide/sphingolipid in carcinogenesis and treatment

Sphingolipids play a crucial role in the multistep process of carcinogenesis and are strongly interconnected in the metabolic network, contributing to normal cell function. Specific mutations in tumor suppressor genes and oncogenes can result in alterations to sphingolipid levels.[17] Modified sphingolipids are involved in cell metastasis, progression and proliferation in certain cancer types. Therefore, developing activators and inhibitors of sphingolipid translation is an important approach for anticancer drug development.[18]

Ceramides, through their cell stress responses, play an important role in cancer biology and are involved in abnormalities in sphingolipid signaling in various cancers. Attenuated ceramide levels or increased S1P levels are correlated with the stages of cancer pathogenesis.[19]

The enzyme acid ceramidase, which converts ceramide to sphingosine, may play a role in prostate cancer development, as it is overexpressed in 60% of primary prostate cancer tissues.[56] Another study found that elevated levels of C16:0-Cer were associated with positive lymph node status, suggesting that certain ceramide analogues have the potential to be used as therapy for chemo- and endocrine-resistant breast cancer.[20] In the case of head and neck squamous cell carcinoma (HNSCC) carcinogenesis, a study showed that ceramide may be one of the important substrates for its development.[21]

Drugs affecting ceramide levels

The drug fenretinide has shown antitumor activity in vitro and in vivo in several tumor types, without toxicity in mice in preclinical studies. It decreases de novo synthesis of ceramide by binding to dihydroceramide desaturase (DES). This leads to an increase in dihydroceramide levels, which induces autophagy and inhibits cell growth of cancer cells.[22]

The glycosphingolipid α-GalCer (KRN-7000, α-galactosylceramide-pulsed antigen-presenting cells) is a synthetic, invariant, and natural killer T-cell ligand. Dendritic cells are enriched with the glycosphingolipid, capture antigens and activate multiple types of T cells for their antitumor effects.[23]

Safingol ((2S, 3S)]-2-aminooctadecane-1,3-diol) serves as an inhibitor and affects the ceramide/dihydroceramide ratio. This results in a signal inhibitory effect and induces apoptosis.[24]

Fingolimod, also known as FTY720 or Gilenya (2-amino-2-[2-(4-octylphenyl)ethyl]propane-1,3-diol) is a structural analogue of sphingosine and a functional antagonist of the sphingosine-1-phosphate receptor (S1PR). The internalization of S1PR induced by Fingolimod results in the sequestration of T lymphocytes in lymph nodes.[18,25] One potential anticancer mechanism is its ability to limit the conversion of sphingosine to S1P.[26] The ceramide and drug specific involvement in tumorigenesis processes and the site of action is visible in the Figure 4.

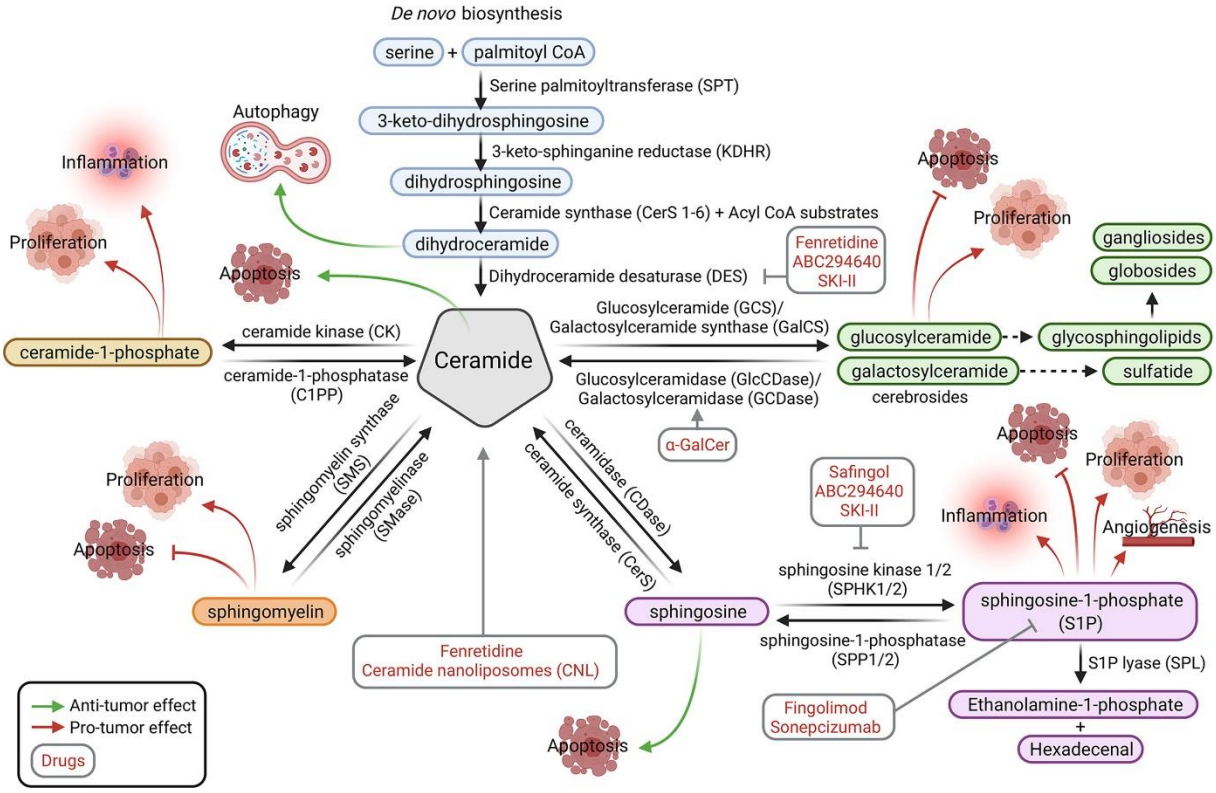

Figure 4. Ceramide - Involvement in tumorigenesis processes and site of action of individual ceramide-associated drugs [18]

1.3 Glycosphingolipids (GSL)

GSL are constructed by a ceramide backbone attached to at least one sugar unit. In an organism simple or more complex sugar head groups are added stepwise and bound to their activated nucleotide precursor. It is assumed that GSL are not freely bound on the cell surface but form a membrane complex together with proteins (glycosylphosphatidylinositol), sphingomyelin and cholesterol.[27] Different GSLs have different functions in the organism depending on their localization. Monoglycosylceramides (cerebrosides) are present in epithelial cells of the human intestine. Di-, tri-, and tetraglycosylceramides are used in more complex compounds for the characterization of blood group antigens.[28] In the plasma membrane, GSLs are important protagonists in infectious diseases as receptor/co-receptor for bacteria, toxins and viruses.[29]

GSLs are categorized based on their sugar residues and charge (neutral or acidic), as well as their chain lengths and double bonds within the fatty acid chains. Based on these characteristics, several GSL series result, which exhibit a great diversity in their function through their sugar residues, as shown in Figure 5.[30]

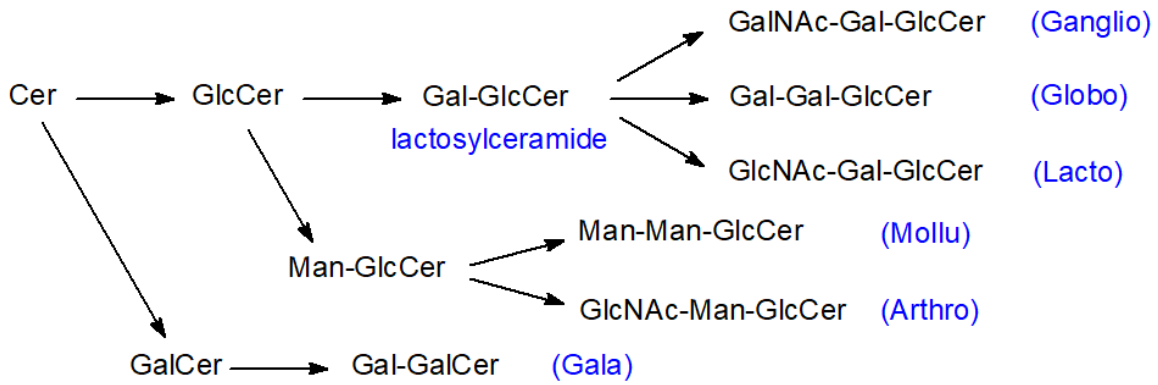

Figure 5. biosynthetic pathway of the glycosphingolipid series [30]

The three neutral glycosphingolipids: glucosylceramide (GclCer), galactosylceramide (GalCer) and lactosylceramide (LacCer) often serve as biological precursors of more complex structures. GlcCer and GalCer are referred to as cerebrosides and have a monosaccharide head group attached to the ceramide. Binding of a galactose unit via a β-1,4-glycosidic bond gives LacCer, which is the major lipid for all larger and important GSLs. [13]

Acidic glycosphingolipids are surrounded by a negative charge and are divided into the four categories: Gangliosides (one or more sialic acid groups), Glucuronglycosphingolipids (glucuronic acid moiety), Sulfatoglycosphingolipids (sulfate group), and Phosphoglycosphingolipids (phosphate group). [13] The remaining GSL series are mostly present as neutrally charged molecules.

1.3.1 Lactosylceramide

Lactosylceramide serves as a precursor in the biosynthesis of most GSLs in higher animals. In this molecule, lactose is beta-glycosidically bound to the 1-hydroxyl group of the ceramide. In addition, the Gala series with galactose as the sugar part is an exception (β-galactosylceramides).[28] The structure of LacCer and GalCer are shown for a better illustration in Figure 6.

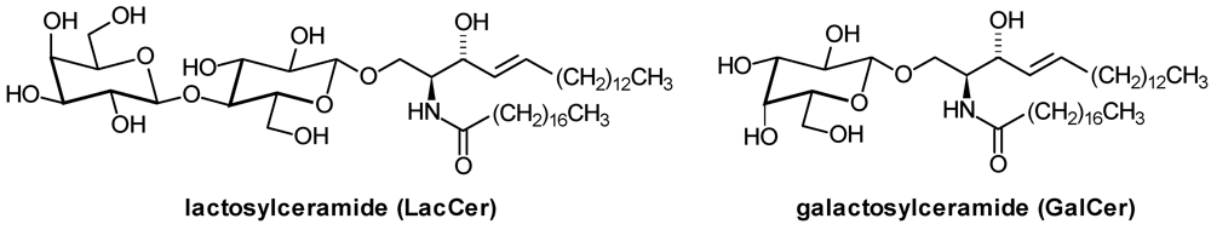

Figure 6. structure of Lactosylceramide (LacCer) and galactosylceramide (GalCer) [28]

1.3.2 Globoside

Globosides are neutral glycosphingolipids in which N-acetylgalactosamine (NAG) is present along with two or more monohexoses, including glucose and galactose. The triose Gb3 is abundant on the cell membrane of mammalian tissue cells (e.g. erythrocytes) and has a specific binding affinity toward certain toxins (Gb3 serves as a receptor for verotoxins and shiga toxins).[29] Furthermore, Gb3 is a component in apoptosis because it interacts with the Fas (CD95) receptor. IGb3 differs from Gb3 in its glycosidic binding and is an antigen for natural killer T cells. In the context of ganglioside GM2, Gb4Cer has been identified as an important storage substance in Sandhoff disease (β-hexosaminidase-β-subunit deficiency).[28] Forssman GSL has been characterized as a blood group antigen in humans and is present in combination with other Globo series in the kidney.[31] Gb5 is known as a cell surface marker and is used to define human embryonic stem cells.[28] Globo-H, which is rather less studied, has been detected in mesenchymal stem cells in umbilical cord blood.[32] Gb3 and Gb4 are the starting point for the precursor molecules of the blood group antigens, which end after the whole biosynthesis process with a fucose in the sugar chain.[28] An short overview of the GSL structures for the blood group antigens is shown in Figure 7 and shows the importance of globosides for the formation of the human blood group system. Globosides are different from gangliosides from their lack of N-acetylneuraminic acid (NANA). For a better understanding, the globo-series is listed in Table 2 and the globosides studied in this project are shown in Figure 8 and Figure 9.

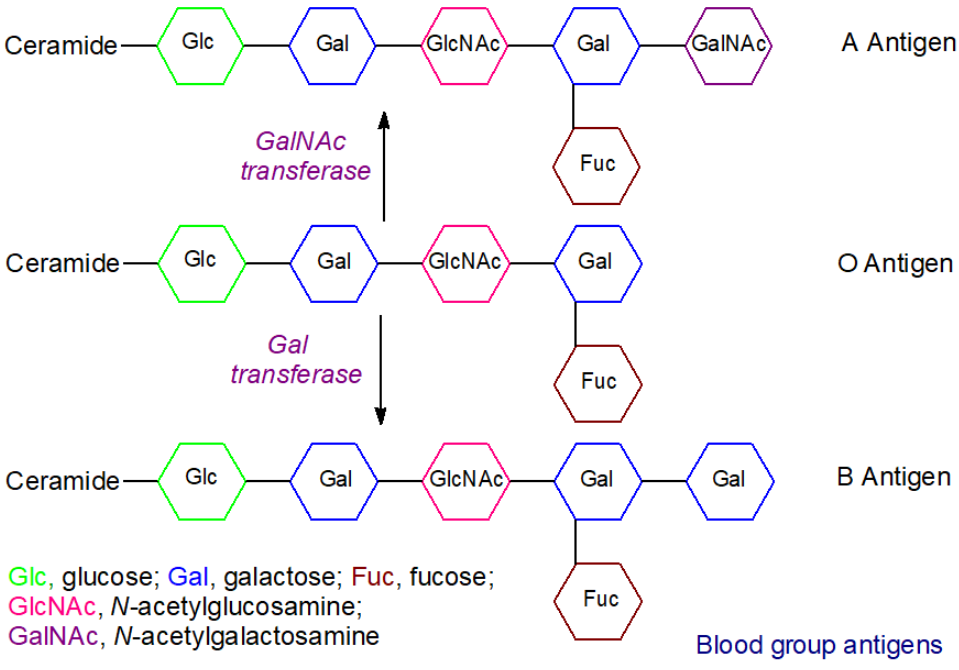

Figure 7. GSL sugar structures of the blood group antigens [28]

Structures of the Globo series

Galα4Galβ4Glcβ1Cer	GB3
Galα3Galβ4Glcβ1Cer	Iso-Gb3
GalNAcβ3Galα4Galβ4Glcβ1Cer	GB4
GalNAcβ3Galα3Galβ4Glcβ1Cer	Iso-Gb4
GalNAcα3GalNAcβ3Galα4Galβ4Glcβ1Cer	Forssmann
Galβ3GalNAcβ3Galα4Galβ4Glcβ1Cer	Gb5 (SSEA-3a)
Fucα2Galβ3GalNAcβ3Galα4Galβ4Glcβ1Cer	Globo-H (SSEA-3b)
SAα3Galβ3GalNAcβ3Galα4Galβ4Glcβ1Cer	Monosialyl-Gb5 (SSEA-4)
SAα3Galβ3GalNAc6SAα2β3Galα4Galβ4Glcβ1Cer	Disialyl-Gb5

Table 2. Structures of the Globo series [28]

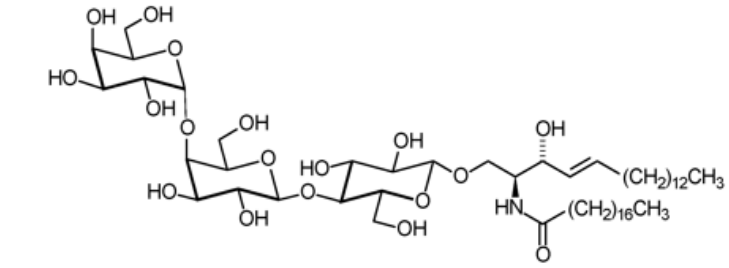

Globotriaosylceramide (Gb3Cer)

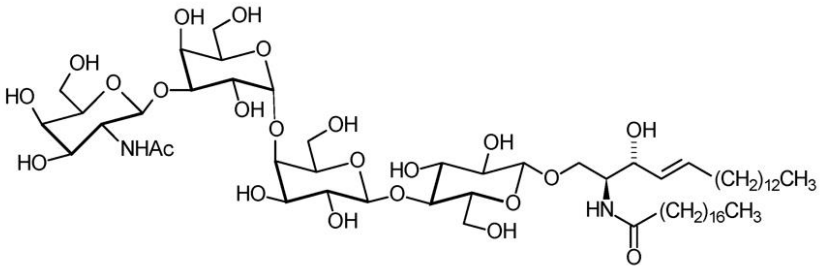

Globotetraosylceramide (Globoside; Gb4Cer)

Figure 8. structure of Gb3Cer and Gb4Cer [28]

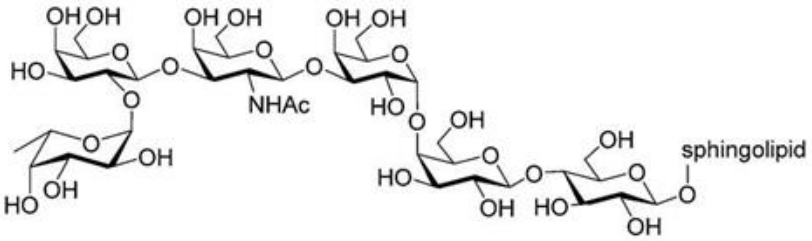

Figure 9. structure of Globo-H (created with ChemDraw 21.0.0)

1.3.3 Ganglioside

Acidic glycosphingolipids containing one or more sialic acid residues (N-acetylneuraminic acid or sialic acid) in their carbohydrate moiety are specifically referred to as gangliosides. Gangliosides are among the larger groups of glycosphingolipids and are found in many human tissues and fluids. They play a critical role in the maintenance, development and function of the nervous system. Therefore, they are found primarily in the peripheral nervous system, retina, and brain.[33] Their structural feature is the sialic acid units. Due to the variability of the carbohydrate unit, gangliosides are divided into several groups and are mostly found in the outer plasma membrane of neurons. The sugar unit of the molecule extends into the cytoplasm and the ceramide backbone is anchored in the cell membrane. Both the different number and variability of carbohydrate bonds, as well as chain lengths, number/position of double bonds, and hydroxylation, contribute to the diversity of gangliosides.[34]

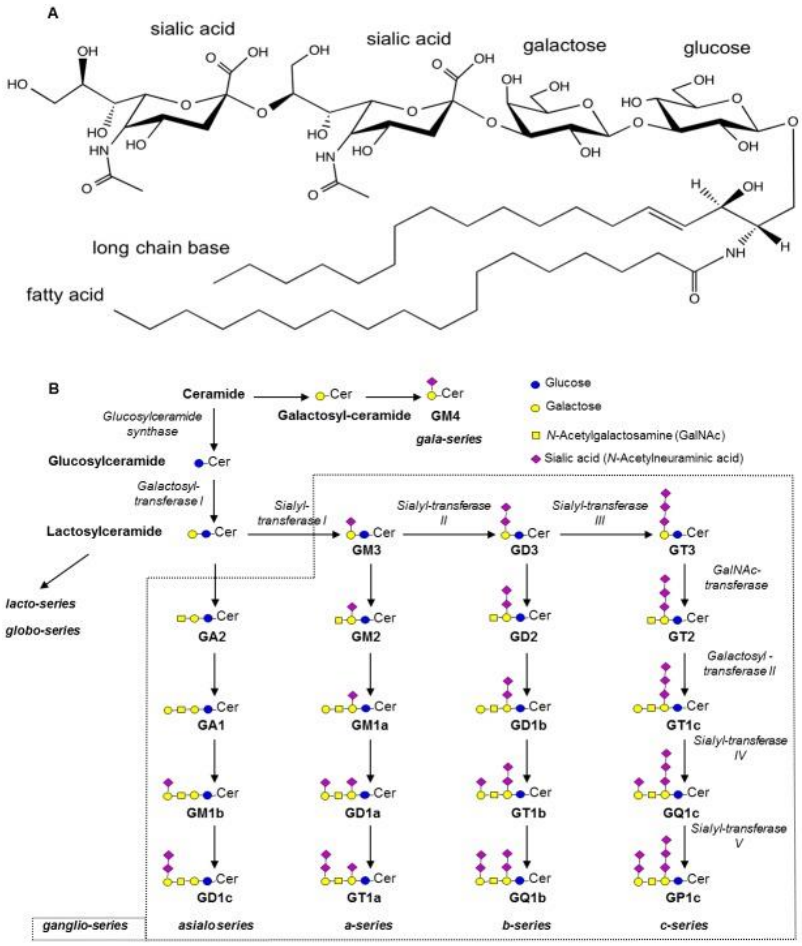

Figure 10 A. structure of GD3 34:1, B. ganglioside biosynthesis (adapted from Sibille et al. [33])

The symbols in Figure 10 are corresponding to the nomenclature by Schnarr et al.[35] and as example is the structure of GD3 34:1 shown. Gangliosides are acidic glycosphingolipids containing one or more sialic acid residues (N-acetylneuraminic acid or sialic acid) in their carbohydrate moiety. They are classified into the asialo a-, b-, c-series, depending on the number of sialic acid residues attached to the galactose residue. Except for GM4, which is built up from galactosylceramide (GalCer), the gangliosides are biosynthesized from lactosylceramide (LacCer). The respective addition of the respective sugar and sialic acid results in the classes shown above. In addition, gangliosides with sialic acid residues are classified with N-acetylgalactosamine binding with α.[33, 36] The general nomenclature is based on the description of Svennerholm et al. as accepted by IUPAC-IUB from Chester et al.[35] The first letter G stands for gangliosides, the second letter for the number of sialic acids ("A" = 0, "M" = 1, "D" = 2, "T" = 3, "Q" = 4, "P" = 5), and the third letter for the number of neutral sugars (5-n sugars).

To find out more about the biological function and effect of sphingolipids and glycosphingolipids in particular, liquid chromatography-tandem mass spectrometry (LC-MS/MS) based methods are commonly used. It is currently an accurate tool for simultaneous structure-specific investigation and quantitative measurement of these lipid compounds. LC-MS/MS methods offer high sensitivity, low detection limits, quantitative precessions and high sample throughput rates. The combination of fragmentation workflow with high resolution mass spectrometry enables potential isomer specific analysis. The use of different LC phases (such as normal, reversed phase) and several solvent compositions lead to a better separation of isobaric and isometric species. [37]

1.3.4 Impact of GSLs on cancer development

Cancer is an uncontrolled proliferation of malignant cells (carcinomas, sarcomas), which in almost all cases has a negative impact on the health of the organism. The typical proliferation and metastasis to other tissue areas results in a process that is sometimes difficult to stop and if left untreated, very often leads to the death of the affected organism. In principle, a healthy organism exhibits a balanced equilibrium in the formation and regeneration of cells (homeostasis). In addition, the induction of programmed cell death (apoptosis) helps to maintain the balance between cell death and growth. [38]

Due to certain mutations/gene defects, growing cancer cells do not receive inhibitory signals that could prevent them from initiating this process. Cancer is thus the result of mutations of individual genes involved in differentiation and growth. In addition to cancer-causing substances that enter the body through the environment, genetic predispositions and metabolic changes within cells can lead to these mutations in the genome. Since GSLs play an important role in the maintenance of many physiological processes in cell, abnormalities in GSL levels may have different consequences in tumor development. This finding has been investigated in many studies and promising results on GSLs related to different types of cancer have been elaborated. Figure 11 shows the influences of changes in GSL in the up- and downregulation of cancer, as published in various studies. [38]

Cancer	Upregulation or promotion	Downregulation or inhibition
Breast	**GD2** and/or **GD3** (Cazet et al., 2010, 2012; Battula et al., 2012; Liang et al., 2013; Lin et al., 2014; Sarkar et al., 2015) **ST8SIA1** (Ruckhaberle et al., 2009; Liang et al., 2017) **Gb5** (Cheung et al., 2016) **GD1α** (Bos et al., 2009; Vandermeersch et al., 2015; Drolez et al., 2016)	**GD1b** (Ha et al., 2016) **Gg4** and **B3GALT4** (Guan et al., 2009, 2010; Guo et al., 2015)
Lung	**Gb3** (Tyler et al., 2015) **GM2** (Yamada et al., 2011) **NeuGcGM3** (Hayashi et al., 2013; Alfonso et al., 2014; Piperno et al., 2015; Palomo et al., 2016)	**α-GalCer** (Hasegawa et al., 2014; Ando et al., 2015; Ito et al., 2015; Yamashita et al., 2016) **GALC** (Peng et al., 2015)
Colorectal	**Gb3** (Distler et al., 2009) **Gb4** (Park et al., 2012) **GCS** (Haynes et al., 2012) **NEU3** (Shiozaki et al., 2009; Yamaguchi et al., 2012; Mozzi et al., 2015; Takahashi et al., 2015)	**GD1a** and **GM1** (Kwak et al., 2011) **α-GalCer** (Yoshioka et al., 2012; Dong et al., 2016) **GM3** (Chung et al., 2014)
Melanoma	**NeuGcGM3** (Tringali et al., 2014) **d-GM3** (Yan et al., 2013) **GD2** and **GD3** (Furukawa et al., 2014; Dobrenkov et al., 2016; Gargett et al., 2016; Kaneko et al., 2016; Makino et al., 2016) **B4GalT5** (Shirane et al., 2014)	**α-GalCer** (Neumann et al., 2015; Albertini et al., 2016)
Leukemia	**NeuGcGM3** (Fernandez-Marrero et al., 2011; Casadesus et al., 2013) **GCS** (Watters et al., 2013; Wang et al., 2014) **Lc3**, **GM3**, and **nLc4** (Wang et al., 2012)	**α-GalCer** (Weinkove et al., 2013) **GM3** (Jin et al., 2014; Delannoy et al., 2017) **GlcCer** (Schwamb et al., 2012)
Prostate	**GD1a** and **SPG** (Hatano et al., 2011, 2012) **sialyl-Gb5** (Sivasubramaniyan et al., 2015; Hofner et al., 2016) **LacCer** (Skotland et al., 2017) **Gg4** (Van Slambrouck et al., 2009, 2014)	**DSGb5** (Shimada et al., 2014)
Ovarian	**P1** (Jacob et al., 2014) **GD3** (Webb et al., 2012)	**GM3** (Prinetti et al., 2011)
Renal	**GM3** (Lin et al., 2012) **DSGb5** (Kawasaki et al., 2015) **LacCer** (Chatterjee et al., 2013)	**GlcCer** (Chatterjee et al., 2013)
Bladder	**GCS** (Sun et al., 2012)	**GM3** (Wang et al., 2013)
Gastric	**Gb3** (Geyer et al., 2016)	

Figure 11. overview of puplished papers for different GSL in the up- and downregulation of cancer [39]

The expression of Globotriaosylceramide (Gb3) is increased in Hsp70 membrane-positive tumor cells [40] und in human breast carcinoma compared to normal tissue. [41] Further Gb3 is a potential marker and target for neck and head Cancer.[42] High levels of Gb3 expression had an impact on the acquisition of cisplatin resistance in non-small cell lung cancer cells.[43] Gb4 enhanced activation of MAPK/ERK signal transduction in HCT116 human colorectal carcinoma cells through direct interaction with EGFR.[44] Recent research has shown that Globo-H suppresses immune function in breast cancer cells.[45] Antibodies against Gb3, Gb4 and Globo-H have been successfully used as antitumor agents. In addition, their corresponding vaccines represent a promising approach for cancer immunotherapy.[46]

A high level of ganglioside GD3 expression in lymphoid T-cell leukemia and melanoma and GD2 in breast cancer, neuroblastoma and small cell lung cancer was confirmed.[47] In particular, the sialic acid structures of GD3 and GD2 enhance the malignant properties of cancer cells. [48,49] However, monosialylgangliosides (GM1, GM2, and GM3) can also suppress the malignant properties of cancer cells.[50,51] Some of these functional approaches may yield antibody vaccines, such as ractotumomab against NeuGcGM3, which can prolong the life of lung cancer patients.[52]

In healthy human tissues, GM3 is typically found, but numerous human tumors display the N-glycolylated ganglioside NeuGcGM3. As NeuGcGM3 is selectively expressed in tumor cells, it holds significant potential as a target for immunotherapy, particularly via the racotumomab alum vaccine [53] oder des rekombinanten monoklonalen Antikörpers 14F7.[54] Upregulated GM3 expression during differentiation of human acute monocytic leukemia THP-1 cells into macrophages was shown from Delannoy et al.[55]

Aim of the project

The aim was to develop a comprehensive glycosphingolipid LC-MS/MS method for the analysis commercially available GSL standards. As a proof of principle, colon cancer cell samples were screend for GSLs. Additionally, a selected panel of the GSLs found were assigned based on their fragmentation by interpretation of MS2 spectra. To cover many chemical properties of these lipid structures, five specific GSL classes were selected for method development based on their literature references to their molecular structure and carcinogenesis.

2. Material and methods

2.1 Requirements for sample and standard preparation

At the beginning of each lipidomics workflow, the respective samples/standards are prepared for analysis. The low stability of lipids must be taken into account when collecting and storing lipid sample material. Improper handling or storage may lead to degradation of lipid structures by oxidation, peroxidation, or hydrolysis. In addition, possible enzymatic activity must be prevented when testing and storing organic material, which can also lead to lipid degradation. Therefore, it is recommended to store samples in sealed containers and at very low temperatures (-80°C) to ensure stability.[57, 58]

Depending on the starting material and sample composition, different methods are used for lipid extraction. The two most common methods are the classical liquid-liquid extraction for rough overview measurements and the solid phase extraction for targeted lipid analyses. Other solvent systems are used for lipid extraction due to the non-polar lipid structures, unlike metabolite extraction.[59]

The best-known lipid extractions include Folch method [60], which is based on extraction with the solvents methanol and chloroform (2:1, v/v), and Bligh-Dyer method [61], which also uses methanol and chloroform. However, in a different ratio (1:2, v/v). The methods have been adapted over the years to the specific lipid classes and the sample material at hand. Since chloroform has a higher toxicity and requires a complicated sample handling process (removal of aqueous phase due to higher density), solvent alternatives were sought. Besides ethyl acetate [62] hexane [63] and isopropanol [64], methyl tert-butyl ether (MTBE) [65] was established as a common solvent choice. The MTBE method was shown to be more efficient than the Folch extraction method in comparative studies.[66] It was illustrated that the choice of solvent has a rather lower effect on the extraction of major lipid classes, but may have higher effect on minor lipid classes (ceramides). Therefore, it is more reasonable to choose solvents depending on the analytical problem and lipid class.

2.2 Lipid based Liquid chromatograhy

There are currently two main methods available in mass spectrometry for studying a lipidome. The shotgun lipidomics method is used for direct infusion of samples into the MS and liquid chromatography (LC) is used for pre-separating samples with a column before injection.

Coupling a liquid chromatography with a mass spectrometer can offer many advantages. Column separation gives us a chromatographic selectivity that can be used to identify substance classes based on the obtained parameters. The chemical interactions of the analytes with the stationary phase and mobile phase gives an overview of the distribution of each sample and is well suited for assigning lipid classes.[67]

Specific separations of substances are possible through the use of a suitable separation column and the correct adjustment of the eluent. The most common systems are: normal-phase liquid chromatography (NP-LC), hydrophilic interaction liquid chromatography (HILIC) and reversed-phase liquid chromatography (RP-LC).[68] Each design has its own areas of application, as well as advantages and disadvantages. Lipids are amphiphilic, meaning they have both hydrophobic and hydrophilic components. Regarding in lipid analysis, NP-LC is based on polar interactions between lipids and the typically column is unmodified silica with free silanol groups. The HILIC is an alternative to NP-LC and is generally suitable for hydrophilic and amphiphilic analytes. Normal phase or HILIC methods can separate lipids based on their hydrophilic properties, which allow the lipid class separation based on head-group specificity.[69] The most commonly used separation column in lipidomics is RP-LC. They separate lipid classes and fatty acyl isomers based on their carbon number and the number of double bonds in the fatty acyl chains.[67] By combining lipid fragment information with chromatographic selectivity and retentivity, less confusing lipid identifications are made achievable. The reduced ion suppression by the separation of other analytes and contaminants help to increase lipid sensitivity.[70] Throw the analysis with LC also a better separation of isobaric and isomeric lipids is possible. Liquid chromatography has wide applications in various fields to address lipidomics tasks. There are also some other separation chromatography methods for lipids, which are characterized by their separation technique: two-dimensional liquid chromatography (2D-LC), supercritical fluid chromatography (SFC) and gas chromatography (GC).[71]

Multiple reviews, including Liebisch et el. from 2017 [72], have highlighted the challenge of distinguishing between lipid species and their non-endogenous internal standards during separation. Reversed phase (RP) separation results in different matrix effects and solvent compositions of the internal standard and analyte, a change in ionization efficiency may occur. Therefore, RP separation should aim to minimize ion suppression by separating lipid species while maintaining similar retention times for internal standards and all lipid species within a class. Generally, RP-UPLC is preferred for analyzing already separated classes rather than complex lipid extracts.

2.2.1 Reversed phase-chromatography with Lipids

The separation of analytes in a non-polar reversed phase-chromatography column is according to the hydrophobicity of the lipid analytes and selected eluents. The length of the fatty acyl chain, the quantity of double bonds and the shape of the lipids are the key determinants of their hydrophobicity. As a result, lipid species from several lipid classes that share fatty acyl chains might elute simultaneously, which can result in isobaric overlaps.[70] Long run periods must be used to produce sufficient chromatographic separation of lipid isobars. In Ováciková et al. 2016 [69], the run time was 140 min and 400 lipid species from 14 lipid classes were identified in the human plasma. In Narváez-Rivas and Zhang's study from 2016, they achieved the same level of identification in 24 minutes.[73] Moreover, the use of UPLC pumps, which operate at a higher pressure level, show a increase in sensitivity, resolution and speed of analysis.

In 2017, Breitkopf et al. identified 1500 lipid species from 18 classes in human plasma using a QExactive Plus Orbitrap. They used two solvent mixtures: ACN:water (6:4) and IPA:ACN (9:1). Both containing 10 mM ammonium formate and 0.1% formic acid.[74] These solvent mixtures are used for all analysis in this project.

2.2.2 Retention time

Retention time is affected by several factors, such as the column length and type, solvents, temperature and binding properties of a compound.[75] Therefore, standardizing the retention time is a valuable technique for making them comparable across various methods. Recently, retention time indexing (RTI) has been implemented in LC-MS instruments. This method could potentially be useful for further verifying the lipid identification of suspects and unknown compounds.

2.3 High resolution mass spectrometry

Mass spectrometry serves as an analytical technique to identify analytes based on their mass-to-charge (m/z) ratio. The analytical method used in this study was developed based on established screening approaches, utilizing RP-UHPLC-ESI-Orbitrap-MS instrumentation, which offers high resolution and accuracy in m/z measurement. High-resolution (HR) instruments have increased sensitivity and selectivity, enabling the identification of a vast number of compounds. Additionally, high resolution allows the separation of isomers and in some cases, even isobaric compounds by distinguishing peaks with minimal mass differences.[76] The chromatographic separation was extended to ensure clear separation and a washing step was incorporated into the method to avoid carry-over effects. The method was validated with reference standards and blanks.

2.3.1 Targeted lipid analysis

Targeted analysis refers to the process of identifying analytes by utilizing standards under identical analytical conditions. To identify specific glycosphingolipid classes the open-source software Skyline[78,79] was used. This software arranges the obtained data based on their retention time, the peak area of the respective ion with specific mass to charge ratio (e.g.: LacCer d34:1-> M+H: 862.6250). This involved setting peak boundaries to integrate LC peaks and exporting peak areas of the targeted lipid species. The skyline settings were adapted for the project. Transition Lists of the selected lipid classes were generated for sykline in positive and negative ion modes. Some transitions for MS2 analysis in Skyline were also generated by using the LipidCreator[77] tool within Skyline.

2.3.2 Untargeted lipid analysis

Untargeted analysis involves the screening of metabolites of unknown compounds without prior knowledge of the sample.[80] In such experiments, MS2 spectra are crucial as the produced fragments are specific to the compound. These fragments, in combination with the knowledge of the exact mass, can be used for annotations by comparing them with fragmentation libraries. [81] Untargeted lipid anaylsis can be performed with Lipid Search from Thermo Fisher Scientific by using filters in silico database, but was not included in this method validation project. The analytical approach depends on the analytical question and a short overview of the process finding is shown in Figure 12.

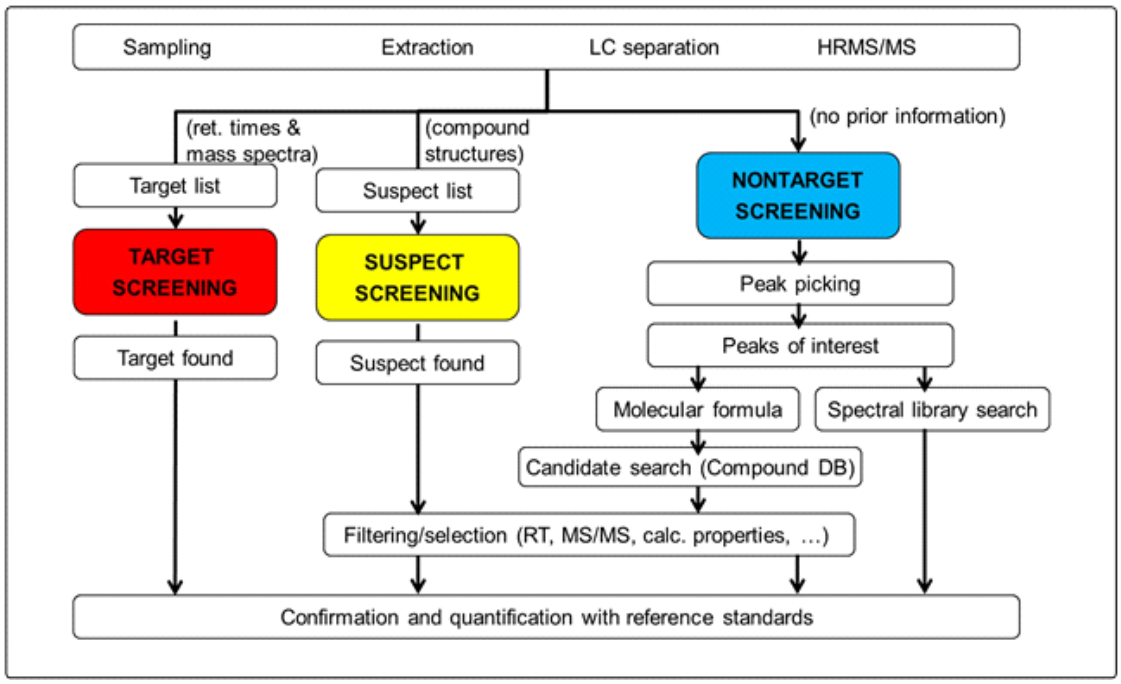

Figure 12. overview of different analytical approaches in screening by Schymanski et al.[82]

2.3.3 Data acquisiton modes

There are three basic data acquisition modes for HRMS. The first mode, Full-MS, captures MS spectra on the MS1 level, while the other two modes, parallel reaction monitoring (PRM) and data dependent acquisition (DDA), record MS/MS spectra on the MS2 level. Full-MS is an acquisition mode that doesn't involve fragmentation and records all ions within a specified m/z range. This mode requires no prior knowledge and is useful for lipid quantification on the MS1 level.[83] On the other hand, PRM and DDA are both fragmentation-based acquisition modes. In PRM, similar to a product ion scan using QqQ, a precursor ion is selected and fragmented and all resulting fragments are measured with high resolution. PRM scans are suitable for lipidomics quantification on the MS2 level. In a DDA experiment, Top N precursor ions are separately fragmented, leading to high-resolution product ion scans for each precursor ion. DDA is typically combined with Full-MS for untargeted lipid analysis to identify lipid species and was used in this project.[84,85]

For targeted analysis of glycosphingolipids, low-resolution triple quadrupole mass spectrometers typically utilize the distinct fragment ions. These ions can be detected using two MS/MS operating modes, namely precursor ion scan and multiple reaction monitoring (MRM). The precursor ion scan mode involves fragmenting all mass-selected ions from the source and monitoring a diagnostic ion.[86,87]

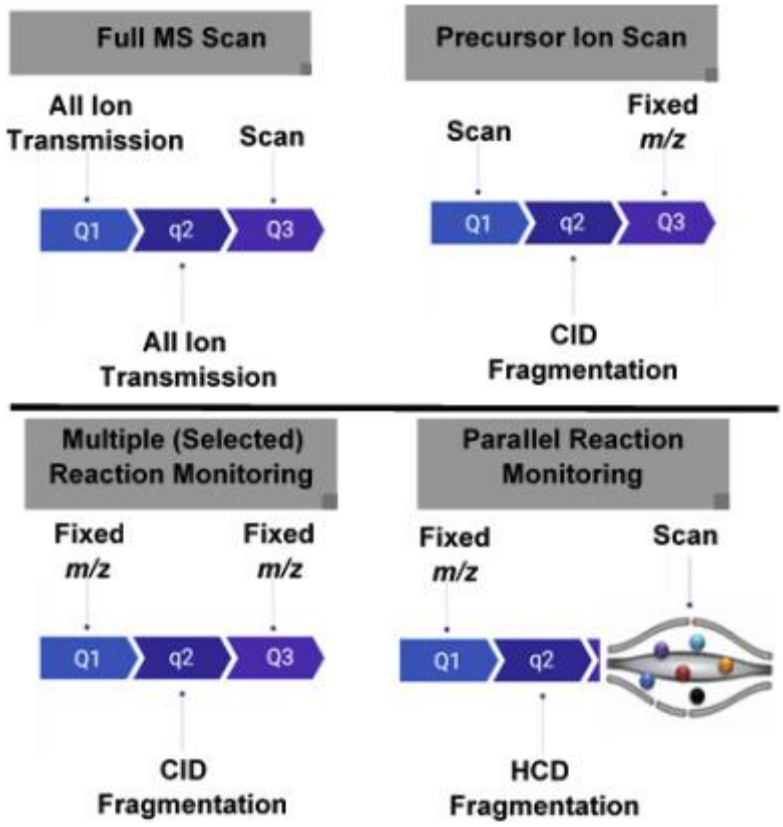

Figure 13. differences in the data acquisition mode when measuring with a CID-MS/MS [88]

All ions generated from the source are detected without fragmentation during a full scan. In precursor ion scan, all ions produced from the source are isolated and fragmented while scanning, with the aim of detecting the precursor ion that generates a particular, predefined fragment ion. During multiple reaction monitoring (MRM), a predetermined precursor-product ion pair is monitored and in parallel reaction monitoring (PRM), a specific ion is selected by mass, fragmented and all product ions being subsequently detected. The data acquisition mode with all the different applications for a CID-MS/MS is shown in Figure 13.

2.3.4 Lipid identification

Lipid identification and quantification are interdependent processes. To identify lipids, an untargeted analysis can be conducted to profile all lipidome in a sample of interest. Once a panel of lipids is identified, it becomes the foundation for a targeted analysis that focuses only on specific lipids for quantification purposes. The main goal of lipid identification is to obtain structural details of a lipid. The Lipidomics Standards Initiative (LSI) has established guidelines to ensure reliable lipid identification. These guidelines recommend using HRMS measurements to accurately identify lipids and separate them if they have similar masses.[89] MS/MS measurements can differentiate between various lipid classes and molecular species.

Additional criteria for lipid identification can be obtained by using separation techniques, such as retention time in chromatography-based methods and CCS (collision cross section) value for IMS (ion mobility spectrometry) measurements. Lipids that have been identified should follow the annotation of Liebisch et al., as presented in chapter 1.1. Several MS-based techniques have shown promise in achieving structural resolution of lipids, including Full-MS and/or MS/MS for carbons and double bonds, MS/MS for fatty acyl constituents, MS/MS considering the ratio of fatty acyl fragments or pretreatment with phospholipase A2 for positional isomers, ozone-induced dissociation (OzID) for double bond position and IMS for double bond cis/trans conformation. According to Schymanski et al.[82] MS-based lipid identifications are level 3 identifications. This means that they provide information on possible structures but not enough information for one exact structure.

Due to their low abundance and low ionization efficiency, particularly in the case of heavily glycosylated ones, glycosphingolipids are challenging to detect compared to other lipids. To enhance their detectability and permit more precise and multiplexed quantification, chemical derivatization (labeling) approaches are frequently utilized.[88]

2.3.5 MS-based approaches for quantification

Multiple methods based on MS exist for quantifying lipids accurately. LC-MS with Full-MS quantification entails the measurement of all m/z ratios, from which those linked to a particular lipid species are assessed. MS/MS quantification, in contrast, involves the measurement of precise precursor/product ion pairs for each lipid species, resulting in an enhancement of sensitivity and specificity.[90]

Most frequently quantification is carried out with external standardization (ESTD) or internal standardization (ISTD). For example, an external calibration method with internal standardization using ^{13}C enriched lipids as ISTDs is obtained by lipidome isotope labeling of yeast (LILY).[83] The concentration of LILY lipids is unknown. Therefore a calibration curve is established by plotting the ratio of the ion intensity of ESTD to ISTD against the concentration of ESTD. Using this curve, the concentration of an analyte can be determined by calculating the ratio of the ion intensity of the analyte to the ion intensity of the ISTD.

2.4 Chemical reagents

The used mobile phase solvents (water, acetonitrile and isopropanol) and solvents for the standard/sample preparation (isopropanol, water) were of LC-MS grade and ordered at Thermo Fisher (Vienna, Austria), Merck (Vienna, Austria) or VMR International (Vienna Austria). Ammonium formate and formic acid were ordered at Sigma Aldrich (Steinheim, Germany).

2.4.1 Eluents for the liquid chromatography

For the accuracy, the individual solvents were weighed and labeled directly in the glass bottles used for the measurement. The composition of the eluents are listed in Table 3 and Table 4.

Eluent A: ACN/H_2O 6:4 (v/v) 10 mM AF 0.1 % FA

	solvent	for 1 L	for 500 mL
1	H_2O	400 g	200 g
2	AF	630.6 mg in 1 mL H_2O	315.3 mg in 0.5 mL H_2O
3	ACN	469 g	234 g
4	conc. FA	1 mL	0.5 mL

Table 3. composition of eluent A for LC

Eluent B: IPA/ACN 9:1 (v/v) 10 mM AF 0.1 % FA

	solvent	for 1 L	for 500 mL
1	IPA	707 g	354 g
2	AF	630.6 mg in 1 mL H_2O	315.3 mg in 0.5 mL H_2O
3	ACN	78 g	39 g
4	conc. FA	1 mL	0.5 mL

Table 4. Composition of eluent B for LC

2.5 Reference Standards

To validate the method for analyzing five particular glycosphingolipid classes, three distinct standards were purchased from the Cayman Chemical Company and prepared for analysis by LC-MS.

Standard 1: 29358 - Neutral Glycosphingolipid Mixture (1 mL stock solution) is solved in chloroform:methanol (2:1, v/v) and contains hydroxy/non-hydroxy galactosylceramides, lactosylceramides, globotriaosylceramides and globotetraosylceramides, which are visible on a TLC in Figure 14. Concentration: 1 mg/mL, storage: -20°C, stability >= 2 years

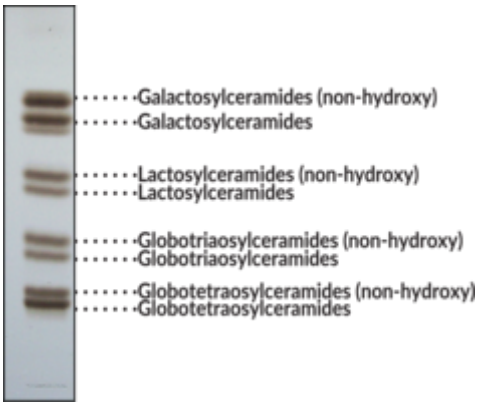

Figure 14. TLC on ingredients of item number 29358 - Cayman Chemical Company[156]

Standard 2: 29360 - Disialoganglioside Mixture (1 mL stock solution) is solved in chloroform:methanol:water (2:1:0.1, v/v/v) and contains the disialogangliosides G_{D1a}, G_{D1b}, and G_{D3}, which are visible on a TLC in Figure 15. Concentration: 0.5 mg/mL, storage: -20°C, stability >= 2 years

Figure 15. TLC on ingredients of item number 29360 - Cayman Chemical Company[156]

Standard 3: 29361 - Lactosylceramide, Ganglioside GM3 and GD3 Mixture (1 mL stock solution) is solved in chloroform:methanol:water (2:1:0.1, v/v/v) and contains LacCers, the monosialoganglioside GM3, and the disialoganglioside GD3, which are visible on a TLC in Figure 16. Concentration: 0.5 mg/mL, storage: -20°C, stability >= 2 years

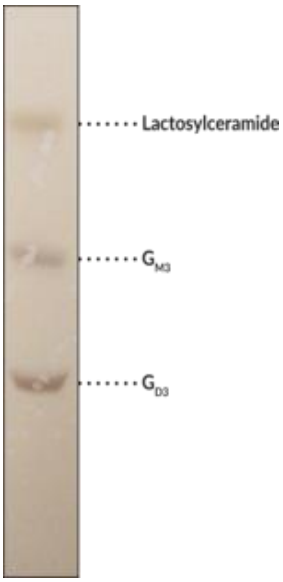

Figure 16. TLC on ingredients of item number 29361 - Cayman Chemical Company[156]

2.5.1 Standard preparation method

Calculation of the used concentration: The manufacturer did not provide precise information on the composition and amount of each individual substance. It was assumed that the proportions of the analytes were approximately equal to each other. Using the indicated total concentration and the molar masses of the individual lipids, 50 µM and 5 µM standards were prepared for liquid chromatography. The 5 µM standard series was shown in preliminary tests to be the desired concentration for further analyses.

Average mol mass of the each standard lipid content:

The mean mol mass of each standard was estimated from the included lipids, averaged and used for the calculation in Table 5 and Table 6. (LacCer ~ 800 g/mol, Disialoganglioside ~ 1870 g/mol, GM ~ 1200-1600, Gb3 ~ 830, Globoside ~ 800-1350)

29358
1000 µg/mL / 1000 g/mol * 1000 = 1000 µM
29360
500 µg/mL / 1800 g/mol * 1000 = 277.8 µM
29361
500 µg/mL / 1000 g/mol * 1000 = 500 µM

Table 5. calculated molar concentration of each standard

50 µM standard (500 µL)	5 µM standard (200 µL)
29358	(dilution of the 50 µM standard)
25 µL standard + 475 µL solvent	20 µL 50 µM standard
29360	180 µL solvent
90 µL standard + 410 µL solvent	**standard pool (100 µL)**
29361	10 µL of each 50 µM standard
50 µL standard + 450 µL solvent	70 µL solvent
solvent: IPA:H2O (65:35)	

Table 6. used standard concentration for the method validation

Centrifugation, drying and reconstitution

The reference standards were dried by removing the solvent in a Genevac EZ-2 Series Personal Evaporator (SP Scientific, Ipswich, UK). Afterward the reconstituion of the dried material was performed in 1 mL IPA:H2O (65:35) by shaking, vortexing and ultrasonication (30°C, 15 min).[55] The used 5 µM standards and the 5 µM pool of each standard for the LC-MS analysis was prepared using the table 4 scheme.

Lipid-QC: In-house standard preparation method

For internal standardization lipids enriched with ^{13}C were utilized. These lipids were manufactured using the LILY procedure[83] and prepared with a in-house protocol for the LC-MS measurement (10 mL dried EtOH extract unlabeled; redissolved in 0.6 mL MTBE, 0.2mL MeOH, 0.2 mL water; upper phase collected in 2 mL Eppendorf tube; dried in SpeedVac; redissovled in 2 mL IPA; centrifuged; 10µL aliquote in 2mL Eppendorf tubes; dried in SpeedVac; stored at -80°C). The at -80°C stored dried lipid yeast QC samples were slowly heated to room temperature and re-suspended in 100 µL IPA for the LC-MS analysis.

2.6 HCT116 colon cancer sample

The analyzed sample in this work was a HCT116 colon cancer cell line, which were bred by the cancer therapy research group at the medical university vienna (Walter Berger, Dina Baier).[91] These samples are included in a project on specific lipid alterations accompanying the response and development of resistance against chemo-/targeted therapy. The aim was the targeted and untargeted analysis of whole cell lysates and lipid droplets. For their measurement they used treated (KP1339), untreated (DMSO), resitent and unresitent HCT116 cell lines in lipid droplets and whole cell samples. The measurement in this work with the validated GSL method was carried out with the untreated whole cell samples of the HCT116 cell line from the project.

Cells	HCT116
	HCTR/KP (KP1339-resistant HCT116)
Medium	McCoy's 5A (M8403) medium with 10% FBS and 0.219 g/L glutamine
Time points	24 h treatment (KP1339) vs. untreated (DMSO only)
Culture format	6-well plate, n=6 wells per condition with 2 ml/well. ca. 200 000- 1 000 000 pro cells, blank controls per conditions
Medium change	with treatment

Table 7. HCT116 cell conditions

2.6.1 HCT116 sample preparation method

The isolation from cultured cells was carried out from the team of the cancer therapy research group at the medical university vienna and the cell conditions are listed in Table 7. HCT116 cells were cultured in McCoy's 5A GlutaMAXTM medium (36600-021, Life Technologies) supplemented with 10% not-heat inactivated fetal bovine serum (10270-106, Life Technologies) and 100 µg ml-1 antibiotic Penicillin-Streptomycin (10 000 U/mL, 15140-122, Life Technologies). Cells were trypsinised with 0.05% trypsin and passaged after every 48h in a 1:10 ratio into Nunc EasYFlask 75 cm2 Nucleon Delta Surface (156499, Thermo Scientific) flasks. N2 quenching: 1 mL cell medium was transferred in 1,5 mL Eppendorf tubes and the remaining medium was sucked away. The cells were washed three times with 2 mL PBS and then quenched with liquid nitrogen. The plates were stored at -80°C until extraction. The lipids were isolated using the SIMPLEX extraction protocol with addition of 13C labelled internal standard (yeast).[92] In each cell well, 500 µL of cold MeOH was added and the cells were detached using a cell scraper. The cell suspensions were then transferred to 5 mL Eppendorf tubes using a pipette. The plates were washed twice with 250 µL of cold MeOH per well and the suspensions were transferred to the Eppendorf tubes again. 250 µL ^{13}C-LILY standard in MTBE and 2940 µl of cold MTBE was added. The cell suspension mix was incubated for 1 h at 4°C under agitation. Afterward the phases were seperated by adding 800 µL water. The extract was centrifuged at 2000 rcf for 5 min and the upper phase was collected (lipid containing fraction). Two of the biological replicates were combined and samples were dried in a GenVac and dissolved in 200 µL IPA for analysis. For the protein precipitation, MeOH was added to the remaining phase in a final ratio of 4:1, v/v MeOH/H2O (2700 µL MeOH). The samples were incubated for 1 h at 20 °C, followed by 12 min centrifugation (4500 rpm, max. speed) at 4 °C.

The resulting supernatant was transferred (metabolite containing fraction) in a fresh 5 mL Eppendorf tube. The remaining pellet contained the protein fraction. Metabolite and protein fraction were stored at -80°C, but not used in this project. The lipid fraction were prepared with a final volume of 200 µL (dissolved in IPA), pipetted into HPLC vials with inserts and stored at -80°C for lipid analysis (range: 50 nM – 25 µM). For the measurements the whole cell pool sample were heated to room temperature, transferred to fresh Eppendorf tubes, centrifugated (12 min, 4500 rpm, at 4 °C) and evaporated to dryness using a Genevac EZ-2 Series Evaporator. The dried lipid samples were dissolved in 200 µL 65:35 IPA:H2O and transferred into HPLC vials for LC-MS analysis.

2.7 LC-MS/MS measurements

All measurements were carried out utilizing high-performance liquid chromatography with ultra-high efficiency (UHPLC) combined with high-resolution mass spectrometry (HRMS). The HRMS aspect was executed utilizing a Q Exactive HF quadrupole-Orbitrap mass spectrometer (Thermo Fisher Scientific, USA) equipped with a heated electrospray ionization (ESI). Before each standard pool/sample measurement, the instrument was calibrated and checked with the Lipid-QC.

Measurement of the LILY internal standard (Lipid-QC)

To ensure the reproducibility of the results and to test the usability of the LC-MS instrument, a lipid quality assurance measurement was carried out with the LILY internal standard before each measurement day. The LILY internal standard was measured after the calibration of the instrument in a 23 minutes method with a in-house protocol.

Experiment 1: Measurement of the standards and validation of the HESI source parameters

Each standard sample were first measured in postive, negative and Full-MS mode with the description of the 30 minutes method. The blank sample (pure HPLC grade IPA:H_2O / 65:35) was measured two times at the beginning, at the end and after every third sample. The measurement was carried out several times with different ESI source parameters and adjusted to the results.

Experiment 2: Measurement of the HCT 116 colon cancer sample

For the second experiment the HCT116 cancer cell line sample was measured. Each colon cancer sample were measured in postive, negative and Full-MS mode with the description of the 30 minutes method. The blank sample (pure HPLC grade IPA:H_2O/65:35) was measured two times at the beginning, at the end and after every third sample. The measurement was carried out with the new HESI source parameters method.

2.8 Methods

2.8.1 Lipid QC - 23 minutes method

The Lipid QC method was developed for the measurement of six lipid classes (DG, PS, PI, LPE, LPC, PC, PE) in the LILY samples. The whole run time of the measurement was 23 minutes, the injection volume 5 µL, the flow rate (0.25 mL/min) and the column temperature 40°C. For lipid analysis an Acquity UPLC HSS T3 column (2.1 mm × 150 mm, 100 Å, 1.8 µm, Waters, USA) with a VanGuard pre-column (2.1 mm × 5 mm, 100 Å, 1.8 µm, Waters, USA) was used. The mobile phase A consisted of ACN/H2O (3:2, v/v) while mobile phase B was composed of IPA/ACN (9:1, v/v). Both solvents contained 10 mM ammonium formate and 0.1% formic acid. The gradient used was 55% B from 0 to 8.0 minutes and a ramp to 65% B from 8.0 to 13.0 minutes. Further increasing to 85% B between 13.0 and 15.0 minutes, followed by 100% B from 15.0 to 20.0 minutes. Then a quick switch back to 55% B at 20.0 minutes for the rest of the run time. The gradient distribution of the mobile phase A and B can be seen in Figure 17 and Figure 18. The method is the traditional used method for the in-house lipids standard measurement.

No	Time	Flow [ml/min]	%B	Curve
1	0.000	Run		
2	0.000	0.250	55.0	5
3	8.000	0.250	65.0	5
4	13.000	0.250	85.0	5
5	15.000	0.250	100.0	5
6	20.000	0.250	100.0	5
7	20.000	0.250	55.0	5
8	23.000	0.250	55.0	5
9	*New Row*			
10	23.000	Stop Run		

Figure 17. progression of the gradient for the 23 minutes method

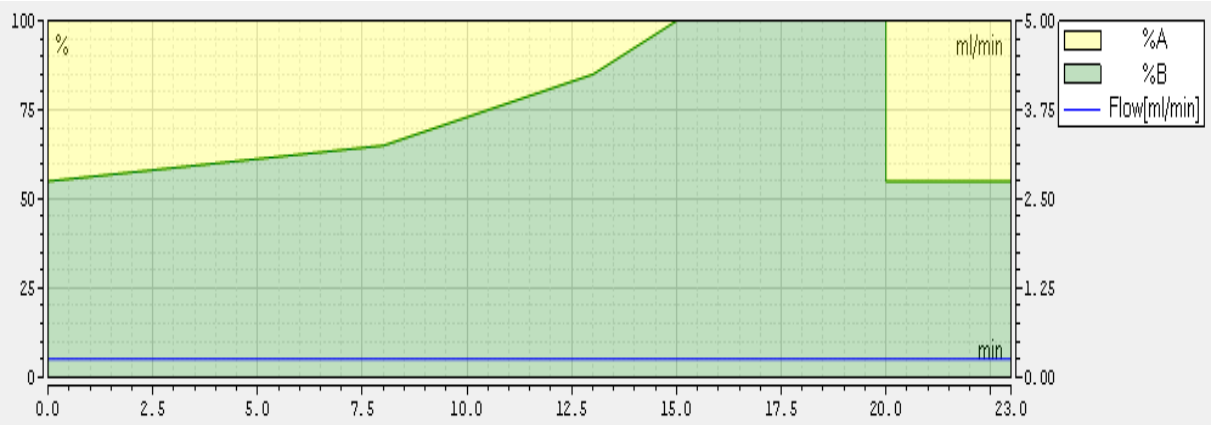

Figure 18. course of the running average gradient for the 23 minutes method

ESI-source settings for the Lipid QC

For the Lipid QC measurement an in-house tunefile (QC HESI 250µL for switching optimized positive/negative mode) was used. The settings are shown in Table 8.

Full MS	positive mode	Full-MS	negative mode
sheath gas	30	**sheath gas**	35
aux gas	5	**aux gas**	10
sweep gas	2	**sweep gas**	2
cappilary temperature	200	**cappilary temperature**	250
RF-lens voltage	30	**RF-lens voltage**	45
aux gas heater temperature	300	**aux gas heater temperature**	300
spray voltage	3.1 kV	**Spray voltage**	2.8 kV
scan range	250 – 2000 m/z	**scan range**	250 – 2000 m/z
MS resolution	60,000	**MS resolution**	60,000
MS AGC target	1 e6	**MS AGC target**	1 e6
MS maximum IT	200 ms	**MS maximum IT**	200 ms
fragmentation	none	**fragmentation**	None
microscans	1	**microscans**	1
lock masses	off	**lock masses**	off

Table 8. ESI-source settings for the Lipid QC

2.8.2 Experiments - 30 minutes method

The second method was developed for the GSL measurement with a run time of 30 minutes. The idea was that a longer run time and the optimation of the mobile phase gradient paramter will show a better GSL class seperation, which also results in a better analysis with the massspectrometry. Therefore the LC-MS workflow in 2022 from Hohenwallner et al.[93] for a ganglioside differentiation was used, adapted and optimized for the overall analysis of several GSL classes. The whole run time of the measurement was 30 minutes, the injection volume 5 µL, the flow rate (0.25 mL/min) and the column temperature 40°C. For lipid analysis an Acquity UPLC HSS T3 column (2.1 mm × 150 mm, 100 Å, 1.8 µm, Waters, USA) with a VanGuard pre-column (2.1 mm × 5 mm, 100 Å, 1.8 µm, Waters, USA) was used. The mobile phase A consisted of ACN/H2O (3:2, v/v) while mobile phase B was composed of IPA/ACN (9:1, v/v). Both solvents contained 10 mM ammonium formate and 0.1% formic acid. The gradient used was 30% B from 0 to 2.0 minutes, a ramp to 55% B from 2.0 to 3.0 minutes and a second to 67% from 3.0 to 17.0 minutes. Further increasing to 100% B between 17.0 and 22.0 minutes, followed by 100% B from 22.0 to 26.0 minutes. Then a switch back to 30% B at 26.0 minutes for the rest of the run time. The gradient distribution of the mobile phase A and B can be seen in Figure 19 and Figure 20.

No	Time	Flow [ml/min]	%B	Curve
1	0.000	Run		
2	0.000	0.250	30.0	5
3	2.000	0.250	30.0	5
4	3.000	0.250	55.0	5
5	17.000	0.250	67.0	5
6	22.000	0.250	100.0	5
7	26.000	0.250	100.0	5
8	26.000	0.250	30.0	5
9	30.000	0.250	30.0	5
10	*New Row*			
11	30.000	Stop Run		

Figure 19. progression of the gradient for the 30 minutes method

Figure 20. course of the running average gradient for the 30 minutes method

2.8.3 Data interpretation of the Lipids via Skyline

The selected and calculated target lists for the GSL classes of single and double charged H-adducts were used to write a transition list for the import into Skyline. For the Lipid-QC a transition list for six lipid classes of single charged H-and NH_4-adducts were used. The results were manualy compared with Skyline. An example of the Lipid-QC measurement and data evaluation can be seen in Figure 21, Figure 22 and Figure 23.

Data representation of a lipid QC measurement

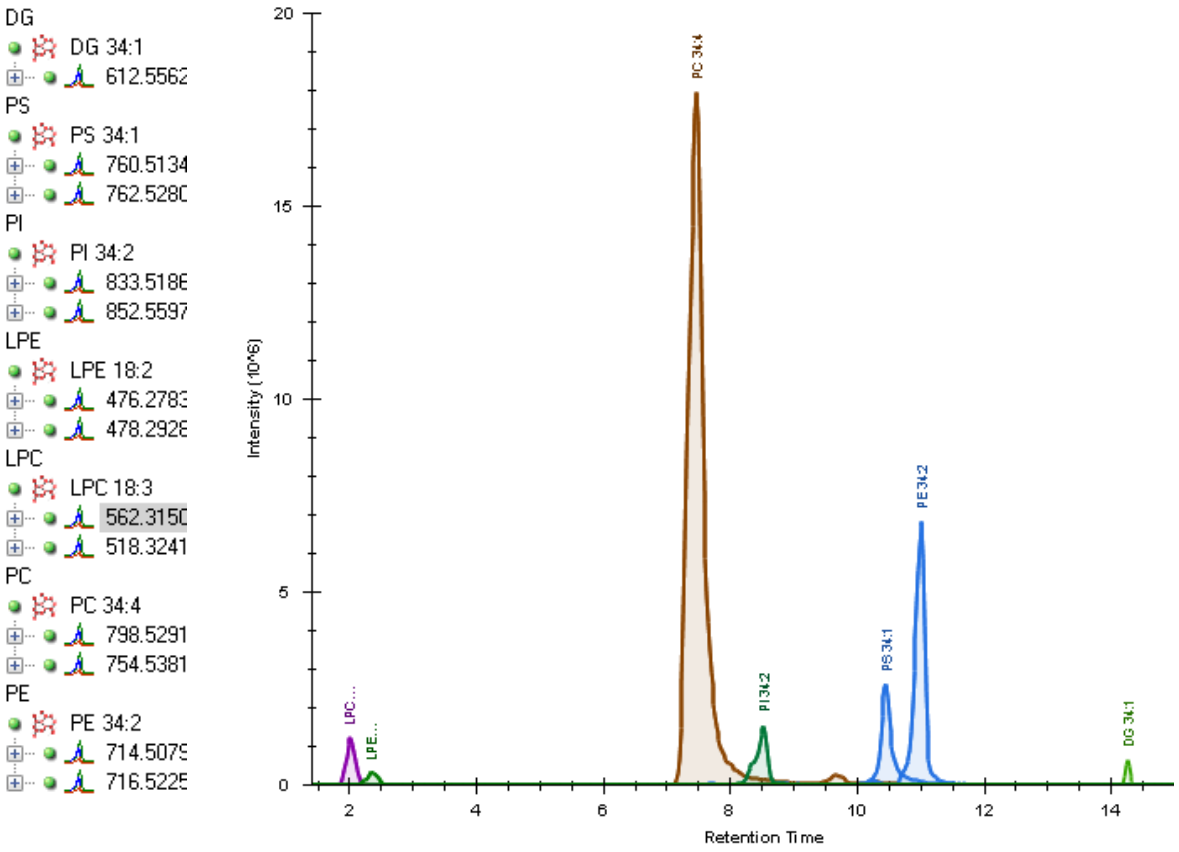

Figure 21. table of transition list of the lipid-QC and the visualization by skyline

In the lipid QC, previously aliquoted samples were examined for their instrumental changes in specific lipid composition. The fluctuations provide information about the performance of the device and are essential before measuring the main samples. The comparison of the peakarea and the retention time of the last 8 lipid QC measurements in Figure 22 and Figure 23 show a appropriate operability of the device. Figure 24 contains the lipid classes of the LILY-Lipid-QC. By comparing the retention times and intensity of the measured LILY-lipid standard, it was possible to identify changes in the instrumental system in advance and ensure reproducibility.

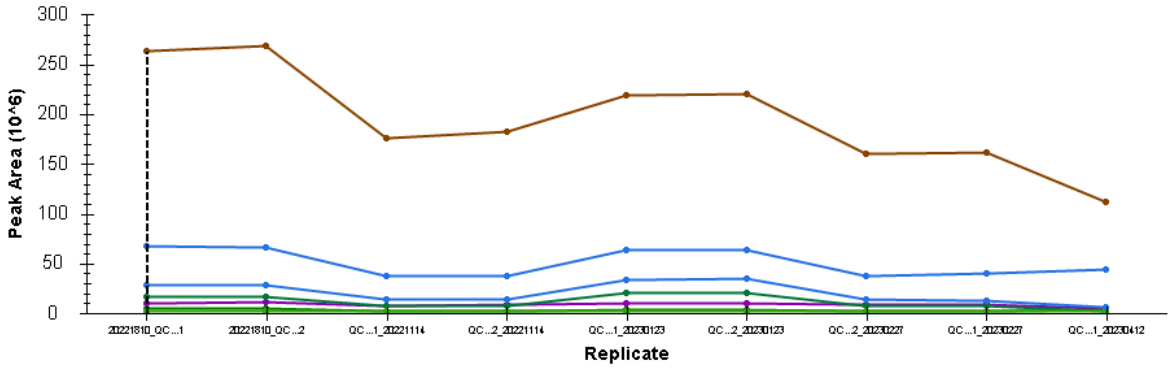

Figure 22. reproducibility comparison of the peakarea of the last 8 lipid QC measurements, created by Skyline

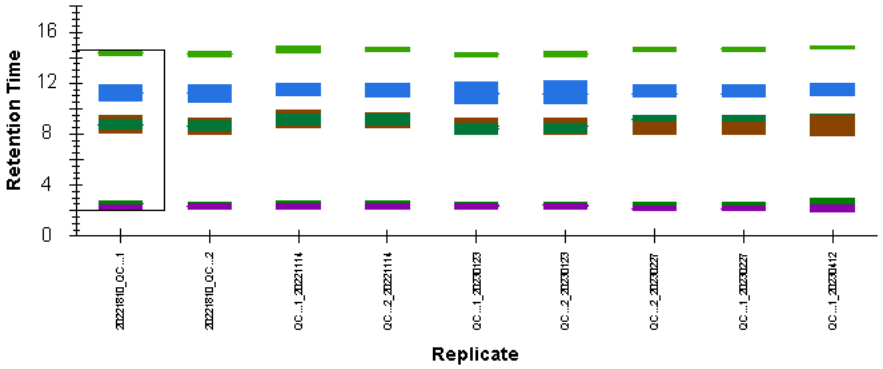

Figure 23. reproducibility comparison of the retention time of the last 8 lipid QC measurements

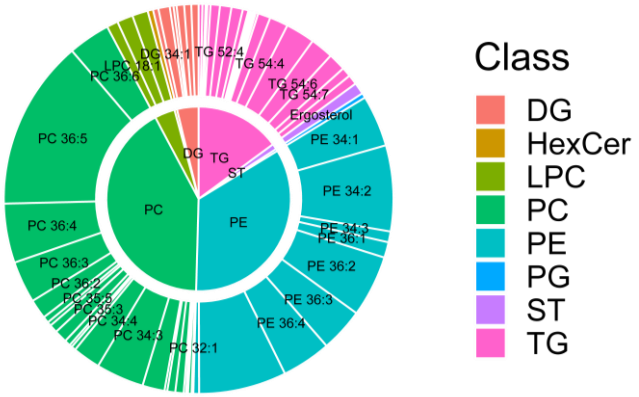

Figure 24. lipid class content of the LILY-Lipid-QC [83]

3. Results and discussion

The aim of this project was to develop a targeted RP-HRMS/MS-based method for qualitative analysis of glycosphingolipids with a focus on lactosylceramide, Gb3, Gb4, Globo-H and GM3, using commercially available standards. The MS acquisition modes were Full-MS for MS1 level and DDA for MS2 level. A precise analysis of the retention times, lipid distribution and fragmentation patterns were carried out using the software Skyline and Freestyle. To ensure high-quality annotations of GSLs, target lists and inclusion lists were created, which were calculated and used for method validation.

3.1 GSL-specific method development

There are several challenges that should be considered when analyzing GSL. Glycosphingolipids have a complex structure with a hydrophilic and a hydrophobic part, making them important compounds in the lipidome.[94] In contrast to phospholipids, many classes usually occur in lower concentrations in tissues (except nerve cells).[95] To perform qualification and quantification of the individual GSL classes, appropriate external and internal calibration of standards is required. In many cases, these are often expensive and only available for specific species or as an overall pool. Although there have been tremendous advances in the automation of lipidomic data analysis in recent decades, universal GSL assays are missing. This is because many approaches are also very specific to sample analyzed and thus there can be no universally applicable method for GSL analysis. The process usually starts with the system or sample under consideration and is then determined by the choice of appropriate sample preparation, extraction method, instrument selection and analysis software. Each lipidomics research assay is a complex analysis and validation process relying on the targeted and optimized method development of the lipids in each environment. In this work relative qualification of annotated GSLs was performed and a comprehensive database including retention times and observed fragmentation patterns was generated.

3.1.1 Targeted analysis of GSLs in the standard pool and cancer sample

A common way to study sphingolipids is to use LC-MS/MS as an analytical tool.[96] LC-MS based methods that use gradient elution face the challenge of continuous changes in the matrix caused by variations in the solvent composition. To address this issue, it is suggested to use retention-time-matched standardization in addition to class-specific standardization.[97] In this

project, no LILY standardization was performed and the focus was on qualitative method development and parameter optimization.

3.1.2 Target- and inclusion list

In order to develop a targeted method to study glycosphingolipids by LC-MS in standard samples, some subgroups of GSL were selected to gain a divers GSL picture. All classes studied found in cancer related studies and their possible functions in cancer development have been highlighted in several published papers. An overview on these studies is given for each class in section 3.1.3.

To cover the whole species range, a target list and inclusion list were compiled as mentioned before. The target list was compiled and calculated utilizing LIPID MAPS database[3], enviPat Web[98] and swiss lipids database[99]. This list includes the LCBs of d18:0, d18:1, t18:0, t18:1, d20:0 or d20:1, as well FAs variants, starting from FAs 2:0 to 38:5 for all studied GSL classes. In addition, several possible m/z adducts ([M]+, [M+H]+, [M+K]+, [M+Na]+, [M+Li]+, [M+NH4]+, [M+OAc]-, [M.-H]-, [M+COOH]-, [M+2H]+ and [M-2H] were calculated and listed for all species. For the acquisition of MS2 spectra in both negative and positive ion mode, inclusion lists with only the m/z values of singly and doubly charged H-adducts of each GSL-class were created. The inclusion lists were created from the target list and also included a combination of LCBs (d18:0, d18:1, t18:0, t18:1, d20:0 or d20:1) and FAs (2:0 to 38:5) for the GSL classes. The selection of FAs and LCBs species was based on several references on the topic of GSL in cancer cells and human plasma and was reassembled for this project.

3.1.3 Cancer studies on GSLs species

In neutral cerebrosides, sphingosine d18:1 was observed to be the most abundant sphingoid base and the fatty acids were mainly based on long fatty acid chains.[100] In addition, sphingosine (d18:1) with non-hydroxy 16:0 fatty acid is the major ceramide species of hESC glycosphingolipids.[101,102] The N-acylated fatty acyl chains have variable lengths ranging from 16 to 26 carbon atoms and may possess a double bond in some species. While C16:0, C22:0, C24:0 and C24:1 are the predominant types, their proportion differs across distinct cell lines.[103] In undifferentiated ES cells, the major constituent ceramides of GSLs are d18:1 sphingosine with N-acyl fatty chain of C16:0, C18:0, C20:0, C22:0 and C24:0.[104]

Lactosylceramide - LacCer

The LacCer d18:1/16:0 was highly determined in a sphingolipid study in human plasma [106] and in an identification study in human ovarian cancer cell line[107]. Among the LacCer, the d18:1/24:1, d18:1/24:0 and d18:1/16:0 were dominant. Also, LacCer d18:1/16:0 and LacCer d18:1/24:0 were significantly higher in cholangiocarcinoma tissues than in the adjacent normal tissues.[108] Moreover, LacCer d18:1/16:0 showed high significance as a potential biomarker for prostate cancer.[109]

Globotriaosylceramide - Gb3

The Gb3 d18:1 species with N-amidated FAs 16:0, 22:0, 24:0 and 24:1 have been identified as potential biomarkers for prostate cancer.[109] Hydroxylated Gb3 species d18:0/16:0 and d18:1/16:0 were found in 86% of the tumors studied, while they were absent in healthy tissue.[110] In Ramos and MDA-MB-231 cells, the most abundant Gb3 isoforms were Gb3 d18:1/16:0, Gb3 d18:1/24:0 and Gb3 d18:1/24:1. In the HT-29 cell line the most abundant types were Gb3 d18:1/16:0, Gb3 d18:1/24:0 and unexpectedly, Gb3 18:1/16:0-OH. Further analysis included the detection and consideration of additional species with minimal presence, such as Gb3 d18:1/22:0 and Gb3 d18:1/18:1.[111] The amounts of Gb3 species were in the order of d18:1/24:1 > d18:1/24:0 > d18:1/16:0 > d18:1/22:0 when GSLs were examined in fibroblasts from patients with adrenoleukodystrophy.[112] The most abundant types of Gb3 in cultured human fibroblasts of adult cell lines were Gb3 d18:1/24:0, Gb3 d18:1/24:1, Gb3 d18:1/22:0, and Gb3 d18:1/16:0.[113]

Globotetrahexosylceramide - Gb4

Gb4 d18:1/24:0 and GM3 d18:1/23:0 were used to study the characteristic size of liposomes that correlate with their antibody-inducing activities in mice. When GSLs were identified in fibroblasts from patients with adrenoleukodystrophy, the predominant species at Gb4 were d18:1/24:0 and d18:1/24:1, respectively.[115] Identification of a Gb4 d18:1 and C24:0 bound to MD-2 complex.[116] ESI-QTOF mass spectra of Gb4Cer receptors from an E. coli binding overlay assay revealed Gb4Cer d18:1, C24:1/C24:0 and Gb4Cer d18:1, C22:1/C22:0 assigned.[117] The Globo-H ceramide is less researched in tumor samples, however one study found that a Globo-H with FAs C16:0 allows cancer cells to evade immune surveillance.[118]

Ganglioside - GM3

Gangliosides (GD1, GM1, GM2, GM3) containing d18:1/18:0 and d20:1/18:0 ceramides are predominant in healthy brain tissue and peritumoral regions. In glioblastomas, an elevated proportion of ceramides with shorter (C16) and longer (C22, C24) fatty acyl chains, unsaturated fatty acyl chains (C24:1) and fatty acyl chains with an odd number of carbon atoms (C17, C19) have been identified.[119] The expression of GM3 (d18:1/22:1) in renal cancer patients was higher than in healthy controls.[120] The fatty acyl components C16, C16OH, C22, C24:1 and C24 with the d18:1 sphingosine base are most abundant in GM3 in human embryonic stem cells and breast cancer stem cells.[121] In patients with hematological disorders, GM3(d18:1/16:0) and GM3(d18:1/24:1) showed a significant positive correlation with C-reactive protein, soluble interleukin-2 receptor and blood lactate dehydrogenase.[122] The GM3 species d34:1 was frequently found in CFPAC1, NCI-H358 and MCF7 in the surface analysis of gangliosides with LC-MS in different cell lines.[123] As example, Table 9 shows the list of specific GSLs in a study of d18:1/16:0 and d18:1/24:0 in burst cancer tissue and peritumor tissue. Furthermore, it could also be proven that the species distribution of the GSL classes, depend on the respective cell line, as shown in Table 10.

GSL	Molecular ions $[M+Na]^+$	Fatty acid*	Sphingosine$^{\Delta}$	Total GSL(%)	
				Breast-cancer tissue	Peritumor tissue
GlcCer	806.7	16:0	d18:1	38.54	43.87
	918.8	24:0	d18:1		
LacCer	1010.8	16:0	d18:1	27.11	21.23
	1122.8	24:0	d18:1		
Gb3	1214.9	16:0	d18:1	13.70	17.71
	1326.9	24:0	d18:1		
Gb4	1459.9	16:0	d18:1	19.27	16.90
	1572.0	24:0	d18:1		
Globo-H	1838.1	16:0	d18:1	0.45	0.16
	1950.9	24:0	d18:1		

Table 9. Major GSLs in breast cancer tissues and paired peritumoral tissues [121]

Spezies	Hep-2	HeLa	HeLa	XF-	SF-	SKOV3	SKVLB	HBMEC	EA.hy 926	GMVE
16:0	10	6	19	21	29	33	50	41	22	53
18:0	2.0	4	4	16	17	22	45	nq	nq	–
20:0	1.4	–	–	1	1	3	1	nq	nq	–
22:0	1.1	35	10	13	11	9	1	7	11	14
22:1	0,1	–	2	–	–	–	–	–	–	–
23:0	nd	–	3	3	2	nd	nd	–	–	–
23:1	nd	–	1	–	–	–	–	–	–	–
24:0	24	42	32	38	28	15	2	20	34	22
24:1	60	8	29	8	12	8	1	32	33	11
26:0	0,1	–	–	–	–	–	–	nq	nq	–
26:1	1.0	–	–	–	–	–	–	nq	nq	–

Table 10. composition of Gb3 species in different cell lines [103]

3.2 Method performance

The measurements were made over a period of several months and therefore the samples were stored at -20°C or -80°C. The selected standard pool concentration was 5 µM per standard and a volume of 5 µL was injected per measurement. The method exhibited good performance in detecting GSL-lipids from various classes, which will be discussed in detail below. Initially, the method's efficacy will be presented, encompassing the detectable standards and the stability of retention time. Subsequently, the outcomes of the experiment will be thoroughly examined.

3.2.1 Chromatographic seperation of the studied GSL classes and species

At the beginning of the validation process, an existing method for a UHPLC-MS for gangliosides[93] was chosen and a test scan was carried out for the respective lipid classes with the standard pool. The results showed a satisfactory separation of the individual GSL classes by the RP-LC. The eluent composition, the duration of the run and the eluent gradient were adopted from this method (30 minutes method) for the further measurements. For the Skyline Transition List, the single and double charged adducts of each GSL class were selected from the target list.

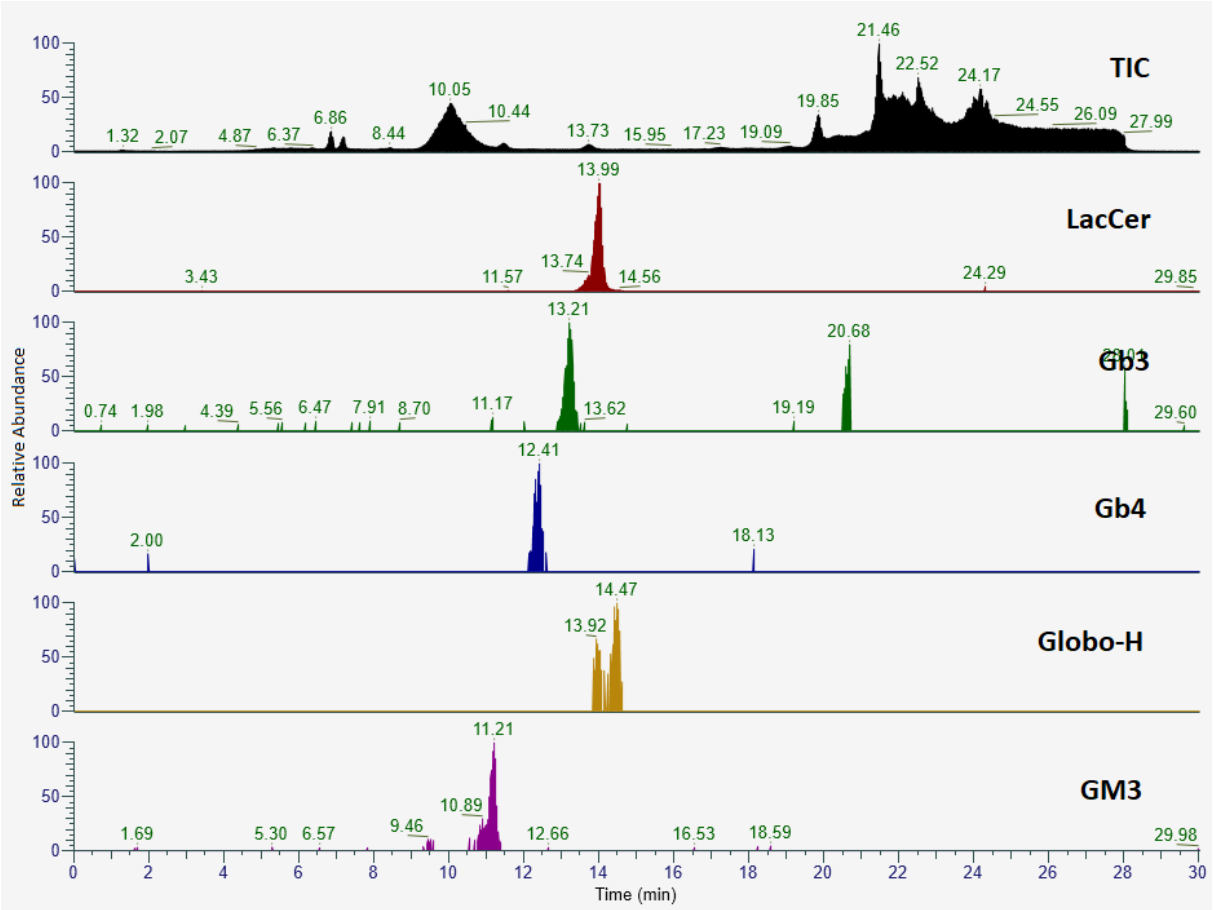

Figure 25. elution order of all studied GSL classes for d18:1_16:0 (d34:1 species) - positive mode, typical total ion current (TIC) chromatogram created using Freestyle 1.8

As expected, the elution order in reverse-phase chromatography depends on the increasing polarities or the headgroup. The elution of each GSL group basically depends on the glycan moiety, as illustrated in Figure 25. More hydrophobic molecules with fewer saccharides, such as LacCer, have the highest retention times, while molecules with more saccharides, like GM3, have the lowest retention times. The d34:1 species are detected by the [M+H]+ adduct of the individual lipids and increasing chain length generally leads to a longer retention time.

The basic structure of all GSLs is ceramide, which is linked to individual saccharide units or sialic acids and characterizes the respective class. The influence of the glycan content on the elution order can also depend on the linkage of the individual saccharide units in the sugar chain.[124] In contrast, gangliosides have differently linked sialic acids between the saccharide units. The sialic acid affects the polarity of the whole molecule, and therefore, the GM3 class elutes earlier than Gb3, even though they have the same number of sugars. The charge and detected production ion depend on the molecule and the ionization technique used for lipid identification.

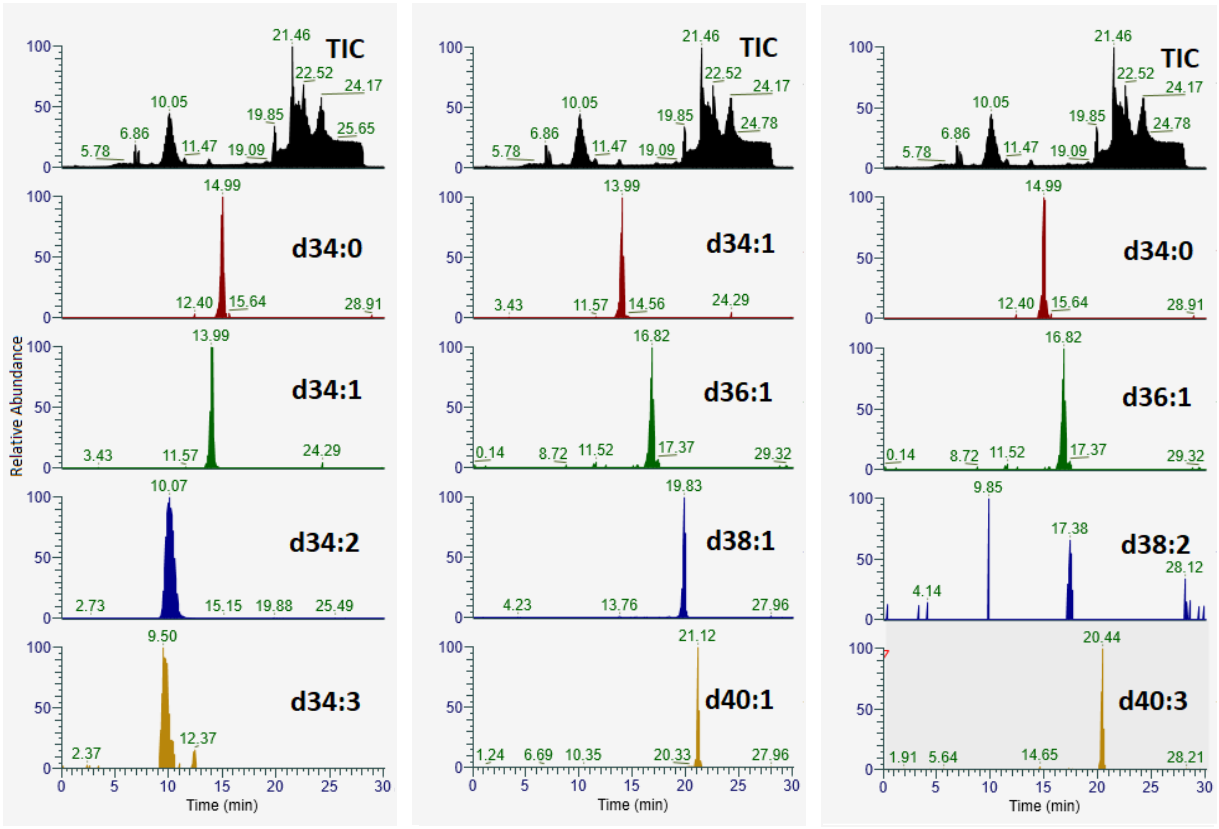

Figure 26. comparison and effects on retention time of different carbon chain lengths and double bonds in lactosylceramide species – positiv mode – created using FreeStyle 1.8

The analysis of the productions in positive and negative mode give a concordant retention time due to the elution of lipids before ionization by the MS instrument. Figure 26 shows the chromatographic profile from the standard pool sample obtained by total ion current (TIC) on selected m/z ions. As visible in Figure 26 A, multiple double bonds in a fatty acyl chain or in LCBs result in a shorter retention time in reverse phase chromatography (as described in the equivalent carbon number (ECN) model)[157]. For illustration the examples of lactosylceramide d34:0, d34:1, d34:2 and d34:3 were used. The change of each double bond decreased the retention time. Three double bonds in the carbon chains (34:3) result in a retention time change of 4 minutes 30 seconds compared to no double bonds (d34:0). Longer fatty acyl chains or LCBs result in a higher retention time, as shown in Figure 26 B. The elution distance between lactosylceramide d34:1 and d36:1 is 2 minutes 50 seconds, to d38:1 4 minutes 30 seconds and to d40:1 7 minutes 7 seconds. A combination of both effects leads to a smaller change in retention time, but where the effect of increasing the carbon chain residues in the fatty acyl chain dominates over that of the double bonds (Figure 26 C). The change in retention time

from d34:0 to d36:1 1 minute 50 seconds, to d38:1 2 minutes 23 seconds and to d40:3 5 minutes 27 seconds. The increase in hydroxylation level (d34:1 / t34:1) also correlated with an increase in retention time. In this case, the d34:1 configuration could consist of multiple isobars (e.g.: from d18:1/16:0 or d20:1/14:0). The exact fatty acyl constituents of lipid species d34:1 cannot be reflected by this chromatogram. Moreover, a more detailed description about the positional isomers, stereoisomers or double bond position cannot be characterized by this instrumental method. While the m/z is the same, the lipid structure interacts with the column differently, enabling chromatographic separation. Another possibility is that different conformations of a given lipid sum composition, such as variations in the position of a double bond, could lead to peak separation. Interpretation of lipid structural spectra with RP-HRMS must be done with caution. If only a single class of lipids is isolated, favorable outcomes can be obtained. The analyze of a mixture of numerous classes with RP, could cause a overlapping of lipid species from diverse lipid classes.[125]

The most commonly used technique for lipid separation is RP chromatography, as the majority of lipids are retained on RP columns. Nonetheless, extended chromatographic times of at least 20-30 minutes are required to distinguish isobaric species.[126,127] It should be noted that HRMS allows the separation of isobaric species, but the quantification of isomeric species without chromatographic resolution is not feasible, particularly for ceramides and related lipid classes. This is relevant for double bond positional isomers and cis/trans isomers, which cannot be distinguished by MS/MS analysis and would be of interest for analysis of lipid function.[128]

3.2.2 Retention time stability

Stable retention times are important, because retention time is a key factor in annotating or identifying a compound and give an analytical feedback on the reproducibility of the method. The measurements were carried out over a period of several months and a comparison of the retention times of the individual measurements provides a good comparison of the condition of the separation column, the running medium and the samples used. The results were checked over the entire measurement period using the lipid-QC and after each measurement using the replicates in the standard pool/HCT116 sample (Figure 27 and Figure 28).

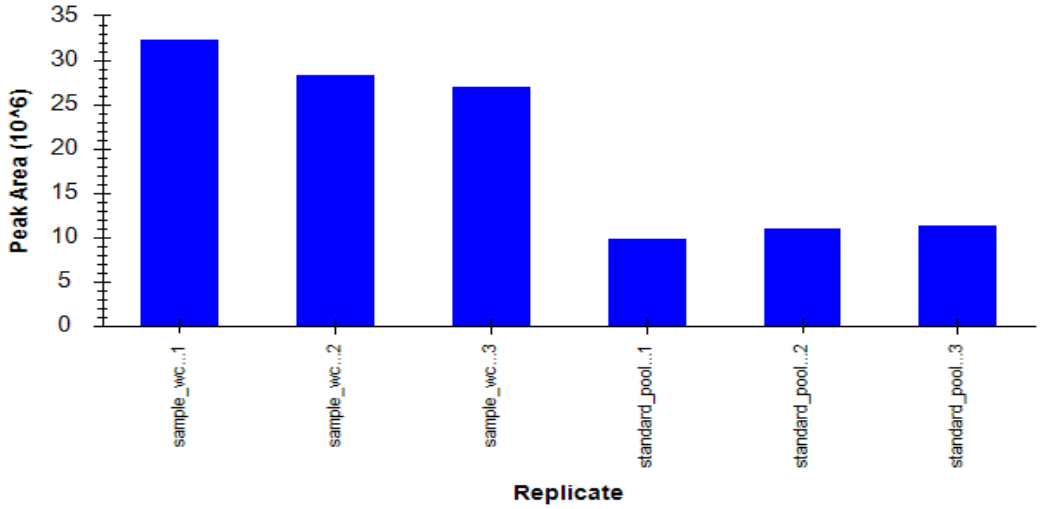

Figure 27. comparison of peakarea in the standard pool/HCT116 sample replicates for LacCer d34:1

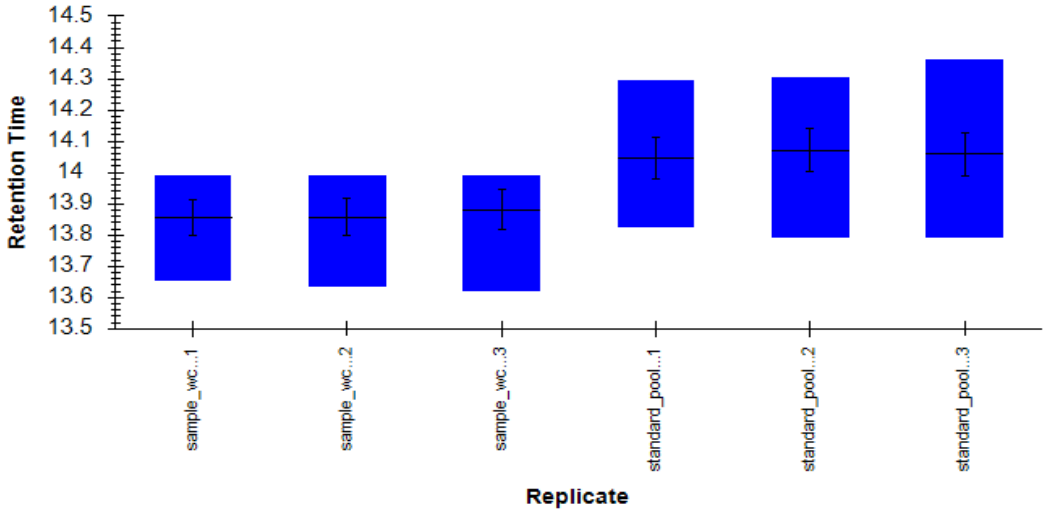

Figure 28. comparison of retention time in the standard pool/HCT116 sample replicates for LacCer d34:1

The replicates of a measurement of d34:1 species of LacCer showed small differences between the individual replicates in both peakarea and retention time. It is noticeable that there is a difference in retention time of LacCer species d34:1 between HCT113 sample and the standard pool. The reason for this difference could be matrix effects due to the different lipid composition in the respective samples. Differences in peak areas among replicates are more likely caused by the lower injection concentration of the samples and not by the matrix itself. It is important to equilibrate the column not only with a blank but also with the lipid target compounds (lipid-QC) and avoid retention time shifts in the LC method. For qualitative analysis, a good signal response is also important for potential isotopologue monitoring and stable retention times.

3.2.3 Ionisation methods for glycosphingolipids

For sphingolipids in general tandem mass spectrometry (MS/MS) is essential in structural elucidation. There are four main ion dissociation (fragmentation) techniques that can be used: 1) collision-induced 2) electron-aided 3) photoinduced and 4) chemical-induced dissociations. These dissociation techniques break bonds at distinct sites within the molecule and the integration of these techniques can offer a comprehensive understanding of the structure of glycosphingolipids. With the capacity to forecast fragmentation pathways, virtual structural databases could be developed to detect both identified and unidentified glycosphingolipids.[129]

The electrospray ionization (ESI) is the most used ionization method in the lipidomic area, but there is also the APCI method, which can be used for neutral lipids.[131]

The measurements in this project were carried out with a heated electrospray ionization (H-ESI). The process of heated-electrospray ionization involves using a heated auxiliary gas along with electrospray ionization (ESI) to convert ions in a solution into gas phase ions. This method is useful for analyzing polar compounds that can form ions in solution. For instance, basic compounds can form a protonated molecule $[M+H]^+$, while acidic compounds can form a deprotonated molecule $[M–H]^-$. When operating in the positive ion polarity mode, the peak at an m/z value of M + 1 is produced by the protonated molecule, where M is the original molecule's mass. On the other hand, when the negative ion polarity mode is used, the peak generated by the deprotonated molecule appears at an m/z value of M – 1, where M refers to the original molecule's mass. The sample ions can have a single charge or multiple charges, and this is determined by the chemical structure of the analyte and the solvent being used as a carrier. Several factors can impact the H-ESI process, including the size of the droplets, surface charge, liquid surface tension, solvent volatility, and the strength of ion solvation. Electrospray efficiency is adversely affected by the presence of large droplets with high surface tension, low volatility, strong ion solvation, low surface charge and high conductivity. Volatile acids and bases are mainly used, but salts above 10 mM concentration and strong acids and bases are extremely detrimental. For highly demanding applications, the HESI-II probe offers improved nozzle performance and better desolvation, resulting in increased sensitivity.[131]

In mass spectrometry, heavily glycosylated sphingolipids show low ionization efficiency due to their reduced hydrophobicity and volatility. This problem is further exacerbated by labile

groups such as sialic acid or fucose. If the method is not tailored to the labile groups, these structures can be cleaved off during ionization and missed.[132]

3.2.4 Setup for the HESI-source parameter validation

The parameters of the HESI source settings of the standard pool sample were checked for their separation, peak width and peak area with Skyline and the fragment patern with freestyle 1.8 after each measurement. After reviewing the results, the individual parameters were then optimized and a new series of measurements started. This process was carried out with different ESI source setting parameters (Table 11 and Table 12) until a promising method for the analysis of the selected lipid classes was reached.

The ESI source parameters for identification of glycosphingolipids were adjusted for positive and negative ion mode. The instrument was used separately for negative and positive ion mode and started with the origin settings: Full MS scans were followed by data-dependent MS2 (ddMS2) scans. During full MS runs, data in the range of 500-2000 m/z were acquired with a resolution of 120,000, an AGC target of 1e6, and a maximum injection time (IT) of 100 ms. During MS2 acquisition, a resolution of 30,000 was used in the range of 400-2000 m/z, with an AGC target of 1e5, a maximum IT of 54 ms, an isolation window of 1.0 m/z, and a normalized collision energy (NCE) of 35. Inclusion lists, which contained the m/z values of single and double charged H-adducts of different glycosphingolipid classes, were used for the acquisition of MS2 spectra in negative and positive ion mode.

3.2.5 HESI-source parameter

The optimization of an analysis of GSL with MS/MS depends on several parameters. Mainly, the settings of the HESI source play an important role in ionization and fragmentation. Therefore, it is useful for method validation to adjust the parameters to the glycosphingolpids. The HESI-source settings of the origin method are parameters that were developed and tested for a measurement with gangliosides.[93] Based on these settings, the different changes of the parameters were tested with standard sample measurements to obtain the method for the five GSL classes. All GSL classes studied are in a mass to charge ratio range of 500 to 2000. This range was maintained for the entire measurement. Variations at the NCE showed different structural information to the glycan and the ceramide part of the GSL in a Q Exactive HF experiment.[133] GSL required a relatively high RF voltage, resulting in a higher hit rate for precursor ions. By increasing the RF level of the S-lens, more ions are fragmented in the S-lens and high m/z productions are more likely to pass through the S-lens than low m/z ions.[134] It is important to note that the optimal source parameters for a glycosphingolipid method in MS will need to be empirically determined through experimentation and optimization.

Slight differences in operating parameters of the optimized method can be seen between negative (sheath gas flow: 40, auxillary gas flow: 15, sweep gas: 4, capillary temperature 200 °C, RF lens voltage: 50, auxillary gas heater temperature: 250 and NCE: 30) and positive mode (sheath gas flow: 30, auxillary gas flow: 5, sweep gas: 2, capillary temperature 250 °C, RF lens voltage: 47, auxillary gas heater temperature: 350 and NCE: 26). The full MS properties (MS1 resolution: 120,000, MS1 AGC target: 1 e6, MS1 maximum IT: 100 ms) and the ddMS2 settings (MS2 AGC target: 1 e5, MS2 maximum IT: 54 ms, loop count: 5, topN: 5, isolation window 1 m/z, appex trigger: 1 to 4 s, charge exclusion: 3 - 8, >8, exlude isotope: on, dynamic exclusion: 5 s, if idle: pick others) were equal in positive and negative mode.

Fragmentation was limited to ions whose m/z ratio appeared in the inclusion list and no other ions were selected. Additionally, any precursors that had already undergone fragmentation in ddMS2 spectra were not fragmented in subsequent measurements. Table 10 provides a concise overview of the used parameters of the RP-HRMS/MS methods.

negative mode	origin method	test methods	new method
sheath gas	35	30, 40	40
aux gas	10	5, 15	15
sweep gas	2	0, 4	4
cappilary temperature	250	200, 300	200
RF-lens voltage	45	40, 43, 47, 50	50
aux gas heater temperature	300	250, 350	250
NCE	27	21, 24, 27, 30, 33	30
Properties of Full MS - negative polarity			
scan range (m/z)	500 - 2000	400 - 2000	400 - 2000
MS1 resolution	120,000	120,000	120,000
MS1 AGC target	1 e6	1 e6	1 e6
MS1 maximum IT	100 ms	100 ms	100 ms
Properties of dd-MS2			
MS2 resolution	30,000	30,000	30,000
MS2 AGC target	1 e5	1 e5	1 e5
MS2 maximum IT	54 ms	54 ms	54 ms
loop count	5	5	5
topN	5	5	5
isolation window	1.5 m/z	1, 1.5, 2 m/z	1 m/z
Appex trigger	-	1 to 4 s	1 to 4 s
charge exclusion	-	3 - 8, > 8	3 - 8, >8
exclude isotope	on	on	on
dynamic exclusion	5 s	5 s	5 s
if idle	pick others	pick others	pick others
Inclusion list	on	on	on

Table 11. overview of the used parameters of the RP-HRMS/MS methods in negative mode

positive mode	origin method	test methods	new method
sheath gas	30	40, 50	30
aux gas	5	0, 10, 15	5
sweep gas	2	0, 4, 6	2
cappilary temperature	220	200, 250, 300	250
RF-lens voltage	45	35, 40, 43, 47	47
aux gas heater temperature	300	250, 350	350
NCE	23	17, 20, 26, 29, 32	26
Properties of Full MS -positive polarity			
scan range (m/z)	500 - 2000	400 - 2000	400 - 2000
MS1 resolution	120,000	120,000	120,000
MS1 AGC target	1 e6	1 e6	1 e6
MS1 maximum IT	100 ms	100 ms	100 ms
Properties of dd-MS2			
MS2 resolution	30,000	30,000	30,000
MS2 AGC target	1 e5	1 e5	1 e5
MS2 maximum IT	54 ms	54 ms	54 ms
loop count	5	5	5
topN	5	5	5
isolation window	1.5 m/z	1, 1.5, 2 m/z	1 m/z
appex trigger	-	1 to 4 s	1 to 4 s
charge exclusion	-	3 - 8, > 8	3 - 8, >8
exclude isotope	on	on	on
dynamic exclusion	5 s	5 s	5 s
if idle	pick others	pick others	pick others
Inclusion list	on	on	on

Table 12. overview of the used parameters of the RP-HRMS/MS methods in positive mode

3.2.6 Comparison of HESI modes

The differences between the negative and positive HESI modes are illustrated by the LacCer analysis in Figure 29 and Figure 30 for the new method and in Figure 31 and Figure 32 for the origin method of the standard pool sample. The adducts are $[M+H]^+$, $[M+2H]^+$ in positive mode

and $[M-H]^-$ and $[M-2H]^-$ in negative mode. The majority of GSLs produced a good signal response in both modes, characterized by sharply defined peak shapes with most widths ranging from 6 to 12 seconds at the baseline. 99% of the GSLs retention times were between 15 and 28 minutes. Some GSLs exhibited a weaker signal response, which could be due to their lower concentration. As mentioned earlier, some lipids classes are susceptible to faster degradation, which may lead to reduced signal responses. Another factor that could contribute to this observation is solubility or interaction with matrix content. It can also be seen that not only are fewer GSL lipids detected in negative than in positive mode, but also the intensities are lower. In addition, the lipid species detection is different. This result has to do with the ionization of the molecules and is due to the structure of the GSLs.

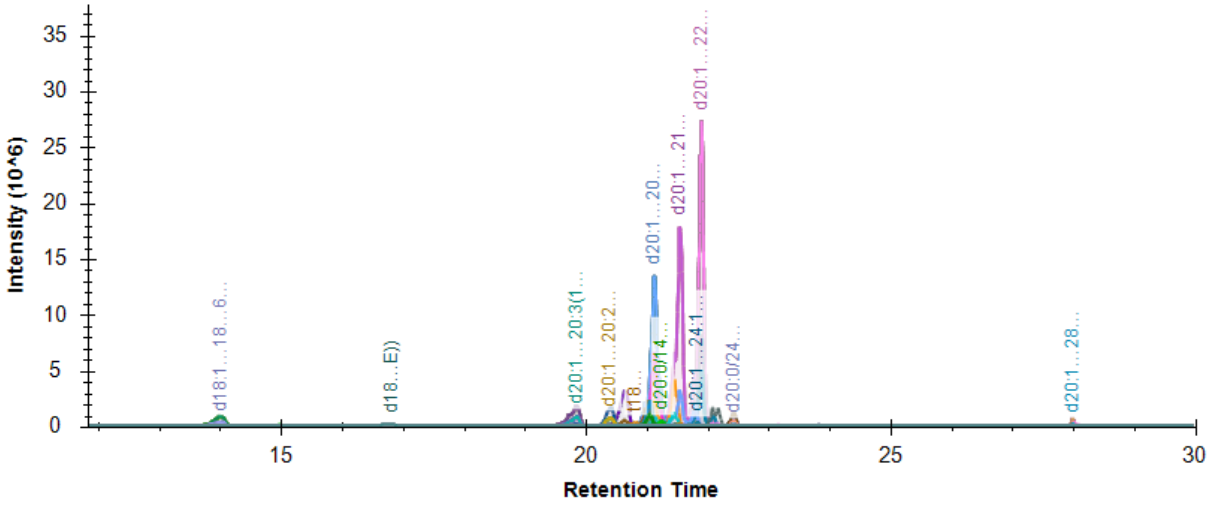

Figure 29. new HESI-source positive method for LacCer analysis (created with Skyline)

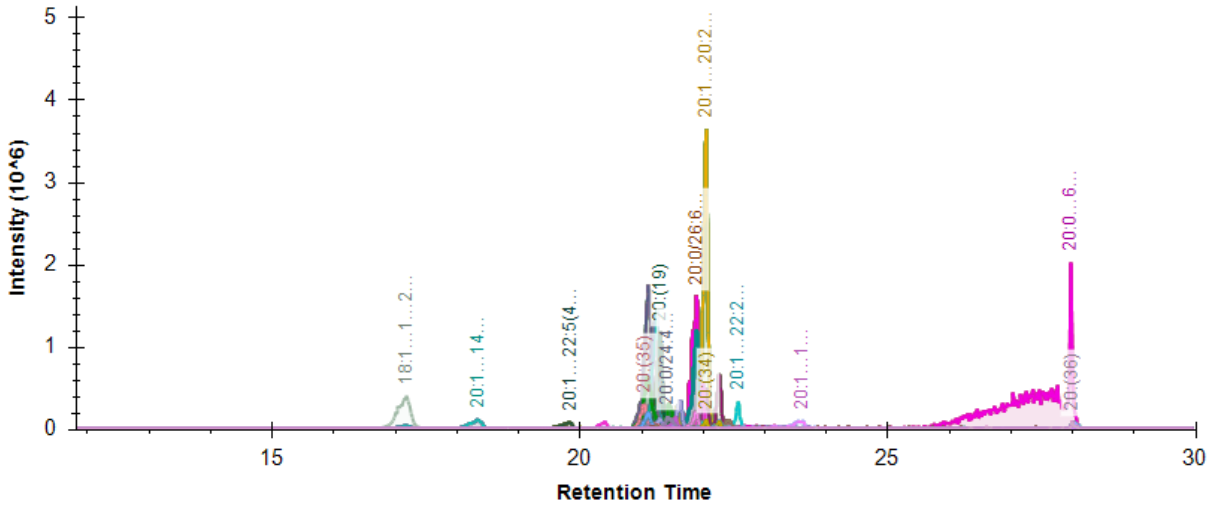

Figure 30. new HESI-source negative method for LacCer analysis (created with Skyline)

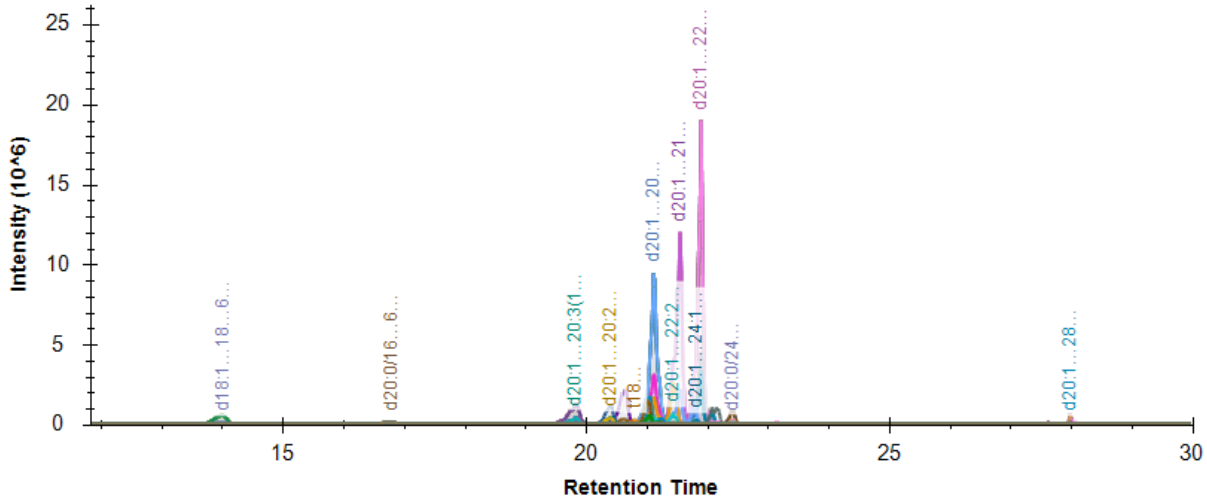

Figure 31. origin HESI-source positive method for LacCer analysis (created with Skyline)

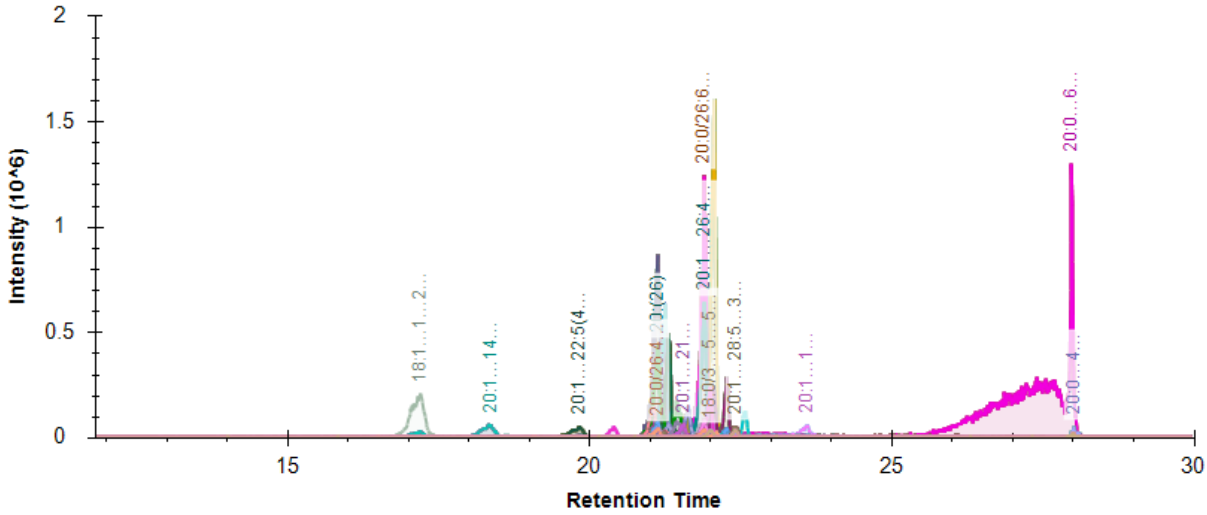

Figure 32. origin HESI-source negative method for LacCer analysis (created with Skyline)

Lactosylceramides bind two saccharide units and globotetraosylceramides (Gb4) bind three saccharide units and one N-acetylgalactosamine unit. These two groups were chosen for illustration. The results of the positive mode comparison of Gb4 are visible in Figure 33 and Figure 35 for the origin method and in Figure 34 and Figure 36 for the new method. The new method is not only an improvement for glycosphingolpids that have saccharide units in the chain (LacCer, Gb3) but also for GSLs that have additionally included N-acetylgalactosamines or N-Acetylneuraminic acid (Gb4, GloboH, GM3). In the direct overview comparison of all species between the original method for gangliosides and the new method for the five GSL classes, a significant increase in the intensity of most of the detected LacCer and Gb4 can be seen in Figure 37and Figure 38.

Higher intensities also result in a higher peakarea. This leads to a better detection of the individual lipid species. Figure 29-36 shows the comparison between the original method and the optimized new method for the most abundant lactosylceramides and globotetraosylceramides. The increase in intensity and peak area is evident in the other GSL species in the sample, indicating the improvement in detectability of the GSL lipids by the new method.

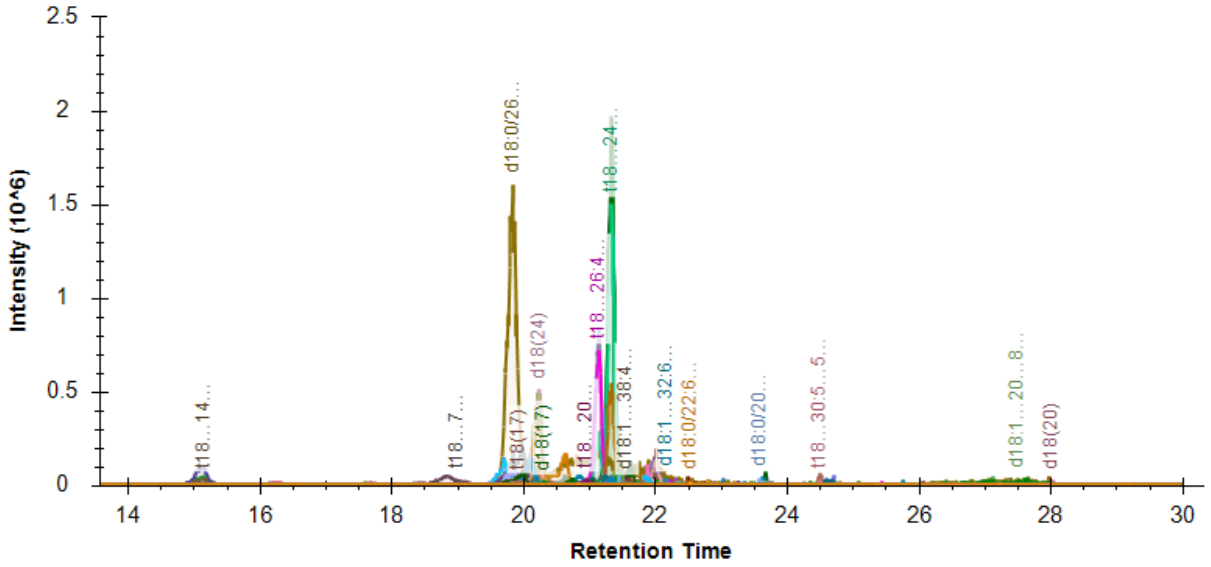

Figure 33. origin HESI-source positive method for Gb4 analysis (created with Skyline)

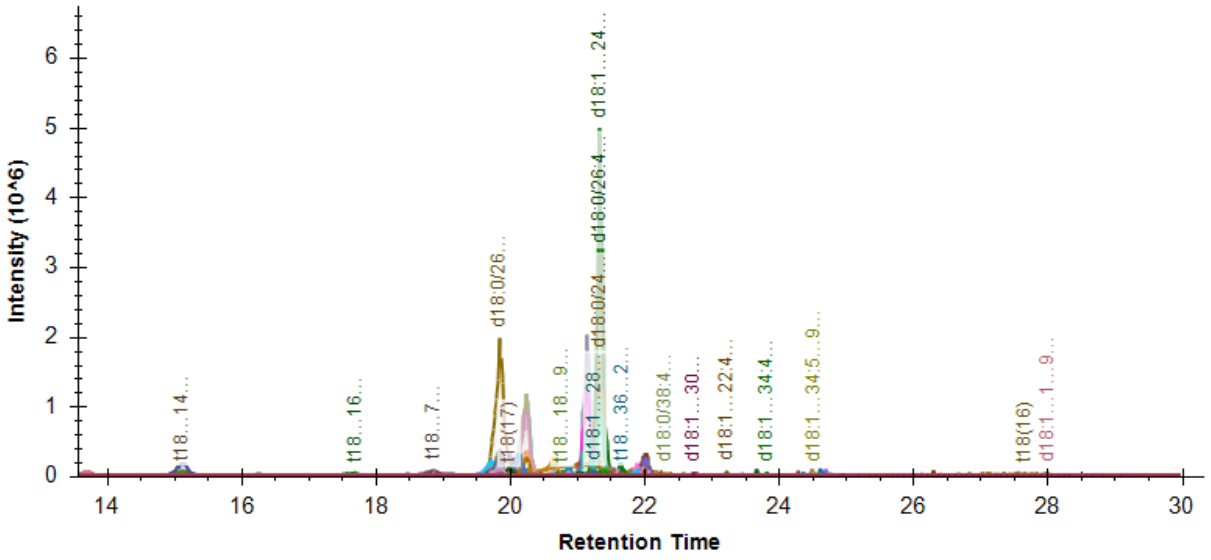

Figure 34. new HESI-source positive method for Gb4 analysis (created with Skyline)

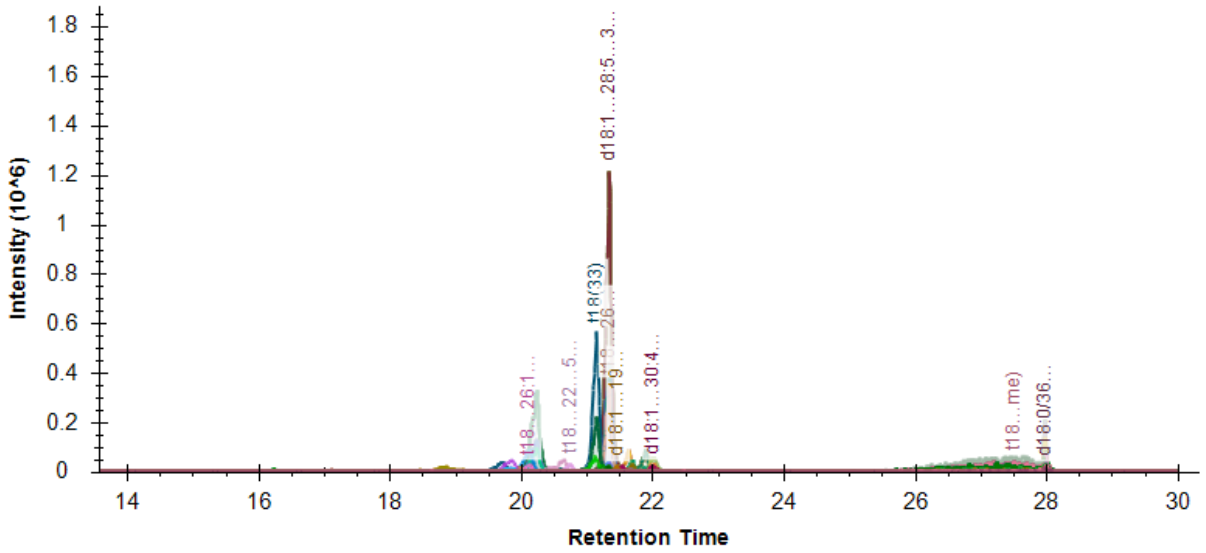

Figure 35. origin HESI-source negative method for Gb4 analysis (created with Skyline)

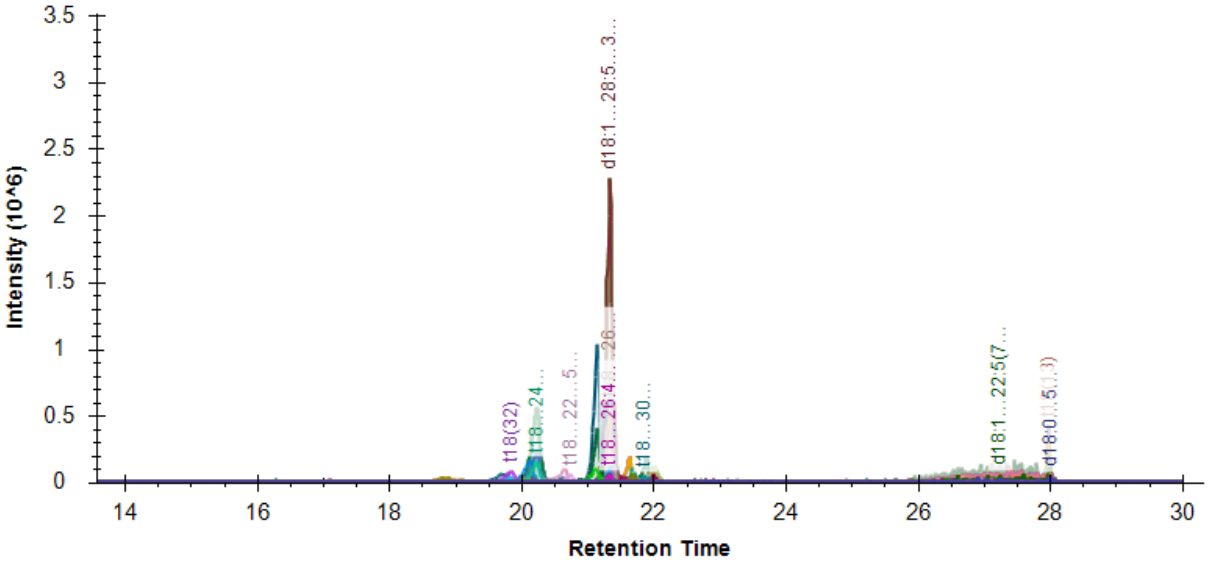

Figure 36. new HESI-source negative method for Gb4 analysis (created with Skyline)

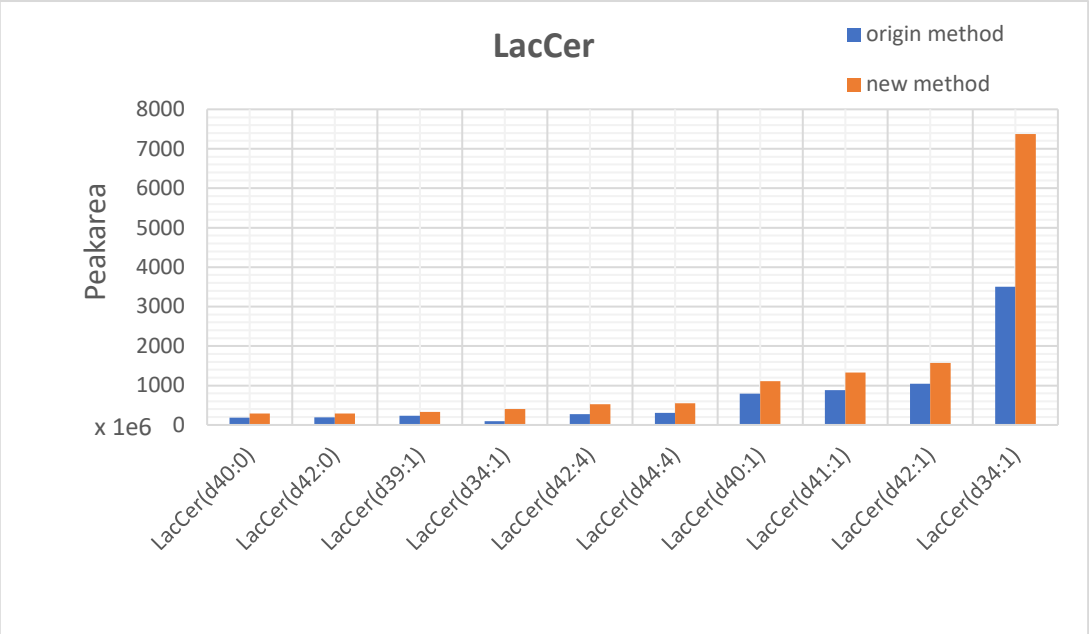

Figure 37. comparison highest Peakarea origin/new method for LacCer analysis in standard pool

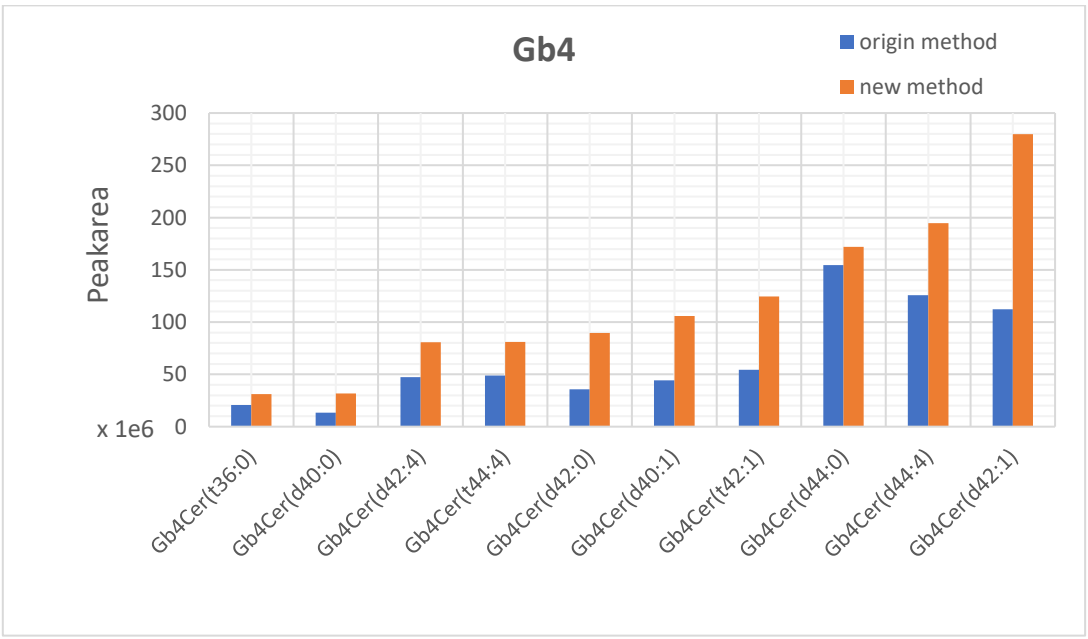

Figure 38. comparison highest Peakarea origin/new method for Gb4 analysis in standard pool

3.3 Analysis of colon cancer samples using the developed glycosphingolipid assay

As proof of concept, the efficacy of the workflow was demonstrated for analyzing human cancer cells. The new method was employed to analyze and evaluate the HCT116 cell line. The analysis revealed the presence of all GSL classes at various species levels, as depicted in Figure 39 for LacCer and Figure 41 for Gb4. The HCT116 colon cancer cell line was compared to the origin reference method, which are shown in this project with the ten most occurred species of LacCer (Figure 40) and Gb4 (Figure 42). The new method convinces with higher peak areas and peak intensities for all five studied GSL classes.

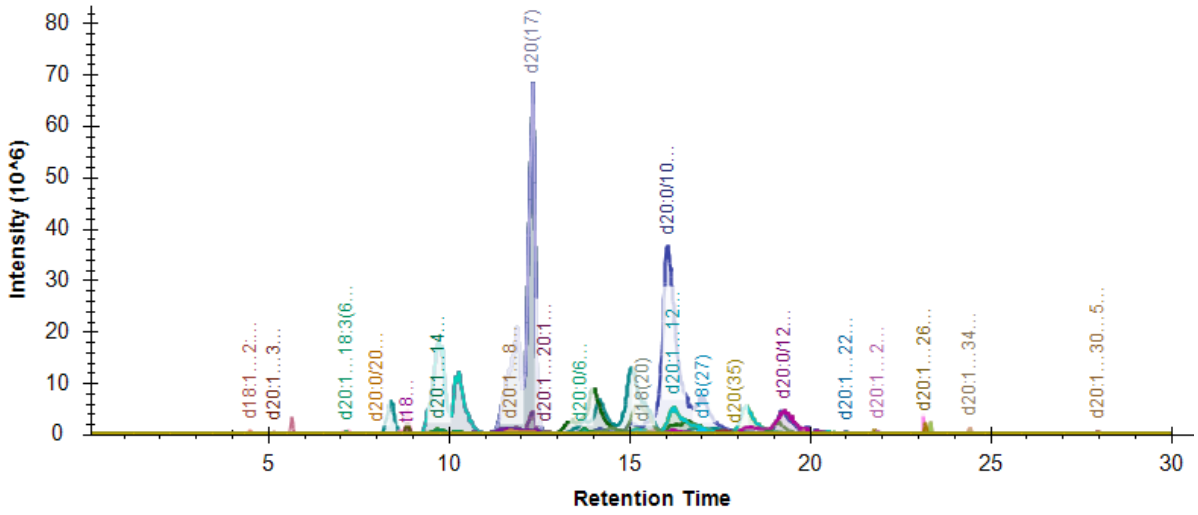

Figure 39. new method positive mode for LacCer analysis in HCT116 sample (created with Skyline)

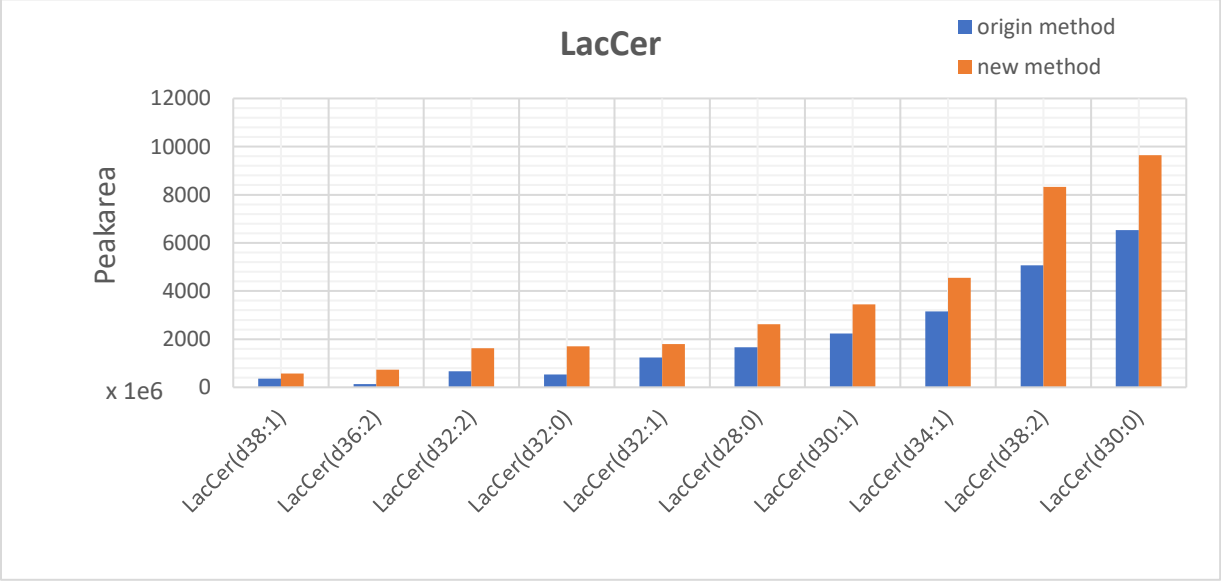

Figure 40. comparison highest Peakarea origin/new positive mode method for LacCer analysis in HCT116 sample

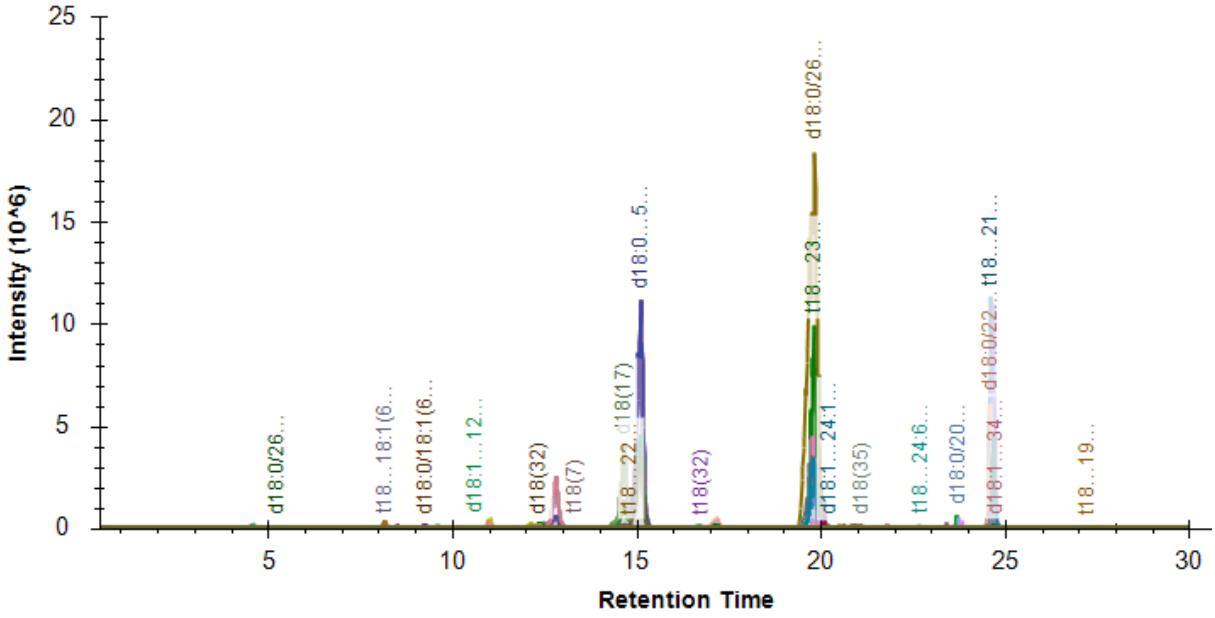

Figure 41. new method positive mode for Gb4 analysis in HCT116 sample (created with Skyline)

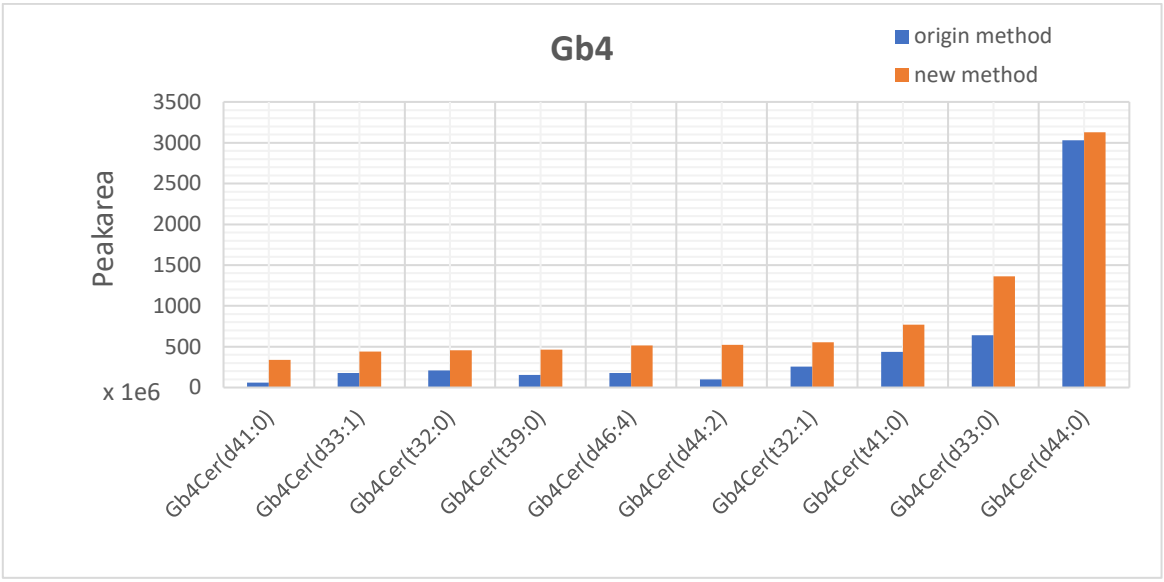

Figure 42. comparison highest Peakarea origin/new positive mode method for Gb4 analysis in HCT116 sample

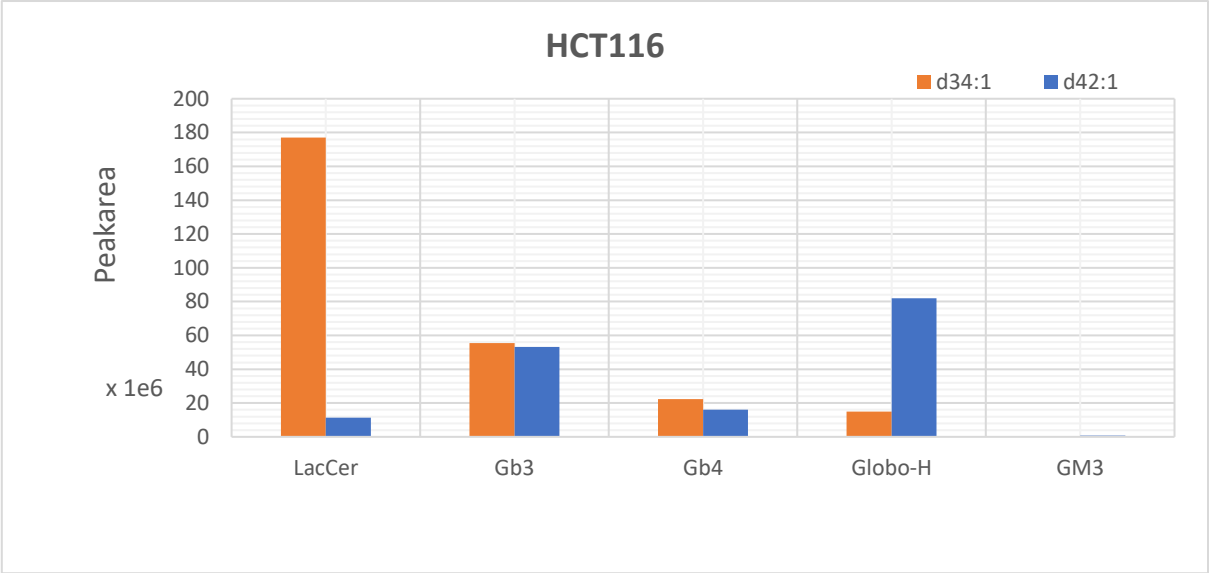

Figure 43. comparison Peakarea new method for d34:1/d42:1 species in HCT116 sample

Figure 43 demonstrates the distinct distribution of individual lipid species within a class. Species d34:1 and d42:1 were selected for display as they have significant roles in various cancer types and have been widely studied in functional and expression studies. The d34:1 species is more prevalent in lactosylceramide than d42:1. The globosides Gb3 and Gb4 have a nearly balanced ratio and in Globo-H the d42:1 species predominates. Only very small amounts have been detected for these two species for ganglioside GM3 with a higher d34:1 proportion.

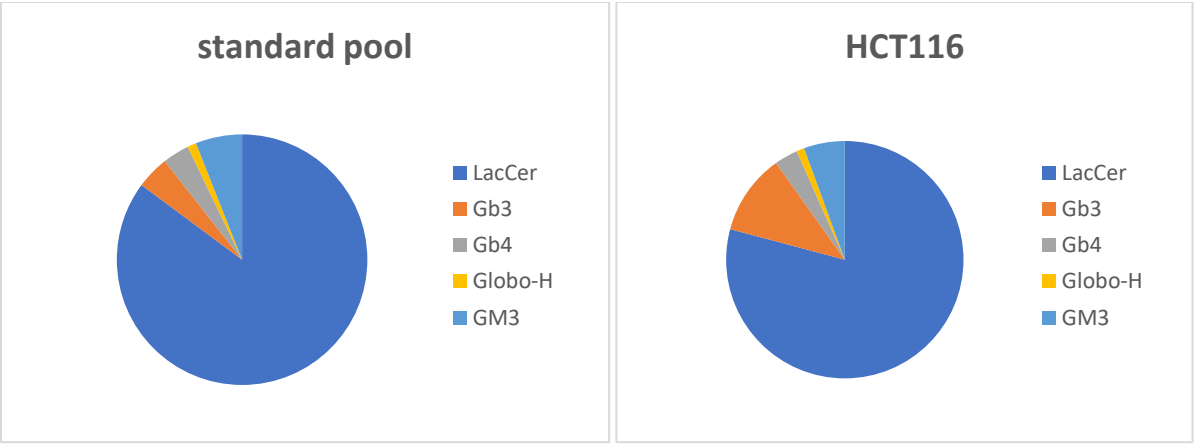

Figure 44. distribution of GSL classes in standard pool and HCT116 sample

There are clear differences in lipid species and peakarea between lactosylceramides and Gb4, as well as all other studied GSL classes. The highest abundant GSL in standard pool samples

and in the colon cancer sample, is the lactosylceramide class (Figure 44), based on the peakareas. This result is due to the fact that LacCer is considered a precursor in the biosynthesis of the other GSL classes and is accordingly present in a higher amount and could be also caused by potential in-source fragmentation of the other classes, which will be investigated in follow-up studies. The cause of the species differences among the classes cannot be found using the applied experimental setup. However, this is suspected to be due to their different functions and distributions in the cell. The most represented LacCer species in the standard pool is d34:2 and d30:0 in the cancer sample. Regarding Gb3, the major species is d42:1 in the standard pool, while in the cancer sample, it is t56:4. Furthermore, the highest signals for Gb4 were observed for d42:1 in the standard pool and d44:0 in the cancer sample. Additionally, the major species for Globo-H in the standard pool is d36:0 and t44:4 in the cancer sample. Finally, for GM3, the most abundant species in the standard pool is d48:5 and d48:4 in the cancer sample.

The applied LC-MS/MS method does not enable direct localization of double bonds. The lipids are detected in FullMS as species and were represented as the amount of all isomers occurring in the species (d34:1 = d18:1/16:0, d18:0/16:1, d20:1/14:0 or d20:0/14:1). In order to determine the exact number of double bonds in the LCB and the fatty acyl chain, it is possible to draw conclusions about the respective lipids on the basis of the fragmentations in MS2.

3.3.1 GSLs in standard pool and HCT116 samples

The annotation of GSLs was mainly based on MS1 information and was determined for the overview diagrams using the single $[M+/-H]^+$ and double $[M+/-2H]^+$ adducts of the lipids present in the samples. To simplify the analysis, the pooled standard sample was used and showed similar results in a separate comparison measurement with the single standards. It can be assumed that there are no or minimal matrix effects due to the mixing and that the analysis of the three pooled standards is acceptable. The pooled standard served as the starting point for method development and was convincing in terms of the results obtained and reproducibility. The HCT116 sample, which was processed with the SIMPLEX extraction and the standard pool indicate the presence of all studied GSL classes. All samples were measured in positive and negative ionization mode. In general, dihydroxylated sphingoid bases (d) are reported more frequently than trihydroxylated bases (t) in the literature for

humans. [153] In the analyzed biological samples, d- ceramide species were also more prevalent than t- ceramide species in MS1.

standard pool	
Class	*Species*
LacCer	d34:1, d42:1, d41:1, d40:1, d44:4, d42:4, d34:1, d39:1, d42:0, d40:0
Gb3	d42:1, t42:1, d44:4, d40:1, t44:4, d42:0, d42:4, t42:0, d40:0, d42:2
Gb4	d42:1, d44:4, d44:0, t44:1, d40:1, d42:0, t44:4, d42:4, d40:0, t36:0
Globo-H	d36:0, d35:0, d37:0, t42:1, t36:1, d34:0, d33:0, d38:3, t32:1, d40:6
GM3	d38:5, d40:7, d20:1, d40:4, t38:5, d41:0, d46:5, d38:0, d36:0, d42:0
HCT116 sample	
Class	*Species*
LacCer	d30:0, d38:2, d34:2, d30:1, d28:0, d32:1, d32:0, d32:2, d36:2, d38:1
Gb3	t56:4, d50:5, d48:6, d48:6, t46:5, d44:0, d36:1, t48:6, t46:4, d28:1
Gb4	d44:0, d33:0, t41:0, t32:1, d44:1, d36:4, t39:0, t32:0, d33:1, d41:0
Globo-H	t44:4, d34:0, d40:5, d40:4, d38:6, t38:0, d42:1, t44:5, d37:1, d38:5
GM3	d48:4, d50:7, d50:4, d48:1, d43:1, d46:4, d50:6, d22:0, t36:0, d38:0

Table 13. most occurring species of the researched GSL classes identified in the standard pool sample and the HCT116 cancer cell line using negative and positive ion mode

The differences of the ten most occurring species for all studied GSLs is shown in Table 13. In addition to the dihydroxylated and trihydroxylated species, there are also strong differences in the chain length of the individual GSLs. Furthermore, the analysis shows that LacCer is the most abundant GSL class, followed by GM3, Gb3, Gb4 and Globo-H in the standard pool and followed by Gb3, GM3, Gb4 and Globo-H in the HCT116 sample. It should be noted that only very low intensities and species were detected in the standard pool sample for the Globo-H class. The signals from Globo-H lipids were excluded due to their low intensity in the identification by MS2 spectra.

3.4 GSL annotation based on fragmentation patterns in MS2

The structural diversity of GSLs arises from the variations in their LCBs and FAs, their sugar moieties, their N-acetylgalactosamines (GalNAc) moieties, their N-Acetylneuraminic acid (sialic acid) moieties and functional groups. All of these molecular properties lead to a large number of possible structures, which are part of the GSL lipidome.[135] GSL annotation should not be performed based on retention times by LC or by m/z adducts in Full-MS mode. Lipid classes, isomeric or isobaric molecules could provide a false assignment. Therefore, using fragmentation patterns with ddMS2 spectra, a more accurate structure elucidation is performed. In this project, the validated method was shown to provide good fragmentation of certain GSLs. Using the MS2 fragment spectra, the selected lipid species are viewed and conclusions about the structure are collected. Based on the numerous references in the literature (chapter 3.1.3), for all GSL classes studied (LacCer, Gb3, Gb4, Globo-H, GM3), the species d34:1 and d42:1 were selected and considered in more detail for detection in the standard pool and in the cancer sample.

Distinguishing between isomers is important, because they can have different biological effects. Variants in structure can result from the headgroup and lipid tail. The head group variants include molecules that differ in connectivity (positional isomers) or spatial orientation (stereoisomers).[136] The distinction from the Gb3 and iGb3 isomer based on the connectivity of terminal Gal to the second hexosyl and the sialic acid bond position on the hexosyl ring can also be either α2-3 or α2-6.[137,138]

Furthermore, hydroxyl groups and carbon-carbon double bonds in N-fatty acid acyl groups lead to isomeric and isobaric species. For example, GalCer d18:1(n-14)/23:1(n-9)(OH) and GalCer d18:1(n-14)/23:1(n-7)(OH) differ only in the Position of the double bond at n-7 vs. n-9. Identifying such variants presents a challenge to traditional mass spectrometry techniques.[139] Newer instruments have been developed to address these issues with special fragment techniques.[140,141]

3.4.1 Nomenclature of GSL fragments

The nomenclature of for carbohydrate fragmentations in MS/MS spectra of glycoconjugates was first addressed early by the Domon et al.[142] and further by Qinghon et al.[143] As already described in chapter 1.1 Fahy et al. together with the Lipid MAPS consortium, proposed a comprehensive classification system and developed a structural database for lipids that are

biologically relevant in 2005. Liebisch et al.[7] also proposed a shorthand notation for annotating lipid structures derived from mass spectrometry data in 2013. Based on this classification, Koelmel et al.[3] systematically characterized high-resolution MS data with exact mass and fragmentation patterns. The descriptions of Qinghon et al.[143] and the review work of Barrientos et al.[139] can be used to classify newly discovered glycolipid fragments.

The fragments are classified based on whether they include the non-reducing end (A, B, and C) or the reducing end (X, Y, and Z). The B, C, Y, and Z fragments signify glycosidic bond cleavages that establish carbohydrate sequence, whereas A and X indicate cross-ring cleavages that identify linkage positions. The superscripts in cross-ring cleavages represent which bond is cleaved. For example, cleaving the bonds between C1-C2 and C5-O generates the 1,5X ion. The ceramide fragment ions comprise E, S, T, U, and O". These result from cleaving the glycosidic bond between the ceramide and the glycan. Among these fragments, O" and E are the main fragment ions. The O" fragment is indicative of the long-chain base composition (shown in Figure 45).[143,139]

A

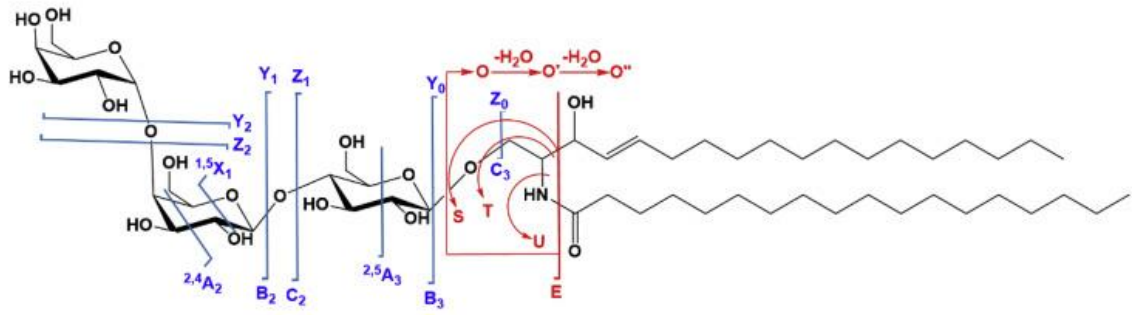

B

Glycan headgroup		Long-chain base				
Ganglioside	Sulfatide	d16:1	d18:0	d18:1	d20:0	d20:1
m/z 290	*m/z* 97	*m/z* 236	*m/z* 266	*m/z* 264	*m/z* 294	*m/z* 292

Figure 45. sections and nomeclature of the individual fragments of GSL with MS/MS

The negative mode reveals the presence of m/z 290 and m/z 97. When combined with accurate mass measurement, ions with m/z 266 (d18:0), m/z 264 (d18:1), m/z 236 (d16:1), and m/z 292 (d20:1) can identify the lipid composition in positive mode.[144] The increase in mass by 162 and 204 m/z suggests that a hexose and N-acetylhexosamine, respectively, have

been eliminated. These ions are useful in targeted tandem mass spectrometric methods for the known and also helpful in the structural elucidation of novel glycosphingolipids.[139]

3.4.2 Glycosidic fragments

In addition to the identification of peaks from Full-MS data, some species were annotated based on structural information obtained from the MS2 spectra. The fragmentation patterns suggested that cerebrosides, globosides and gangliosides are present, which contain sphingosine (S) and sphinganine (DS) as sphingoid bases. In an GIPC annotation from Blaas and Humpf's findings of sphingolipids fragments derived from the FA or LCB segment of the ceramide are frequently less detectable in negative mode.[145] In this project, the finding in the negative mode for GSL is also clearly worse than in the positive mode for most species. By using the positive ion mode of fragments, the structural elucidation of the LCB unit could be performed comprehensively. By studying LCB fragmentation and losses of sugar units, conclusions can be made about the fatty acyl chain. Based on the fragment formation provided, fragment lists could be generated for the GSL classes studied.

Table 14 summarizes the possible detected fragments in analyses of the five glycosphingolipid classes. All detected fragments are singly charged. The bonds are commonly cleaved before and after the adjacent oxygen atom, as displayed in Figure 45. Furthermore, most of the detected precursors contain H-adducts or water loss aducts. In the case of glycoside neutral losses, it should be noted that single or double water splitting can occur, as can be seen in Figure 46 in an MS2 spectrum of LacCer d34:1. The different sugar units that occur (glucose, galactose) were designated as hexoses, because they are not differentiated by this MS instrument. The calculation of the fragments was based on LIPID enviPat Web[98] and LIPID MAPS database[3]. The mass tolerance was set at 5 ppm. For fragments in the low m/z range little differences end up in quite high ppm values.

Ceramide fragment ions	**Sugar ring fragment ions**
FA	$C_6H_{10}O_5$,[Hex]
FA – H_2O	$C_5H_9O_4$,[X_1]
LCB – H_2O	$C_4H_7O_4$,[A_1]
LCB – 2xH_2O	**Ceramide neutral losses**
LCB – CH_4O_2	M - Cer
Glycosidic neutral losses	**Glycosidic fragment ions**
Lactosylceramide (LacCer)	**Lactosylceramide (LacCer)**
M - Hex(-O), [Y_1, Z_1]	Hex(-O), [B_1, C_1]
M - Hex-Hex(-O), [Y_0, Z_0]	Hex-Hex(-O), [B_2, C_2]
Globoside (Gb3)	**Globoside (Gb3)**
M - Hex(-O), [Y_2, Z_2]	Hex(-O), [B_1, C_1]
M - Hex-Hex(-O), [Y_1, Z_1]	Hex-Hex(-O), [B_2, C_2]
M - Hex-Hex-Hex(-O), [Y_0, Z_0]	Hex-Hex-Hex(-O), [B_3, C_3]
Globoside (Gb4)	**Globoside (Gb4)**
M - HexNAc(-O), [Y_3, Z_3]	HexNAc(-O), [B_1, C_1]
M - HexNAc-Hex(-O), [Y_2, Z_2]	HexNAc-Hex(-O), [B_2, C_2]
M - HexNAc-Hex-Hex(-O), [Y_1, Z_1]	HexNAc-Hex-Hex(-O), [B_3, C_3]
M - HexNAc-Hex-Hex-Hex(-O), [Y_0, Z_0]	HexNAc-Hex-Hex-Hex(-O), [B_4, C_4]
Ganglioside (GM3)	**Ganglioside (GM3)**
M - NeuAc(-O), [Y_2, Z_2]	NeuAc(-O), [B_1, C_1]
M - NeuAc-Hex(-O), [Y_1, Z_1]	NeuAc-Hex(-O), [B_2, C_2]
M - NeuAc-Hex-Hex(-O), [Y_0, Z_0]	NeuAc-Hex-Hex(-O), [B_3, C_3]

Table 14. Overview of the fragment calculation of the respective lipid class

Subtracting all saccharides from the precursor mass generates the fragment that includes the complete ceramide component, comprising both LCB and FA. However, these fragments were not detected for GSL classes. The "Glycosidic neutral losses" section mentions these fragments, which may not necessarily produce the m/z value of ceramide but can also result in partial saccharide losses in more complex glycosphingolipids. An additional list of potential m/z values were used to identify the neutral loss of the ceramide component. The use of knowledge obtained from neutral losses and glycosidic fragment ions presents an opportunity to sequence the glycan section.

3.4.3 Ceramide fragments

The differentiation of dihydroxy and trihydroxy bases in ceramide fragments require a high-resolution MS. Species that are isobaric due to the addition of an extra hydroxyl group, one less carbon atom or one additional double bond can be identified. For example, the positive LacCer d34:1 and LacCer t33:2 species have m/z values of 861.6172 and 861.5808. The utilization of HRMS enables differentiation between d- and t-species. Typically, only one chain fragment, either LCB or FA, is detected for sphingolipids. Previous research has labeled these ceramide fragments as LCB fragments[146] and rare FA fragments.[124]

The most occurring LCB species are d18:1 and d20:1, which are present in all glycosphingolipids. Fragments detected in MS2 spectra of different glycosphingolipids during this study, indicating shorter or longer chains, could potentially arise from FA fragments. This observation requires further validation with GSL species standards. The LCB frequently yields fragments with the loss of water and the number of water losses depends on LCB hydroxylation. Generally, two or three distinct fragments resulting from the same LCB species are observed. Glycosphingolipids are composed of only two chains, detecting one chain is sufficient to determine the length and saturation of the associated chain based on the molecule's precise mass.

Figure 47 shows an MS/MS fragmentation of a dihexosylceramide of the d34:1 species (LacCer d18:1/16:0) at a retention time of 14 minutes. MS2 fragmentation was based on the precursor ion $[M+H]^+$ at m/z 862.6259. The highest m/z fragment signal in MS2 comes from the water molecule loss $[M-H2O]^+$ at 844.6115. Smaller signals were observed for the loss of both sugar units at m/z 538. 5199 $[Y_0]^+$, at m/z 520.5087 $[Y_0\text{-}H_2O]^+$ for the additional loss of one water molecule and at m/z 502.4985 $[Y_0\text{-}2xH_2O\ ]^+$ due to the loss of a second water molecule. These

three signals are characteristic of the d34:1 species. The m/z 282.2784 $[O']^+$, m/z 264.2683 $[O'']^+$ and m/z 252.2678 $[O'\text{-}CH_2O]^+$ reflect the fragmentation pattern of the d18:1 long chain base and the m/z 133.0857 $[X_1]+$ for a fragment of a sugar moiety. Interpreting the entire MS2 spectrum, LacCer d18:1/16:0 can be assumed. Similar fragmentation patterns have been observed for other compounds such as LacCer d18:1/16:0 [147], GM3 d18:1/16:0 [93] oder GlcCer d18:1/12:0 [148]. All assigned fragments are listed in Table 15. Each GSL class and different isomers can be identified based on their characteristic fragments. Fragments with only one bond cleaved are anticipated to exhibit higher intensity compared to those where two bonds need to be cleaved.[149]

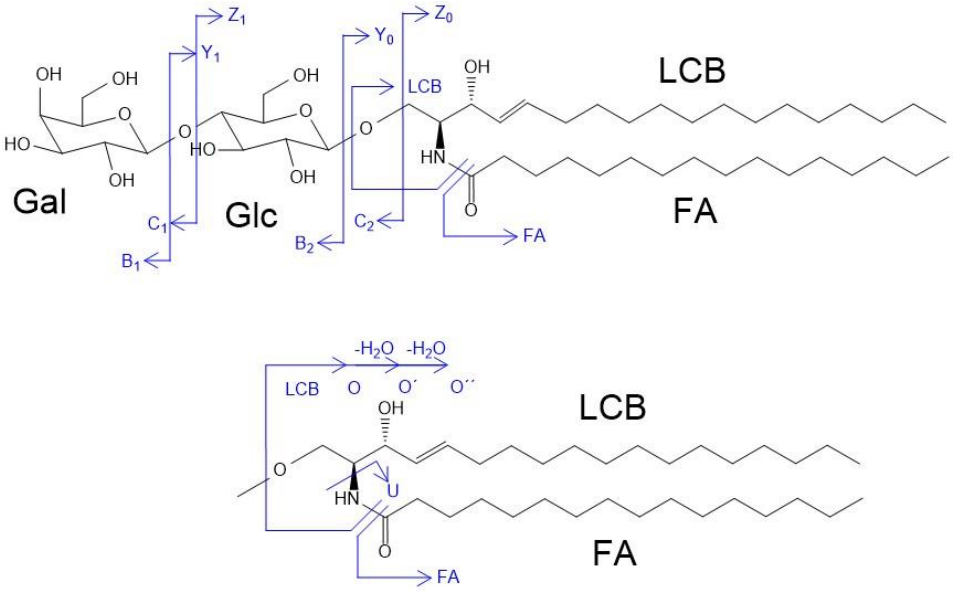

Figure 46. Structure and fragmentation behavior of LacCer d34:1 (d18:1/16:0)

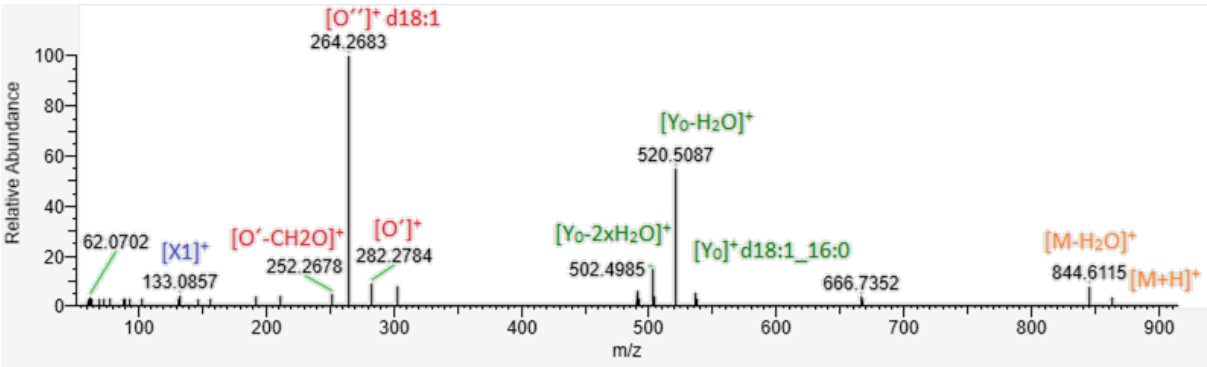

Figure 47. MS2 spectrum of LacCer d34:1 (d18:1/16:0) in positive mode (spectrum created using Freestyle 1.8)

MS2 (+) LacCer(d18:1/16:0)

fragment ion	sum formula	exp. m/z	cal. m/z
$[M+H]^+$	C46H88NO13	862.6259	862.6250
$[M-H_2O]^+$	C46H86NO12	844.6115	844.6145
$[Y_0]^+$	C34H68NO3	538.5195	538.5199
$[Y_0-H_2O]^+$	C34H66NO2	520.5087	520.5088
$[Y_0-2xH_2O]^+$	C34H64NO	502.4985	502.4982
$[O´]^+$	C18H36NO	282.2784	282.2791
$[O´´]^+$	C18H34N	264.2683	264.2686
$[O´-CH_2O]^+$	C17H34N	252.2678	252.2686
$[X_1]^+$	C5H9O4	133.0857	133.0495

Table 15. observed fragmentation in MS2 of LacCer d34:1 in positive mode (d18:1/16:0)

Figure 49 shows MS/MS fragmentation of Gb4 of the d42:1 species (Gb4 d18:1/24:0) at a retention time of 21 minutes and 30 seconds in positive mode and 21 minutes and 34 seconds in negative mode. In positive mode, MS2 fragmentation is based on the precursor ion $[M-H]^-$ at m/z 1337.8632. The highest m/z fragment signal in MS2 comes from the remaining molecule after the loss of a hexose (Gal) and an N-acetylgalactosamine (HexNAc or NAc-Gal) at 956.7344 $[Z_2]^+$. Smaller signals were observed for the loss of N-acetylgalactosamine and two sugar units at m/z 794.6849 $[Z_1]^+$, for the loss of N-acetylgalactosamine and three sugar units at m/z 650.6470 $[Y_0]^+$, for the loss of one water molecule at m/z 632.6345 $[Y_0-H_2O]^+$ and for the loss of a second water molecule at m/z 614.6243 $[Y0-2xH_2O]^+$. These signals are characteristic of the d42:1 species. The m/z 282.2789 $[O']^+$, m/z 264.2684 $[O'']^+$ and m/z 252.2678 $[O'-CH_2O]^+$ reflect the fragmentation pattern of the d18:1 long chain base. The m/z 366.1402 $[B_2]^+$ and m/z 204.0867 $[B1]^+$ reflect the fragmentation of two and one sugar units, respectively. Based on the entire MS2 spectrum, it can be assumed that the compound is Gb4 d18:1/24:0.

In negative mode (Figure 50), MS2 fragmentation proceeds based on the precursor ion $[M+H]^+$ at m/z 1339.8840. The highest m/z fragment signal in MS2 comes after the loss of one N-acetylgalactosamine (HexNAc or NAcGal) at m/z 1134.7875 $[[Y_3]^-$ and one additional hexose at m/z 972.7406 $[Y_2]^-$. Smaller signals were observed for the loss of N-acetylgalactosamine and two sugar units at m/z 810.6812 $[Y_1]^-$, and for the loss of N-acetylgalactosamine and three sugar units at m/z 648.6288 $[Y_0]^-$. The m/z 263.2620 $[O'']^-$ signal is characteristic of the d18:1 long chain base again. The m/z 177.0417 $[Hex+O]^-$ and m/z 161.0455 $[Hex]^-$ reflect the fragments of one sugar unit. All assigned fragments are listed in Table 16 and Table 17. In the case of glycoside neutral losses, it should be noted that single or double water splitting can occur, as seen in Figure 48 in an MS2 spectrum of LacCer d34:1.

In contrast to the positive mode, no clear identification of the ceramide is visible in the negative mode and no water loss is visible in any fragment. However, in the negative mode, all single cleaved fragments of the sugar units are visible and can be easily identified. The positive and negative spectra of GSL reveals that glycan fragments are more commonly present in negative ion mode and positive ion mode exhibits a higher abundance of ceramide fragments. Similar MS/MS fragmentation patterns and fragmentation masses for Gb4 d42:1 (d18:1/24:0) are available in the literature.[150,151,152]

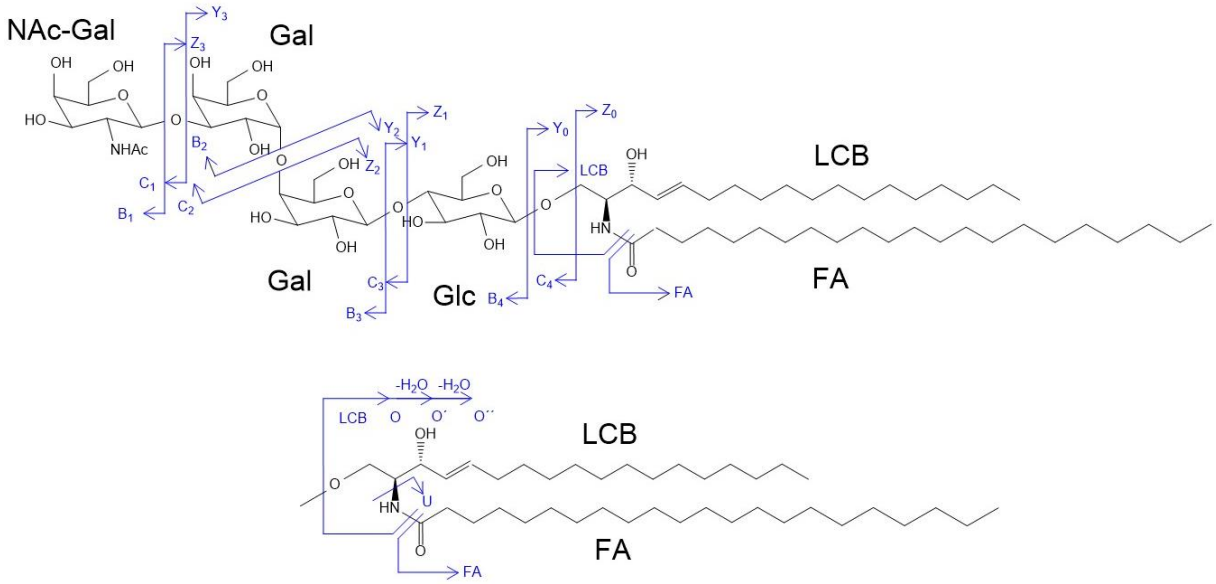

Figure 48. Structure and fragmentation behavior of Gb4 d42:1 (d18:1/24:0)

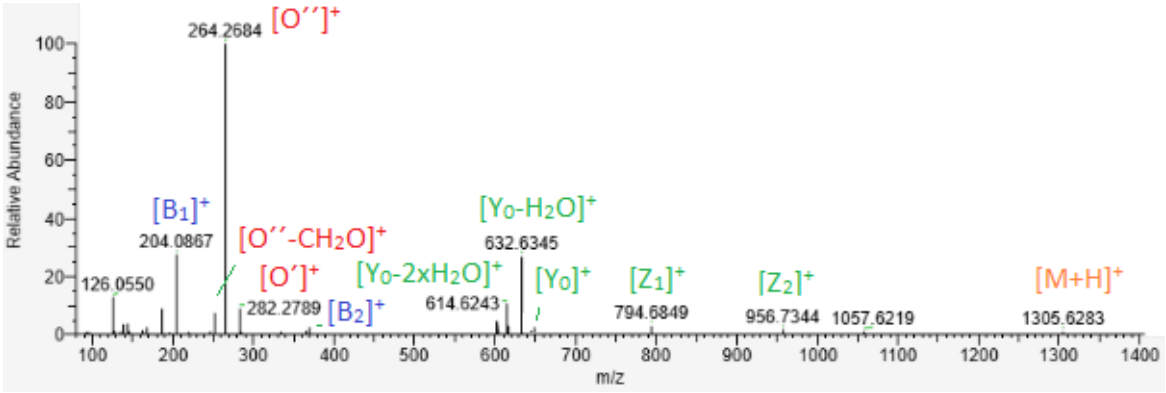

Figure 49. MS2 spectrum of Gb4 d42:1 (d18:1/24:0) in positive mode (spectrum created using Freestyle 1.8)

MS2 (+) Gb4(d18:1/24:0)

fragment ion	sum formula	exp. m/z	cal. m/z
$[M+H]^+$	C68H126N2O23	1339.8840	1339.882
$[Z_2]^+$	C54H102NO12	956.7344	956.7397
$[Z_1]^+$	C48H92NO7	794.6849	794.6868
$[Y_0]^+$	C42H84NO3	650.6470	650.6446
$[Y_0\text{-}H_2O]^+$	C42H82NO2	632.6345	632.634
$[Y_0\text{-}2xH_2O]^+$	C42H80NO	614.6243	614.6234
$[B_2]^+$	C14H24NO10	366.1402	366.1395
$[O´]^+$	C18H36NO	282.2789	282.2791
$[O´´]^+$	C18H34N	264.2684	264.2686
$[O´´\text{-}CH_2O]^+$	C17H34N	252.2690	252.2686
$[B_1]^+$	C8H14NO5	204.0867	204.0866

Table 16. observed fragmentation in MS2 of Gb4 d42:1 in positive mode (d18:1/24:0)

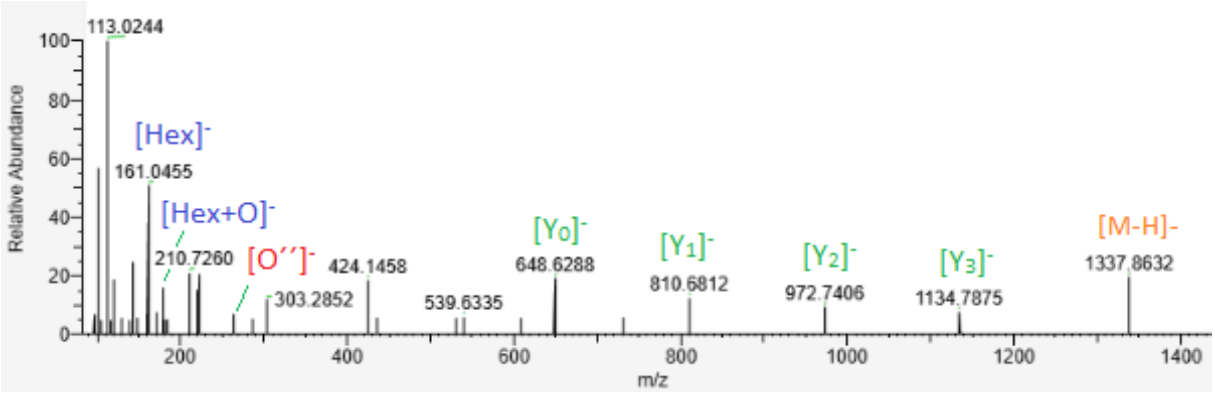

Figure 50. MS2 spectrum of Gb4 d42:1 (d18:1/24:0) in negative mode (spectrum created using Freestyle 1.8)

MS2 (-) Gb4(d18:1/24:0)

fragment ion	sum formula	exp. m/z	cal. m/z
$[M-H]^-$	C68H125N2O23	1337.8632	1337.8679
$[Y_3]^-$	C60H112NO18	1134.7875	1134.7885
$[Y_2]^-$	C54H102NO13	972.7406	972.7357
$[Y_1]^-$	C48H92NO8	810.6812	810.6828
$[Y_0]^-$	C42H82NO3	648.6288	648.6300
$[O´´]^-$	C18H33N1	263.2620	263.2618
$[Hex+O]^-$	C6H9O6	177.0417	177.0405
$[Hex]^-$	C6H9O5	161.0455	161.0455

Table 17. observed fragmentation in MS2 of Gb4 d42:1 in negative mode (d18:1/24:0)

Individual lipids from the classes studied were considered for the d34:1 and d42:1 species in MS2 and an overview finding for fragmentation was made. The number of detected ddMS2 spectra is related to the given inclusion list and the masses to be fragmented. During the project this list was adapted several times and possible changes were observed. Thereby, the classical singly charged adducts $[M+H]^+$, $[M-H]^-$ and the doubly charged $[M+2H]^+$, $[M-2H]^-$ adducts, showed the most hits. Masses resulting from other adducts, such as $[M+NH_4]^+$, $[M+OAc]^-$ and $[M+COOH]^-$, were calculated and tested for the lactosylceramide class. The overview results were poor and therefore they were removed from the inclusion list. The precursors $[M+K]^+$, $[M+Na]^+$ and $[M+Li]^+$ were not tested in any inclusion list due to the

assumption that potassium, sodium or lithium were very low or absent in the sample extract or the running medium. Based on the ddMS2 spectrum, $[M+H]^+$, $[M-H]^-$, $[M-H_2O]^+$ and $[M-H_2O]^-$ emerge as the most abundant precursors for the positive and negative modes.

The fragment pattern was extracted using FreeStyle™ 1.8, which were further compared to spectral files at NIST/mzVault (Freestyle 1.8), mzCloud and LIPID MAPS. Unfortunately, no MS2 fragment spectra are available to date for the studied GSL lipids and could not be compared to any database. However, in LIPID MAPS there is the possibility to generate fragment ions for many sphingolipid classes and thus allows the generation of fragment lists.

For even more accurate structure information (stereoisomers), instruments with higher resolution and stronger fragmentation techniques or nuclear magnetic resonance (NMR) are needed. Besides CID (collision induced dissociation), HCD (higher energy collisional dissociation), ozone induced dissociation, ultraviolet photodissociation (UVPD), newer methods such as electron impact excitation of ions from organics (EIEIO) are also possible for fragmentation.

3.5 Conclusion and outlook

The aim of this project was to develop a LC-MS-based method for glycosphingolipid profiling with a focus on latosylceramides, globosides and gangliosides using a GSL standard pool and HCT116 human colon cancer sample. The extraction method for the HCT116 cell line was based on the SIMPLEX [92] workflow and was successful in isolating the desired lipids, especially the GSLs. Lipid extracts were analyzed by RP-HRMS/MS on a Orbitrap high-resolution mass spectrometer in positive and negative mode using an ACN/H_2O/IPA-based gradient with a total run time of 30 min. This approach showed satisfactory peak shape and effective separation of the GSL categories with different saccharide variations. All GSL classes (lactosylceramides, globosides (Gb3, Gb4, Globo-H) and gangliosides (GM3)) could be separated by the reversed phase LC method and most of them eluted between minute 5 and 28. It should be noted that extending the method by an additional 5 minutes, may ensure an improvement in separation and identification. The retention times of the individual GSL classes depend on the sugar chain length and the LCB/FAs length, as described in chapter 3.2.1. Following the elution order of the d34:1 species for all GSL (Figure 25), GM3 eluted first, ahead of Gb4, Gb3, Globo-H and LacCer. Hydroxylated saturated long-chain fatty acids with a chain length of 38 carbon atoms were detected alongside very short-chain fatty acids with 2 carbon atoms, including odd FA chains. The ten most occurred species of each GSL class were considered for method comparison.

RP-HRMS/MS enables the separation and identification of isomers with different LCB and fatty acid compositions. The HESI-source settings were adjusted to the studied GSL classes and analyzed in several validation measurements. Reproducibility was ensured by LipidQC with ^{13}C enriched LILY lipids for class specific and retention time checking analysis. Full-MS acquired MS1 data was analyzed with Skyline and comprehensive target lists for single and double charged H-adducts for the five GSL classes were created. An overview of the highest occurring GSL classes and species was provided by the detected peak areas in the chromatograms. The variations in lipid species of the most abundant GSL classes were detected. The most prominent ceramide moiety was d18:1-LCB for the standard pool and d18:0-LCB for the HCT116 cell line, which match with the results from the GSL cancer literature (chapter 3.1.3). The investigated colon cancer sample revealed over 50 species in different levels in each GSLs class. The differences of the lipid species in the HCT116 cell line can be explained by varying

functions and altered expression in cancer cells in general. Detected lipid species can have underlying isomers and isobars, which provide potential false assignment in Full-MS (chapter 3.4.1). Small mass shifts could also lead to false associations in the t-species assignment. By utilizing fragmentation patterns alongside ddMS2 spectra, a more precise and correct determination of the structure is possible. The MS2 spectra assigned was possible in both modes and used for the assignment of a selected panel of GSLs. However, less fragmentation occurred in the negative mode, which could be explained by decreased ionization efficiency or a general performance problem of the instrument. The re-measurement with a maintained instrument and the change of some HESI-source settings could achieve better results in negative mode. The developed workflow was the first step towards a comprehensive assay for GSL classes by RP-MS/MS and could pave the way to a more comprehensive understanding of GSL structures and their occurrence in cancer. Overall, the method proved to be fit for purpose for GSL analysis in different complex samples revealing structural details up to the molecular lipid species level.

The developed method is not capable of resolving different double bond positions, which can exhibit different biological activities, as described in chapter 1.1. For this purpose, different analytical strategies for additional GSL structural details have to be applied such as novel fragmentations strategies or chemical derivatization. Additionally, follow-up studies will need to focus on the quantitative aspect of the developed lipidomic research methods for glycosphingolipids e.g. by spiking labeled GSL standards in the sample of interest. For annotation purposes, targeted GSL analysis was performed based on the open-source program Skyline. To enable non-targeted GSL analysis in a sample of interest, other software solution are necessary for automated GSL assignment (e.g. LDA[155]). The use of novel high-resolution MS setups enabling further fragmentation (MS3, MSn) will also improve the developed GSL workflow.

4. References

1. Bou Khalil, M., Hou, W., Zhou, H., Elisma, F., Swayne, L. A., Blanchard, A. P. & Figeys, D. Lipidomics era: accomplishments and challenges. Mass spectrometry reviews, 29(6), 877-929. (2010)

2. Fahy, Eoin, et al. A comprehensive classification system for lipids1. Journal of lipid research 46(5), 839-861. (2005)

3. Koelmel, J. P., Ulmer, C. Z., Jones, C. M., Yost, R. A., & Bowden, J. A.. Common cases of improper lipid annotation using high-resolution tandem mass spectrometry data and corresponding limitations in biological interpretation. Biochimica et Biophysica Acta (BBA)-Molecular and Cell Biology of Lipids, 1862(8), 766-770. (2017)

4. Kelley, N. S., Hubbard, N. E., & Erickson, K. L. Conjugated linoleic acid isomers and cancer. The Journal of nutrition, 137(12), 2599-2607.(2007)

5. Churruca, I., Fernández-Quintela, A., & Portillo, M. P. Conjugated linoleic acid isomers: differences in metabolism and biological effects. Biofactors, 35(1), 105-111. (2009)

6. Fahy, Eoin, et al. Update of the LIPID MAPS comprehensive classification system for lipids1. Journal of lipid research 50: S9-S14.(2009)

7. Liebisch, Gerhard, et al. Shorthand notation for lipid structures derived from mass spectrometry. Journal of lipid research 54(6), 1523-1530. (2013)

8. Schmelzer, K., Fahy, E., Subramaniam, S., & Dennis, E. A. The lipid maps initiative in lipidomics. Methods in enzymology, 432, 171-183. (2007)

9. Piomelli, Daniele, Giuseppe Astarita and Rao Rapaka. A neuroscientist's guide to lipidomics. Nature Reviews Neuroscience 8(10), 743-754. (2007)

10. Rutherford, C., et al. Regulation of cell survival by sphingosine-1-phosphate receptor S1P1 via reciprocal ERK-dependent suppression of Bim and PI-3-kinase/protein kinase C-mediated upregulation of Mcl-1. Cell death & disease 4(11). e927-e927. (2013)

11. Dadsena, Shashank, et al. Ceramides bind VDAC2 to trigger mitochondrial apoptosis. Nature communications 10(1), 1832. (2019)

12. Hannun, Y. A., & Obeid, L. M. Principles of bioactive lipid signalling: lessons from sphingolipids. Nature reviews Molecular cell biology, 9(2), 139-150. (2008)

13. Quinville, B. M., Deschenes, N. M., Ryckman, A. E., & Walia, J. S. A comprehensive review: sphingolipid metabolism and implications of disruption in sphingolipid homeostasis. International journal of molecular sciences, 22(11), 5793. (2021)

14. Pewzner-Jung, Y., Ben-Dor, S., & Futerman, A. H. When do Lasses (longevity assurance genes) become CerS (ceramide synthases)?: Insights into the regulation of ceramide synthesis. Journal of Biological Chemistry, 281(35), 25001-25005. (2006)

15. Linn, S. C. Kim HS, Keane EM, Andras LM, Wang E, Merrill AH Jr. Regulation of de novo sphingolipid biosynthesis and the toxic consequences of its disruption. Biochem Soc Trans, 29, 831-835. (2001)

16. Johnson, K. R., Johnson, K. Y., Becker, K. P., Bielawski, J., Mao, C., & Obeid, L. M. Role of human sphingosine-1-phosphate phosphatase 1 in the regulation of intra-and extracellular sphingosine-1-phosphate levels and cell viability. Journal of Biological Chemistry, 278(36), 34541-34547. (2003)

17. Furuya, H., Shimizu, Y., & Kawamori, T. Sphingolipids in cancer. Cancer and Metastasis Reviews, 30, 567-576. (2011)

18. Companioni, O., Mir, C., Garcia-Mayea, Y., & LLeonart, M. E. Targeting sphingolipids for cancer therapy. Frontiers in Oncology, 11, 745092. (2021)

19. Ogretmen, B., & Hannun, Y. A. Biologically active sphingolipids in cancer pathogenesis and treatment. Nature Reviews Cancer, 4(8), 604-616. (2004)

20. Antoon, J. W., Liu, J., Gestaut, M. M., Burow, M. E., Beckman, B. S., & Foroozesh, M. Design, synthesis, and biological activity of a family of novel ceramide analogues in chemoresistant breast cancer cells. Journal of medicinal chemistry, 52(18), 5748-5752. (2009)

21. Mehta, S., Blackinton, D., Omar, I., Kouttab, N., Myrick, D., Klostergaard, J., et al. Combined cytotoxic action of paclitaxel and ceramide against the human Tu138 head and neck squamous carcinoma cell line. Cancer Chemotherapy and Pharmacology, 46, 85–92. (2000)

22. Rahmaniyan M, Curley RW, Obeid LM, Hannun YA, Kraveka JM. Identification of Dihydroceramide Desaturase as a Direct in Vitro Target for Fenretinide. J Biol Chem 286, 24754–64. (2011)

23. Stolk, D. A., De Haas, A., Vree, J., Duinkerken, S., Lübbers, J., Van de Ven, R., ... & van Kooyk, Y. Lipo-based vaccines as an approach to target dendritic cells for induction of T-and iNKT cell responses. Frontiers in Immunology, 11, 990. (2020)

24. Ling, L. U., Tan, K. B., & Chiu, G. N. Role of reactive oxygen species in the synergistic cytotoxicity of safingol-based combination regimens with conventional chemotherapeutics. Oncology Letters, 2(5), 905-910. (2011)

25. Chi, H. Sphingosine-1-phosphate and immune regulation: trafficking and beyond. Trends in pharmacological sciences, 32(1), 16-24. (2011)

26. Shaw, J., Costa-Pinheiro, P., Patterson, L., Drews, K., Spiegel, S., & Kester, M. Novel sphingolipid-based cancer therapeutics in the personalized medicine era. Advances in cancer research, 140, 327-366. (2018)

27. Schengrund, C. L. Lipid rafts: keys to neurodegeneration. Brain research bulletin, 82(1-2), 7-17. (2010)

28. Farwanah, H., & Kolter, T. Lipidomics of glycosphingolipids. Metabolites, 2(1), 134-164. (2012)

29. Hanada, K. Sphingolipids in infectious diseases. Japanese journal of infectious diseases, 58(3), 131. (2005)

30. Christie W. W. LipidMaps(2023)

https://www.lipidmaps.org/resources/lipidweb/lipidweb_html/lipids/sphingo/oligocer/index.htm

31. Holgersson, J., Jovall, P. Å., Samuelsson, B. E., & Breimer, M. E. Blood group type glycosphingolipids of human kidneys. Structural characterization of extended globo-series compounds. Glycoconjugate journal, 8, 424-433. (1991)

32. Suila, Heli, et al. Are globoseries glycosphingolipids SSEA-3 and-4 markers for stem cells derived from human umbilical cord blood?. Journal of molecular cell biology 3(2), 99-107. (2011)

33. Sibille, Estelle, et al. Ganglioside profiling of the human retina: Comparison with other ocular structures, brain and plasma reveals tissue specificities. PLoS One 11(12), e0168794. (2016)

34. Sipione, S., Monyror, J., Galleguillos, D., Steinberg, N., & Kadam, V. Gangliosides in the brain: physiology, pathophysiology and therapeutic applications. Frontiers in neuroscience, 14, 572965. (2020)

35. Varki, A., Cummings, R. D., Esko, J. D., Stanley, P., Hart, G. W., Aebi, M & Seeberger, P. H. Essentials of Glycobiology (2022)

36. Kolter, Thomas. Ganglioside biochemistry. International Scholarly Research Notices 2012 (2012)

37. Merrill Jr, Alfred H., et al. "Sphingolipidomics: high-throughput, structure-specific, and quantitative analysis of sphingolipids by liquid chromatography tandem mass spectrometry." Methods 36(2) 207-224. (2005)

38. Weinberg R.A. The Biology of Cancer. Garland Science, New York (2013)

39. Zhuo, Dinghao, Xiang Li, and Feng Guan. "Biological roles of aberrantly expressed glycosphingolipids and related enzymes in human cancer development and progression." Frontiers in physiology 9, 466. (2018)

40. Gehrmann, Mathias, et al. "Tumor-specific Hsp70 plasma membrane localization is enabled by the glycosphingolipid Gb3." PloS one 3(4), e1925. (2008)

41. Stimmer, Lev, et al. Human breast cancer and lymph node metastases express Gb3 and can be targeted by STxB-vectorized chemotherapeutic compounds." BMC cancer 14(1), 1-11. (2014)

42. García-Hevia, Lorena, et al. "Gb3/cd77 is a predictive marker and promising therapeutic target for head and neck cancer." Biomedicines 10(4), 732. (2022)

43. Tyler, A., Johansson, A., Karlsson, T., Gudey, S. K., Brannstrom, T., Grankvist, K., et al. Targeting glucosylceramide synthase induction of cell surface globotriaosylceramide (Gb3) in acquired cisplatin-resistance of lung cancer and malignant pleural mesothelioma cells. Exp. Cell Res. 336, 23–32. (2015)

44. Park, S. Y., Kwak, C. Y., Shayman, J. A., and Kim, J. H. Globoside promotes activation of ERK by interaction with the epidermal growth factor receptor. Biochim. Biophys. Acta 1820, 1141–1148. (2012)

45. Tsai YC, Huang JR, Cheng JY, Lin JJ, Hung JT, Wu YY, Yeh KT, Yu AL. A common cancer-associated glycan, globo-H-ceramide, induces immunosuppression by reducing Notch1 signaling. J Cancer Sci. thermal 5, 264-270. (2013)

46. Danishefsky, S. J., Shue, Y. K., Chang, M. N., and Wong, C. H. Development of Globo-H cancer vaccine. Acc. Chem. Res. 48, 643–652. (2015)

47. Furukawa, K., Ohmi, Y., Ohkawa, Y., Bhuiyan, R. H., Zhang, P., Tajima, O. & Furukawa, K. New era of research on cancer-associated glycosphingolipids. Cancer science, 110(5), 1544-1551. (2019)

48. Ohkawa Y, Miyazaki S, Hamamura K, et al. Ganglioside GD3 enhances adhesion signals and augments malignant properties of melanoma cells by recruiting integrins to glycolipid-enriched microdomains. J Biol Chem. 285, 27213-27223. (2010)

49. Hamamura K, Furukawa K, Hayashi T, et al. Ganglioside GD3 promotes cell growth and invasion through p130Cas and paxillin in malignant melanoma cells. Proc Natl Acad Sci USA.;102, 11041-11046. (2005)

50. SJ Yoon , K. Nakayama , T. Hikita , K. Handa , SI Hakomori . Epidermale Wachstumsfaktor-Rezeptor-Tyrosinkinase wird durch GM3-Wechselwirkung mit N-verknüpften GlcNAc-Termini des Rezeptors moduliert . Proc Natl Acad Sci USA. 103, 18987-18991. (2006)

51. Y. Dong , K. Ikeda , K. Hamamura et al. Die GM1/GD1b/GA1-Synthase-Expression führt zu reduzierten Krebsphänotypen mit Modulation der Zusammensetzung und Raft-Lokalisierung von Gangliosiden in einer Melanom-Zelllinie . Krebs Wissenschaft. 101, 2039-2047. (2010)

52. Gabri, MR, Cacciavillano, W., Chantada, GL, and Alonso, DF. Racotumomab for the treatment of lung cancer and refractory malignancies in children. Expert Opin. biol. ther. 16, 573-578. (2016)

53. Alfonso, S., Valdes-Zayas, A., Santiesteban, E. R., Flores, Y. I., Areces, F., Hernandez, M., et al. A randomized, multicenter, placebo-controlled clinical trial of racotumomab-alum vaccine as switch maintenance therapy in advanced non-small cell lung cancer patients. Clin. Cancer Res. 20, 3660–3671. (2014)

54. Piperno, G. M., Lopez-Requena, A., Predonzani, A., Dorvignit, D., Labrada, M., Zentilin, L., et al. Recombinant AAV-mediated in vivo long-term expression and antitumour activity of an anti-ganglioside GM3(Neu5Gc) antibody. Gene Ther. 22, 960–967. (2015)

55. Delannoy, C. P., Rombouts, Y., Groux-Degroote, S., Holst, S., Coddeville, B., Harduin-Lepers, A., et al. Glycosylation changes triggered by the differentiation of monocytic THP-1 cell line into macrophages. J. Proteome Res. 16, 156–169. (2017)

56. Liu, X., Cheng, JC, Turner, LS, Elojeimy, S., Beckham, TH, Bielawska, A., et al. Saure Ceramidase-Hochregulierung bei Prostatakrebs: Rolle bei der Tumorentwicklung und Implikationen für die Therapie. Gutachten zu therapeutischen Zielen, 13, 1449–1458. (2009)

57. Rustam, Y. H.; Reid, G. E. Analytical Challenges and Recent Advances in Mass Spectrometry Based Lipidomics. Anal. Chem. 90 (1), 374–397. (2018)

58. Giles, C.; Takechi, R.; Lam, V.; Dhaliwal, S. S.; Mamo, J. C. L. Contemporary Lipidomic Analytics: Opportunities and Pitfalls. Progress in Lipid Research. 71, 86–100. (2018)

59. Cajka, T.; Fiehn, O. Toward Merging Untargeted and Targeted Methods in Mass Spectrometry-Based Metabolomics and Lipidomics. Anal. Chem. 88 (1), 524–545. (2016)

60. Folch, J.; Lees, M.; Stanley, G. H. S. A Simple Method for the Isolation and Purification of Total Lipides from Animal Tissues. J. Biol. Chem. 226 (1), 497–509. (1957)

61. Bligh, E. G.; Dyer, W. J. A Rapid Method of Total Lipid Extraction and Purification. Can. J. Biochem. Physiol. 37 (8), 911–917. (1957)

62. Hammad, S. M., Pierce, J., Soodavar, F., Smith, K., Al Gadban, M., Rembiesa, B., Klein, R., Hannun, Y., Bielawski, J., Bielawska, A. Blood sphingolipidomics in healthy humans: impact of sample collection methodology. J. Lipid Res. 51, 3074–3087 (2010).

63. Hara, A. & Radin, N. S. Lipid extraction of tissues with a low toxicity solvent. Anal. Biochem. 90, 420–426. (1978)

64. Yao, L., Lee, S. L., Wang, T. & Gerde, J. A. Comparison of lipid extraction from microalgae and soybeans with aqueous isopropanol. J. Am. Oil Chem. Soc. 90, 571–578. (2013)

65. Matyash, V., Liebisch, G., Kurzchalia, T. V., Shevchenko, A. & Schwudke, D. Lipid extraction by methyl- tert -butyl ether for high-throughput lipidomics. J. Lipid Res. 49, 1137–1146. (2008)

66. Reis, A., Rudnitskaya, A., Blackburn, G., Fauzi, N., Pitt, A., Spickett, C. A comparison of five lipid extraction solvent systems for lipidomic studies of human LDL. J. Lipid Res. 54, 1812–1824. (2013)

67. Triebl, A., Hartler, J., Trötzmüller, M. & C. Köfeler, H. Lipidomics: Prospects from a technological perspective. Biochim. Biophys. Acta - Mol. Cell Biol. Lipids 1862, 740–746. (2017)

68. Cajka, T.; Fiehn, O. Comprehensive Analysis of Lipids in Biological Systems by Liquid Chromatography-Mass Spectrometry. TrAC Trends in Analytical Chemistry. 61, 192–206. (2014)

69. Ovčačíková, M., Lísa, M., Cífková, E. & Holčapek, M. Retention behavior of lipids in reversedphase ultrahigh-performance liquid chromatography-electrospray ionization mass spectrometry. J. Chromatogr. A 1450, 76–85. (2016)

70. Han, X. Lipidomics- Comprehensive Mass Spectrometry of Lipids. John Wiley & Sons. (2016)

71. Jurowski, K.; Kochan, K.; Walczak, J.; Barańska, M.; Piekoszewski, W.; Buszewski, B. Analytical Techniques in Lipidomics: State of the Art. Critical Reviews in Analytical Chemistry. 47 (5), 418–437. (2017)

72. Liebisch, G., Ekroos, K., Hermansson, M. & Ejsing, C. S. Reporting of lipidomics data should be standardized. Biochim. Biophys. Acta 1862, 747–751. (2017)

73. Narváez-Rivas, M. & Zhang, Q. Comprehensive untargeted lipidomic analysis using core-shell C30 particle column and high field orbitrap mass spectrometer. J. Chromatogr. A. 1440, 123–134 (2016)

74. Breitkopf, S. B., Ricoult, S., Yuan, M., Xu, Y., Peake, D., Manning, B., Asara, J. A relative quantitative positive/negative ion switching method for untargeted lipidomics via high resolution LC-MS/MS from any biological source. Metabolomics 13, 1–21. (2017)

75. Wehrens, R., Salek, R., Eds. Metabplomics: Pracital Guide to Design and Analysis. (2020)

76. Hollender, J.; Schymanski, E. L.; Singer, H. P.; Ferguson, P. L. Nontarget Screening with High Resolution Mass Spectrometry in the Environment: Ready to Go? Environ. Sci. Technol. 51(20), 11505–11512. (2017)

77. Peng, B., Kopczynski, D., Pratt, B.S. et al. LipidCreator workbench to probe the lipidomic landscape. Nat Commun 11, 2057 (2020).

78. MacLean B, Tomazela DM, Shulman N, Chambers M, Finney GL, Frewen B, Kern R, Tabb DL, Liebler DC, MacCoss MJ. Skyline: an open source document editor for creating and analyzing targeted proteomics experiments. Bioinformatics. 26(7), 966-8. (2010)

79. Adams KJ, Pratt B, Bose N, Dubois LG, St John-Williams L, Perrott KM, Ky K, Kapahi P, Sharma V, MacCoss MJ, Moseley MA, Colton CA, MacLean BX, Schilling B, Thompson JW; Alzheimer's Disease Metabolomics Consortium. Skyline for Small Molecules: A Unifying Software Package for Quantitative Metabolomics. J Proteome Res. 19(4),1447-1458. (2020)

80. Schymanski, E. L.; Singer, H. P.; Slobodnik, J.; Ipolyi, I. M.; Oswald, P.; Krauss, M.; Schulze, T.; Haglund, P.; Letzel, T.; Grosse, S.; Thomaidis, N. S.; Bletsou, A.; Zwiener, C.; Ibáñez, M.; Portolés, T.; De Boer, R.; Reid, M. J.; Onghena, M.; Kunkel, U.; Schulz, W.; Guillon, A.; Noyon, N.; Leroy, G.; Bados, P.; Bogialli, S.; Stipaničev, D.; Rostkowski, P.; Hollender, J. Non-Target Screening with High-Resolution Mass Spectrometry: Critical Review Using a Collaborative Trial on Water Analysis. Anal. Bioanal. Chem. 407 (21), 6237–6255. (2015)

81. Cui, L.; Lu, H.; Lee, Y. H. Challenges and Emergent Solutions for LC-MS/MS Based Untargeted Metabolomics in Diseases. Mass Spectrom. Rev. 37 (6), 772–792. (2018)

82. Schymanski, E. L.; Jeon, J.; Gulde, R.; Fenner, K.; Ruff, M.; Singer, H. P.; Hollender, J. Identifying Small Molecules via High Resolution Mass Spectrometry: Communicating Confidence. Environ. Sci. Technol. 48 (4), 2097–2098 (2014)

83. Rampler, E.; Coman, C.; Hermann, G.; Sickmann, A.; Ahrends, R.; Koellensperger, G. LILY-Lipidome Isotope Labeling of Yeast: In Vivo Synthesis of 13 C Labeled Reference Lipids for Quantification by Mass Spectrometry. Analyst. 142 (11), 1891–1899. (2017)

84. Rampler, E.; Schoeny, H.; Mitic, B. M.; El Abiead, Y.; Schwaiger, M.; Koellensperger, G. Simultaneous Non-Polar and Polar Lipid Analysis by on-Line Combination of HILIC, RP and High Resolution MS. Analyst. 143 (5), 1250–1258. (2018)

85. Kaufmann, A. Analytical Performance of the Various Acquisition Modes in Orbitrap MS and MS/MS. J Mass Spectrom. 53 (8), 725–738. (2018)

86. Lee, Hyeyoung, et al. Multiple precursor ion scanning of gangliosides and sulfatides with a reversed-phase microfluidic chip and quadrupole time-of-flight mass spectrometry. Analytical chemistry. 84(14) 5905-5912. (2012)

87. Ikeda, Kazutaka, Takao Shimizu, and Ryo Taguchi. Targeted analysis of ganglioside and sulfatide molecular species by LC/ESI-MS/MS with theoretically expanded multiple reaction monitorings. Journal of lipid research 49.12 (2008): 2678-2689.(Barrientos, Rodell C., and Qibin Zhang. "Recent advances in the mass spectrometric analysis of glycosphingolipidome–A review." Analytica chimica acta. 1132, 134-155. (2020)

88. Barrientos, Rodell C., and Qibin Zhang. Recent advances in the mass spectrometric analysis of glycosphingolipidome–A review. Analytica chimica acta 1132, 134-155. (2020)

89. Lipidomics-Standards-Initiative (LSI) https://lipidomics-standards-initiative.org/ (accessed Aug 21, 2019).

90. Wang, M.; Wang, C.; Han, X. Selection of Internal Standards for Accurate Quantification of Complex Lipid Species in Biological Extracts by Electrospray Ionization Mass Spectrometry-What, How and Why?: INTERNAL STANDARDS FOR QUANTIFICATION OF LIPIDS IN LIPIDOMICS. Mass Spec Rev. 36 (6), 693–714. (2017)

91. Neuditschko, Benjamin, et al. Interaction with Ribosomal Proteins Accompanies Stress Induction of the Anticancer Metallodrug BOLD-100/KP1339 in the Endoplasmic Reticulum. Angewandte Chemie International Edition 60(10), 5063-5068. (2021)

92. Coman, Cristina, et al. Simultaneous metabolite, protein, lipid extraction (SIMPLEX): a combinatorial multimolecular omics approach for systems biology. Molecular & Cellular Proteomics 15(4), 1435-1466. (2016)

93. Hohenwallner, Katharina, et al. Decoding distinct ganglioside patterns of native and differentiated mesenchymal stem cells by a novel glycolipidomics profiling strategy. JACS Au 2(11), 2466-2480. (2022)

94. Masson, E. A. Y.; Sibille, E.; Martine, L.; Chaux-Picquet, F.; Bretillon, L.; Berdeaux, O., Apprehending ganglioside diversity: a comprehensive methodological approach. Journal of lipid research. 56, 1835. (2015)

95. Huang, Q.; Zhou, X.; Liu, D.; Xin, B.; Cechner, K.; Wang, H.; Zhou, A., A new liquid chromatography/tandem mass spectrometry method for quantification of gangliosides in human plasma. Analytical Biochemistry. 455, 34 (2015)

96. Peng, B.; Weintraub, S. T.; Coman, C.; Ponnaiyan, S.; Sharma, R.; Tews, B.; Winter, D.; Ahrends, R. A Comprehensive High-Resolution Targeted Workflow for the Deep Profiling of Sphingolipids. Anal. Chem. 89 (22), 12480–12487. (2017)

97. Rampler, E.; Criscuolo, A.; Zeller, M.; El Abiead, Y.; Schoeny, H.; Hermann, G.; Sokol, E.; Cook, K.; Peake, D. A.; Delanghe, B.; et al. A Novel Lipidomics Workflow for Improved Human Plasma Identification and Quantification Using RPLC-MSn Methods and Isotope Dilution Strategies. Anal. Chem. 90 (11), 6494–6501. (2018)

98. Loos, M.; Gerber, C.; Corona, F.; Hollender, J.; Singer, H., Accelerated isotope fine structure calculation using pruned transition trees. Analytical Chemistry 2015, 87 (11), 5738-5744

99. Lucila Aimo, Robin Liechti, Nevila Hyka-Nouspikel, Anne Niknejad, Anne Gleizes, Lou Götz, Dmitry Kuznetsov, Fabrice PA David, F. Gisou van der Goot, Howard Riezman, Lydie Bougueleret, Ioannis Xenarios, Alan Bridge, The SwissLipids Knowledgebase for lipid biology, Bioinformatics. 31(17) 2860–2866. (2015) Swiss lipid database: https://www.swisslipids.org/#/

100. Kishimoto, Yasuo. Ceramides and cerebrosides. Metabolism in the Nervous System 179-199. (1983)

101. Barone, A., Säljö, K., Benktander, J., Blomqvist, M., Månsson, J-E., Johansson, BR, Mölne, J., Aspegren, A., Björquist, P., Breimer, ME , Teneberg, S.: Sialyl-Lactotetra: a novel cell surface marker of undifferentiated human pluripotent stem cells. J. Biol. Chem. 289, 18846-18859 (2014)

102. Barone, A., Benktander, J., Ångström, Aspegren, A., Björquist, P., Teneberg, S., Breimer, ME: Structural complexity of non-acidic glycosphingolipids in human embryonic stem cells grown under feeder-free conditions. J. Biol. Chem. 288, 10035–10050 (2013)

103. Sandvig, Kirsten, et al. "Lipid requirements for entry of protein toxins into cells." Progress in Lipid Research 54, 1-13. (2014)

104. Ho, Ming-Yi, Alice L. Yu, and John Yu. "Glycosphingolipid dynamics in human embryonic stem cell and cancer: their characterization and biomedical implications." Glycoconjugate Journal 34, 765-777. (2017)

105. Zhu, Tingting, et al. "Analysis of breast cancer-associated glycosphingolipids using electrospray ionization-linear ion trap quadrupole mass spectrometry." Carbohydrate research 402, 189-199. (2015)

106. Scherer, Max, et al. "Sphingolipid profiling of human plasma and FPLC-separated lipoprotein fractions by hydrophilic interaction chromatography tandem mass spectrometry." Biochimica et Biophysica Acta (BBA)-Molecular and Cell Biology of Lipids 1811(2), 68-75. (2011)

107. Huang, Hao, et al. "LC-MS based sphingolipidomic study on A2780 human ovarian cancer cell line and its taxol-resistant strain." Scientific reports 6(1), 1-13 (2016)

108. Silsirivanit, Atit, et al. "Overexpression of HexCer and LacCer containing 2-hydroxylated fatty acids in cholangiocarcinoma and the association of the increase of LacCer (d18: 1-h23: 0) with shorter survival of the patients." Glycoconjugate Journal 36, 103-111. (2019)

109. Skotland, Tore, et al. "Molecular lipid species in urinary exosomes as potential prostate cancer biomarkers." European Journal of Cancer 70, 122-132.(2017)

110. Engedal, Nikolai, et al. "Shiga toxin and its use in targeted cancer therapy and imaging." Microbial biotechnology 4(1), 32-46. (2011)

111. Meléndez, Ana Valeria, et al. "Novel lectin-based chimeric antigen receptors target Gb3-positive tumour cells." Cellular and Molecular Life Sciences 79(10), 513. (Römer, Winfried, et al. "Novel lectin-based chimeric antigen receptors target Gb3-positive tumour cells." (2022))

112. Fujiwara, Yuko, et al. "Glycosphingolipids with very long-chain fatty acids accumulate in fibroblasts from adrenoleukodystrophy patients." International Journal of Molecular Sciences 22(16), 8645. (2021)

113. Farwanah, Hany, Thomas Kolter, and Konrad Sandhoff. "Mass spectrometric analysis of neutral sphingolipids: methods, applications, and limitations." Biochimica et Biophysica Acta (BBA)-Molecular and Cell Biology of Lipids 1811(11), 854-860. (2011)

114. Okuda, Tetsuya, and Katsuya Kato. "Glycosphingolipids form characteristic-sized liposomes that correlate with their antibody-inducing activities in mice." Biochemical and Biophysical Research Communications 634, 48-54. (2022)

115. Fujiwara, Yuko, et al. "Glycosphingolipids with very long-chain fatty acids accumulate in fibroblasts from adrenoleukodystrophy patients." International Journal of Molecular Sciences 22(16), 8645. (2021)

116. Kondo, Yuji, et al. "TLR4–MD-2 complex is negatively regulated by an endogenous ligand, globotetraosylceramide." Proceedings of the National Academy of Sciences 110(12), 4714-4719. (2013)

117. Meisen, Iris, Michael Mormann, and Johannes Müthing. "Thin-layer chromatography, overlay technique and mass spectrometry: a versatile triad advancing glycosphingolipidomics." Biochimica et Biophysica Acta (BBA)-Molecular and Cell Biology of Lipids 1811(11), 875-896. (2011)

118. Y.-C. Tsai, J.-R. Huang,J.-Y. Cheng,J.-J. Lin, J.-T. Hung, Y.-Y. Wu, K.-T. Yeh,A. L. Yu,J. CancerSci. Ther. 5, 264–270. (2013)

119. Fabris, Dragana, et al. "Aberrant ganglioside composition in glioblastoma multiforme and peritumoral tissue: A mass spectrometry characterization." Biochimie 137, 56-68. (2017)

120. Lin, L., Huang, Z., Gao, Y., Chen, Y., Hang, W., Xing, J., & Yan, X. LC-MS-based serum metabolic profiling for genitourinary cancer classification and cancer type-specific biomarker discovery. Proteomics, 12(14), 2238-2246. (2012)

121. Liang, Yuh-Jin. "Glycosphingolipids in human embryonic stem cells and breast cancer stem cells, and potential cancer therapy strategies based on their structures and functions." Glycoconjugate Journal 39(2), 177-195. (2022)

122. M. Nishikawa,M. Kurano,T. Nitta, H. Kanoh,J.-i Inokuchi,Y. Yatomi,Sci.Rep. 9, 6308–634. (2019)

123. Lee, Jua, et al. Comprehensive profiling of surface gangliosides extracted from various cell lines by LC-MS/MS. Cells 8(11) 1323. (2019)

124. Domon B., Costello C. E. Structure elucidation of glycosphingolipids and gangliosides using high-performance tandem mass spectrometry. Biochemistry. 27, 1543 (1988)

125. Narváez-Rivas, M. & Zhang, Q. Comprehensive untargeted lipidomic analysis using core-shell C30 particle column and high field orbitrap mass spectrometer. J. Chromatogr. A 1440, 123–134 (2016)

126. Triebl, A., Trötzmüller, M., Hartler, J., Stojakovic, T. & Köfeler, H. C. Lipidomics by ultrahigh performance liquid chromatography-high resolution mass spectrometry and its application to complex biological samples. J. Chromatogr. B 1053, 72–80 (2017)

127. Ovčačíková, M., Lísa, M., Cífková, E. & Holčapek, M. Retention behavior of lipids in reversedphase ultrahigh-performance liquid chromatography-electrospray ionization mass spectrometry. J. Chromatogr. A 1450, 76–85 (2016)

128. Huynh, K.; Barlow, C. K.; Jayawardana, K. S.; Weir, J. M.; Mellett, N. A.; Cinel, M.; Magliano, D. J.; Shaw, J. E.; Drew, B. G.; Meikle, P. J. High-Throughput Plasma Lipidomics: Detailed Mapping of the Associations with Cardiometabolic Risk Factors. Cell Chemical Biology 26 (1), 71-84.e4. (2019)

129. Barrientos, Rodell C., and Qibin Zhang. "Recent advances in the mass spectrometric analysis of glycosphingolipidome–A review." Analytica chimica acta 1132, 134-155. (2020)

130. Holčapek, M.; Jirásko, R.; Lísa, M. Recent Developments in Liquid Chromatography–Mass Spectrometry and Related Techniques. Journal of Chromatography A. 1259, 3–15. (2012)

131. HESI-II Probe User Guide. Thermo Fisher Scientific. https://www.thermofisher.com/order/catalog/product/IQLAAEGABBFACNMAGY

132. Zaia, Joseph. "Mass spectrometry of oligosaccharides." Mass spectrometry reviews 23(3), 161-227. (2004)

133. Barrientos, R. C.; Zhang, Q., Isobaric Labeling of Intact Gangliosides toward. Multiplexed LC-MS/MS-Based Quantitative Analysis. Anal. Chem. 90, 2586. (2018)

134. Thermo Fisher Scientific, Q Exactive HF Software Manual. 2014

135. Farwanah, H., Wirtz, J., Kolter, T., Raith, K., Neubert, R. H., & Sandhoff, K. Normal phase liquid chromatography coupled to quadrupole time of flight atmospheric pressure chemical ionization mass spectrometry for separation, detection and mass spectrometric profiling of neutral sphingolipids and cholesterol. Journal of Chromatography B, 877(27), 2976-2982. (2009)

136. Barrientos, Rodell C., and Qibin Zhang. "Recent advances in the mass spectrometric analysis of glycosphingolipidome–A review." Analytica chimica acta 1132, 134-155. (2020)

137. Li, Yunsen, et al. Sensitive quantitation of isoglobotriaosylceramide in the presence of isobaric components using electrospray ionization-ion trap mass spectrometry. Glycobiology 18(2),166-176 (2008)

138. Ravindran, Madhu Sudhan, Lukas Bahati Tanner, and Markus R. Wenk. "Sialic acid linkage in glycosphingolipids is a molecular correlate for trafficking and delivery of extracellular cargo." Traffic 14(11), 1182-1191. (2013)

139. Barrientos, Rodell C., and Qibin Zhang. "Recent advances in the mass spectrometric analysis of glycosphingolipidome–A review." Analytica chimica acta 1132, 134-155. (2020)

140. Nakajima, Kazuki, et al. "Separation and analysis of mono-glucosylated lipids in brain and skin by hydrophilic interaction chromatography based on carbohydrate and lipid moiety. Journal of Chromatography B. 1031. 146-153. (2016)

141. Boutin, Michel, et al. "Tandem mass spectrometry multiplex analysis of glucosylceramide and galactosylceramide isoforms in brain tissues at different stages of Parkinson disease." Analytical chemistry 88.3 (2016): 1856-1863.

142. Domon, Bruno, and Catherine E. Costello. "A systematic nomenclature for carbohydrate fragmentations in FAB-MS/MS spectra of glycoconjugates." Glycoconjugate journal 5, 397-409. (1988)

143. Ann Q, Adams J, Structure-specific collision-induced fragmentations of ceramides cationized with alkali-metal ions, Anal Chem, 65, 7–13. (1993)

144. Haynes, Christopher A., et al. "Sphingolipidomics: methods for the comprehensive analysis of sphingolipids." Journal of Chromatography B 877(26), 2696-2708. (2009)

145. Blaas, N. & Humpf, H. U. Structural profiling and quantitation of glycosyl inositol phosphoceramides in plants with fourier transform mass spectrometry. J. Agric. Food Chem. 61, 4257–4269. (2013)

146. Ikeda, K.; Shimizu, T.; Taguchi, R., Targeted analysis of ganglioside and sulfatide molecular species by LC/ESI-MS/MS with theoretically expanded multiple reaction monitoring. Journal of lipid research. 49, 2689. (2008)

147. Qu F, Zhang H, Zhang M, Hu P. Sphingolipidomic Profiling of Rat Serum by UPLC-Q-TOF-MS: Application to Rheumatoid Arthritis Study. Molecules. 23(6),1324. (2018)

148. Fu, Zhicheng, et al. "Development of a label-free LC-MS/MS-based glucosylceramide synthase assay and its application to inhibitors screening for ceramide-related diseases." Biomolecules & therapeutics 27(2), 193. (2019)

149. Hájek, Roman, et al. "Hydrophilic interaction liquid chromatography–mass spectrometry characterization of gangliosides in biological samples." Analytical Chemistry 89(22), 12425-12432. (2017)

150. Calvano, C. D., Ventura, G., Sardanelli, A. M., Losito, I., Palmisano, F., & Cataldi, T. R. Identification of neutral and acidic glycosphingolipids in the human dermal fibroblasts. Analytical biochemistry, 581, 113348 (2019)

151. Karlsson, H., Halim, A., & Teneberg, S. Differentiation of glycosphingolipid-derived glycan structural isomers by liquid chromatography/mass spectrometry. Glycobiology, 20(9), 1103-1116. (2010)

152. Wong, M., Xu, G., Park, D., Barboza, M., & Lebrilla, C. B. Intact glycosphingolipidomic analysis of the cell membrane during differentiation yields extensive glycan and lipid changes. Scientific reports, 8(1), 1-10. (2018)

153. Ghiulai, R.; Sarbu, M.; Vukelić, Ž.; Ilie, C.; Zamfir, A., Early stage fetal neocortex exhibits a complex ganglioside profile as revealed by high resolution tandem mass spectrometry. Official Journal of the International Glycoconjugate Organization 31, 245 (2014)

154. FreeStyle Software. ThermoFisher Scientific. https://www.thermofisher.com/at/en/home/technical-resources/technical-reference-library/mass-spectrometry-support-center/liquid-chromatography-mass-spectrometry-software-support/freestyle-software-support.html (2023)

155. Hartler, J.; Triebl, A.; Ziegl, A.; Trötzmüller, M.; Rechberger, G. N.; Zeleznik, O. A.; Zierler, K. A.; Torta, F.; Cazenave-Gassiot, A.; Wenk, M. R.; Fauland, A.; Wheelock, C. E.; Armando, A. M.; Quehenberger, O.; Zhang, Q.; Wakelam, M. J. O.; Haemmerle, G.; Spener, F.; Köfeler, H. C.; Thallinger, G. G., Deciphering lipid structures based on platform-independent decision rules. Nature Methods. 14 (2017)

156. Biomedical Research Products. Cayman Chemical. https://www.caymanchem.com/ (2023)

157. Ovčačíková, M., Lísa, M., Cífková, E. & Holčapek, M. Retention behavior of lipids in reversedphase ultrahigh-performance liquid chromatography-electrospray ionization mass spectrometry. J. Chromatogr. A 1450, 76-85. (2016)